

UNCLASSIFIED

AD NUMBER
ADB069620
NEW LIMITATION CHANGE
TO Approved for public release, distribution unlimited
FROM Distribution authorized to U.S. Gov't. agencies only; Test and Evaluation; Jun 1982. Other requests shall be referred to Air Force Wright Aeronautical Labs., Wright-Patterson AFB, OH 45433.
AUTHORITY
AFWAL ltr, 6 Feb 1987

THIS PAGE IS UNCLASSIFIED

AFWAL-TR-82-4086



**R&D ON COMPOSITION AND PROCESSING
OF TITANIUM ALUMINIDE ALLOYS
FOR TURBINE ENGINES**

United Technologies Corporation Pratt & Whitney Aircraft Group
Government Products Division
West Palm Beach, Florida 33402

July 1982

Interim Report for Period October 1980 to January 1982

Distribution limited to government agencies only; contains Test and Evaluation
June 1982. Other requests for this document must be referred to
~~Research and High Technology Materials Research and Development Division~~
~~Materials Laboratory~~, Air Force Weight Aeronautical Laboratories, Wright-
Patterson Air Force Base, Ohio 46433.

MLLM

SUBJECT TO EXPORT CONTROL LAWS

This document contains information for manufacturing or using munitions of war. Export of the information contained herein, or release to foreign nationals within the United States, without first obtaining an export license, is a violation of the International Traffic-in-Arms Regulations. Such violation is subject to a penalty of up to 2 years imprisonment and a fine of \$100,000 under 22 USC 2778.

Include this notice with any reproduced portion of this document.

**MATERIALS LABORATORY
AIR FORCE WRIGHT AERONAUTICAL LABORATORIES
AIR FORCE SYSTEMS COMMAND
WRIGHT-PATTERSON AIR FORCE BASE, OHIO 46433**

82 12 13 061

ALBU69620

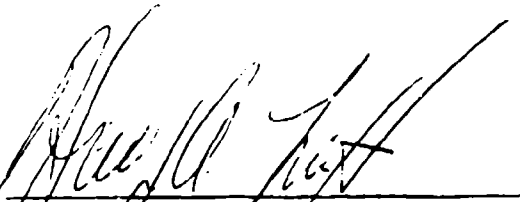
WPK

5200

NOTICE

When Government drawings, specifications, or other data are used for any purpose other than in connection with a definitely related Government procurement operation, the United States Government thereby incurs no responsibility nor any obligation whatsoever; and the fact that the Government may have formulated, furnished, or in any way supplied the said drawings, specifications, or other data, is not to be regarded by implication or otherwise as in any manner licensing the holder or any other person or corporation, or conveying any rights or permission to manufacture, use, or sell any patented invention that may in any way be related thereto.

This technical report has been reviewed and is approved for publication.

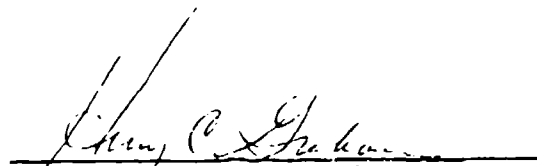


HARRY A. LIPSITT
Project Engineer



NORMAN M. GEYER
Technical Area Manager
Processing & High Temperature
Materials Branch
Metals & Ceramics Division

FOR THE COMMANDER:



HENRY C. GRAHAM, Chief
Processing & High Temperature
Materials Branch
Metals & Ceramics Division

"If your address has changed, if you wish to be removed from our mailing list, or if the addressee is no longer employed by your organization, please notify AFWAL/MLLM, W-P AFB, Ohio 45433 to help maintain a current mailing list".

Copies of this report should not be returned unless return is required by security considerations, contractual obligations, or notice on a specific document.

UNCLASSIFIED

SECURITY CLASSIFICATION OF THIS PAGE (When Data Entered)

REPORT DOCUMENTATION PAGE		READ INSTRUCTIONS BEFORE COMPLETING FORM
1. REPORT NUMBER AFWAL-TR-82-4086	2. GOVT ACCESSION NO. AD-B0696206	3. RECIPIENT'S CATALOG NUMBER
4. TITLE (and Subtitle) R&D ON COMPOSITION AND PROCESSING OF TITANIUM ALUMINIDE ALLOYS FOR TURBINE ENGINES	5. TYPE OF REPORT & PERIOD COVERED Interim Technical Report October 1980-January 1982	6. PERFORMING ORG. REPORT NUMBER FR-16259
		8. CONTRACT OR GRANT NUMBER(s) F33615-80-C-5163
7. AUTHOR(s) M. J. Blackburn M. P. Smith	9. PERFORMING ORGANIZATION NAME AND ADDRESS UTC - Pratt & Whitney Aircraft Group Government Products Division West Palm Beach, FL 33402	10. PROGRAM ELEMENT, PROJECT, TASK AREA & WORK UNIT NUMBERS 24200127
11. CONTROLLING OFFICE NAME AND ADDRESS Materials Laboratory (MLLM) Air Force Wright Aeronautical Laboratories Wright-Patterson AFB, Ohio 45433	12. REPORT DATE June 1982	13. NUMBER OF PAGES 91
	14. MONITORING AGENCY NAME & ADDRESS (if different from Controlling Office)	15. SECURITY CLASS. (of this report) Unclassified
15a. DECLASSIFICATION/DOWNGRADING SCHEDULE		
16. DISTRIBUTION STATEMENT (of this Report) Distribution limited to U.S. Government agencies only. Test and Evaluation; June 1982. Other requests for this document must be referred to AFWAL/MLLM, WPAFB, Ohio 45433		
17. DISTRIBUTION STATEMENT (of the abstract entered in Block 20, if different from Report)		
18. SUPPLEMENTARY NOTES		
19. KEY WORDS (Continue on reverse side if necessary and identify by block number) Titanium Aluminides, Alloy Development, Isothermal Forging, Titanium Ingot Production, Mechanical Properties, Titanium Alloy Microstructures, Titanium Machining, Titanium Casting		
20. ABSTRACT (Continue on reverse side if necessary and identify by block number) Materials based on the intermetallic phases Ti_3Al (α_2) and $TiAl$ (γ) exhibit several attractive features that make them candidates for gas turbine engine applications. Low density, good oxidation resistance and high temperature strength are such characteristics and could result in substitution for the nickel alloys currently used for turbine engine components that operate at intermediate temperatures. Basic alloy development studies over the past eight years have identified the base Ti-Al-Nb-V and Ti-Al-V systems,		

UNCLASSIFIED

Block 20 (Cont'd.)

respectively, as the most attractive base compositions for the two alloy types. In this current program, one alpha-two and several gamma compositions were selected, produced as large ingots and isothermally forged. Extensive mechanical property testing was conducted on these forgings. In addition, various material processing methods such as casting, rolling, extrusion and machining were evaluated.

The alpha-two alloy Ti-25Al-10Nb-3V-1Mo exhibited the best balance of tensile and stress-rupture properties found to date and had a higher elastic modulus. Beta grain size was shown to have major effects on creep, low cycle fatigue and fracture toughness. Alloy stability, as measured by post-exposure tensile ductility, was poor and was tentatively traced to precipitation of an unidentified phase in the beta. Heat treatment modifications were suggested to alleviate this problem. Processing studies showed that many of the methods developed for forging, joining and rolling of conventional titanium alloys can be applied to the alpha-two alloys.

Screening tests conducted on four gamma alloys did not identify an alloy with a better property balance than Ti-48Al-1V-.1C which had been evaluated previously. Properties were more consistent with previous small scale ingots, although ductility and impact strength were somewhat lower, and quite good toughness levels were measured. Alloy stability was excellent after exposure and processing studies established machining procedures and demonstrated that the alloy has fair castability.

TABLE OF CONTENTS

SECTION		PAGE
I	INTRODUCTION	1
II	PROGRAM SCOPE AND APPROACH	2
	1. Background	2
	2. Program Plan	3
	3. Alloy and Process Selection - Alpha-Two Alloy	3
	4. Alloy and Process Selection - Gamma Alloys	4
III	EXPERIMENTAL DETAILS	7
	1. Material Procurement and Processing	7
	a. Large Ingots and Forgings	7
IV	RESULTS AND DISCUSSION	20
	1. Introduction	20
	2. Material Characterization - Alpha-Two Alloy	20
	3. Material Characterization - Gamma Alloys 1-4	44
	a. Screening Tests	44
	b. Material Characterization - Ti-48Al-1V-.1C	48
	4. Processing Studies	64
	a. Net Shape Gamma Alloy Casting	64
	b. Gamma Alloy Machinability	69
	c. Forged Alpha-Two Alloy Compressor Blade	82
	d. Alpha-Two Alloy Sheet Analysis	82
V	ANALYSIS AND CONCLUSIONS	87
	REFERENCES	91

LIST OF ILLUSTRATIONS

FIGURE		PAGE
1	As-received titanium aluminide ingots supplied by RMI. (a) S/N 20007; (b) left to right, S/N 20008, S/N 20009, S/N 20010, S/N 20011.	9
2	Pancake forging preforms machined from RMI titanium aluminide ingots a) S/N 20007; b) S/N 20008; c) S/N 20009; d) S/N 20010; e) S/N 20011. Note fairly extensive porosity on gamma alloy ingots (b-e) compared to the alpha-two alloy a).	10
3	Top and bottom views of as-forged Ti-47Al-2V-2Nb-1Mo alloy pancake.	12
4	Top and bottom views of as-forged Ti-47Al-2V alloy pancake.	13
5	Top and bottom views of as-forged Ti-47Al-2V-.1C alloy pancake.	14
6	Top and bottom views of as-forged Ti-48Al-1V-.1C alloy pancake. Note better die fill and less cracking.	15
7	Top and bottom views of as-forged Ti-25Al-10Nb-3V-1Mo alloy pancake.	16
8	Specimen used to measure tensile, creep and low cycle fatigue capability of titanium aluminide alloy.	17
9	Specimens used for impact and fracture toughness evaluation of titanium aluminide alloys.	18
10	Physical property specimens used for titanium aluminide study. a) thermal expansion; b) modulus of elasticity; c) specific heat; d) conductivity	19
11	Macro- and microstructure of the forged and heat treated Ti-25Al-10Nb-3V-1Mo pancake forging (a). The rim, mid-radius and center microstructures are in b, c and, respectively.	21
12	Microstructures of various titanium aluminide creep specimens tested at 650C/372 MPa (1200F/55 ksi).	24

LIST OF ILLUSTRATIONS (CONT'D.)

FIGURE		PAGE
13	Macrostructure of as-forged Ti-25Al-10Nb-3V-1Mo alloy pancake forging. This was forged on isothermal dies at 1120C (2050F) in one step from a cast ingot.	24
14	Macrostructure of Ti-25Al-10Nb-4V pancake forging from a previous program ⁽⁴⁾ . Top, as-conventionally upset and forged at 1120C (2050F); bottom, heat treated 1150C (2100F)/1/ + salt quench to 815C (1500F)/.5/AC.	25
15	Effect of thermal exposure on hardness of Ti-25Al-10Nb-3V-1Mo tensile specimens.	28
16	Surface of exposed Ti-25Al-10Nb-3V-1Mo alloy tensile specimen showing alpha case contamination, which has a hardness of DPH 700-800.	28
17	SEM fractographs of tested Ti-25Al-10Nb-3V-1Mo tensile specimens.	29
18	General microstructure of Ti-25Al-10Nb-3V-1Mo alloy thin foils cut from tensile specimens.	30
19	Enlarged view of Figure 18 showing the relatively "clean" beta phase in the unexposed specimen 2588 and the darkened beta phase with heavy precipitation in the exposed specimen 2933.	32
20	General microstructure of the unexposed Ti-25Al-10Nb-3V-1Mo tensile specimen 2588 showing spectrum and composition of alpha-two and beta phase.	33
21	S/N curve for smooth Ti-25Al-10Nb-3V-1Mo alloy specimens tested at 650C (1200F).	36
22	S/N curves for notched Ti-25Al-10Nb-3V-1Mo specimens tested at 650C (1200F) based on grain size.	37
23	Selected notched Ti-25Al-10Nb-3V-1Mo LCF specimens showing extremes in grain size but similar microstructures.	38
24	Young's modulus of Ti-25Al-10Nb-3V-1Mo alloy specimen vs. temperature.	40
25	Thermal conductivity of the Ti-25Al-10Nb-3V-1Mo alloy.	42

LIST OF ILLUSTRATIONS (CONT'D.)

FIGURE		PAGE
26	Enthalpy of the Ti-25Al-10Nb-3V-1Mo alloy.	42
27	Heat capacity of the Ti-25Al-10Nb-3V-1Mo alloy.	43
28	Thermal expansion of the Ti-25Al-10Nb-3V-1Mo alloy.	43
29	Cross sections of tested gamma alloy titanium aluminide tensile specimens showing internal porosity (arrow, brackets).	46
30	Grinding cracks and porosity on thread surface of Ti-48Al-1V-.1C tensile specimen. Right, a cross section of a thread root on the same specimen revealing a root crack.	47
31	Microstructures of Ti-48Al-1V-.1C creep specimens showing relative amounts of acicular phase present.	50
32	Continuous oxide layer formed on Ti-48Al-1V-.1C alloy specimens after a thermal exposure of 500 hours at 675C (1250F) plus 100 hours at 730C (1350F) (brackets).	53
33	Fracture mode in precracked slow bend toughness specimens. Left column, Ti-48Al-1V-.1C; right column, Ti-25Al-10Nb-3V-1Mo. Note difference in grain size.	56
34	S/N curves for smooth Ti-48Al-1V-.1C LCF specimens drawn to show effect of grain size on 650C (1200F) life.	57
35	Fracture appearance and microstructures of smooth Ti-48Al-1V-.1C LCF specimens tested at 650C (1200F) and 344 MPa (50 ksi).	58
36	Ti-48Al-1V-.1C smooth LCF specimens tested at 650C (1200F) and 344 MPa (50 ksi). Note origins in coarse grain areas in specimen 3744 (a) and 3749 (b). Fracture path (c) is basically intergranular.	59
37	S/N curve for 815C (1500F) notched low cycle fatigue specimens.	61
38	Young's modulus of the Ti-48Al-1V-.1C alloy.	62
39	Thermal conductivity of the Ti-48Al-1V-.1C alloy.	63

LIST OF ILLUSTRATIONS (CONT'D.)

FIGURE		PAGE
40	Enthalpy of the Ti-48Al-1V-.1C alloy.	63
41	Heat capacity of the Ti-48Al-1V-.1C alloy.	65
42	Thermal expansion of the Ti-48Al-1V-.1C alloy.	65
43	Cast Ti-48Al-1V F100 compressor blade preform showing good fill and definition (a) but surface connected shrinkage porosity at the convex side airfoil platform interface (b, c).	66
44	Cross sections of as-cast Ti-48Al-1V compressor blade preform. Left, black light photo showing centerline shrink; right, normal light photo showing grain flow. (Note this blade was sectioned for fractographic analysis prior to these photos.)	67
45	Typical dendritic appearance of centerline shrinkage in as-cast Ti-48Al-1V compressor blade preform.	68
46	Cross sections of cast + HIP (1190C/103 MPa/3 hours, 2180F/15 ksi/3 hours) Ti-48Al-1V compressor blade preform. Left, black light photo, no indications present; right, natural light photo showing grain flow.	70
47	Microstructure of cast + HIP Ti-48Al-1V compressor blade preform showing residual unhealed porosity.	71
48	Ti-48Al-1V machinability specimen after lathe turning and hole drilling trials. Numbers correspond with specimen numbers in Tables 23 and 24.	72
49	Ti-48Al-1V machinability specimen after milling trials. Numbers correspond with specimen numbers in Table 25.	76
50	Black light photographs of Ti-48Al-1V grinding trial specimens after FPI examination. Note surface cracking on 2BL, 1BS, 3BS and 2AL.	79
51	Effect of peening and subsequent thermal exposure on forged and heat treated Ti-48Al-1V.	81
52	Process procedure for forging Ti-25Al-9Nb-2V compressor blade; left to right, billet, extruded preform, as-forged blade, trimmed blade for final machining.	83
53	Typical microstructures of Ti-25Al-9Nb-2V sheet. a) as-received, annealed; b) beta solution treated and aged; c) welded area after full STA heat treatment.	85

LIST OF TABLES

TABLE		PAGE
1	Actual and Aim Composition in Weight % (Atomic %) of Titanium Aluminide Ingots Procured for Contract F33615-80-C-5163	8
2	Forging Parameters Measured During Isothermal Pressing of Titanium Aluminide Alloys for Contract F33615-80-C-5163	11
3	Transus Temperatures of the Titanium Aluminide Alloys for Contract F33615-80-C-5163	11
4	Tensile Properties of Isothermally Beta Forged and Heat Treated Ti-25Al-10Nb-3V-1Mo Alloy	22
5	Creep Rupture Properties of Isothermally Beta Forged and Heat Treated Ti-25Al-10Nb-3V-1Mo Alloy	22
6	Effect of Thermal Exposure on Tensile Properties of Isothermally Beta Forged and Heat Treated Ti-25Al-10Nb-3V-1Mo Alloy	27
7	Effect of Thermal Exposure on Creep-Rupture Properties of Isothermally Beta Forged and Heat Treated Ti-25Al-10Nb-3V-1Mo Alloy	27
8	Smooth and Notched Charpy Impact Strength of Isothermally Beta Forged and Heat Treated Ti-25Al-10Nb-3V-1Mo Alloy	35
9	Fracture Toughness of Isothermally Beta Forged and Heat Treated Ti-25Al-10Nb-3V-1Mo Pre-cracked Slow Bend Specimens	35
10	Smooth Low Cycle Fatigue Properties of Isothermally Beta Forged and Heat Treated Ti-25Al-10Nb-3V-1Mo Alloy	36
11	Notched (Kt = 2.0) Low Cycle Fatigue Properties of Isothermally Beta Forged and Heat Treated Ti-25Al-10Nb-3V-1Mo Alloy	37
12	Dynamic Modulus of Isothermally Beta Forged and Heat Treated Ti-25Al-10Nb-3V-1Mo Alloy	40
13	Tensile and Stress-Rupture Properties of Forged and Heat Treated Gamma Alloy Pancake Forgings	45
14	Tensile Properties of Isothermally Forged + HIP + Heat Treated Ti-48Al-1V-.1C Alloy	49
15	Stress-Rupture Properties of Isothermally Forged + HIP + Heat Treated Ti-48Al-1V-.1C Alloy	49

LIST OF TABLES (CONT'D.)

TABLE		PAGE
16	Effect of Thermal Exposure on Tensile Properties of Isothermally Forged + HIP + Heat Treated Ti-48Al-1V-.1C Alloy	52
17	Effect of Thermal Exposure on the Creep-Rupture Properties of Isothermally Forged + HIP + Heat Treated Ti-48Al-1V-.1C Alloy	52
18	Smooth Impact Properties of Isothermally Forged + HIP + Heat Treated Ti-48Al-1V-.1C Alloy	54
19	Fracture Toughness of Isothermally Forged + HIP + Heat Treated Ti-48Al-1V-.1C Alloy Precracked Slow Bend Specimens	54
20	Smooth Axial Low Cycle Fatigue of Isothermally Forged + HIP + Heat Treated Ti-48Al-1V-.1C Alloy Specimens	57
21	Notched ($K_t = 2.0$) Axial Low Cycle Fatigue of Isothermally Forged + HIP + Heat Treated Ti-48Al-1V-.1C Alloy Specimens	61
22	Dynamic Modulus of Isothermally Forged + HIP + Heat Treated Ti-48Al-1V-.1C Alloy	62
23	Effect of Lathe Turning Variables on the Machinability of Forged and Heat Treated Ti-48Al-1V	74
24	Effect of Drilling Variables on Machinability of Forged and Heat Treated Ti-48Al-1V	75
25	Effect of Milling Variables on the Machinability of Forged and Heat Treated Ti-48Al-1V	77
26	Effect of Grinding Variables on the Machinability of Forged and Heat Treated Ti-48Al-1V	78
27	Bend Test Data for Alpha-Two Sheet Specimens, V-5816, Ti-25Al-11Nb-2V	86

SECTION I

INTRODUCTION

In the past, major advances in gas turbine engine technology have been associated with the development and incorporation of improved materials including titanium alloys. The high temperature properties of current alpha-beta titanium alloys have improved to the point where the majority of compressors in advanced engines utilize these lightweight materials. Further extension of the use of this class of materials to higher temperature structures in the turbine or after-burner sections of engines is highly desirable; however, conventional titanium alloys offer only limited scope for improvement, and thus, a new approach is needed.

Materials, based on the intermetallic compounds $TiAl$ and Ti_3Al , have been identified which offer considerable advantage over conventional alloys in high temperature environments. Design analysis and payoff studies, conducted for these alloys, have indicated significant weight savings can be achieved in quite a wide range of engine applications. Turbine rotor weight savings from 30 to 40 percent (three to five percent of engine weight) would be achieved with widespread application of the titanium aluminides in rotating hardware; weight savings of up to 16 percent could be achieved in engine applications to static structures such as vanes, cases and bearing supports. It is possible to translate these weight benefits into significant fuel savings with attendant reduction of operating cost.

During the past eight years, Pratt & Whitney Aircraft has participated in Air Force Materials Laboratory sponsored programs directed toward the understanding and exploitation of alloys based on both Ti_3Al and $TiAl$; Contract F33615-75-C-1167 performed alloy and process development on Ti_3Al alloys; Contracts F33615-74-C-1140 and F33615-C-75-1166 have conducted similar development efforts on $TiAl$ alloys. The goals in all programs were to identify alloys from the base systems that exhibited useful properties and develop processing procedures. Results from the first parts of these studies have been presented in previous reports⁽¹⁻⁵⁾.

SECTION II

PROGRAM SCOPE AND APPROACH

1. BACKGROUND

Investigations performed in the mid-1950's by McAndrew and Kessler⁽⁶⁾ at Armour Research Foundation identified several unique characteristics of the TiAl (γ) phase formed in equiatomic titanium-aluminum alloys. In particular, these intermetallic alloys were found to possess high specific strength at elevated temperatures, good oxidation resistance and a high specific modulus of elasticity. Unfortunately, other characteristics, such as essentially zero room temperature ductility and low impact strength plus poor formability characteristics, led to the abandonment of the study. Similar investigations of alloys based on the Ti₃Al (α -two) phase were conducted by McAndrew and Simcoe in the early 1960's^(7,8). Again, attractive elevated temperature properties were found, but rather low room temperature ductility indicated limited engineering usefulness. With the advent of more advanced technologies in physical and process metallurgy by the early 1970's, re-evaluation of the potential of alloys based on these intermetallic compounds was initiated at two organizations, Pratt & Whitney Aircraft and the then Air Force Aerospace Research Laboratory (WPAFB).

As a result of the titanium aluminide efforts conducted over the past eight years, the potential advantages of the use of these materials in advanced gas turbine engines are clear. Basic alloy development studies have identified the most attractive compositional bases, but some opportunities to modify properties by other elements still exist. Much work has been done to scale-up ingot size and investigate additional material processing methods such as casting, extrusion, sheet rolling, machining, etc.

The work described in this report covers the measurement of a wide range of mechanical properties of third generation alloys. In addition, the characteristics of several product forms and finishing methods were evaluated.

2. PROGRAM PLAN

The program was divided into two tasks. In Task I, compositions from the Ti_3Al and $TiAl$ alloy systems showing the best balance of properties were selected. Large ingots were cast in both compositions, and the ingots were then processed using a variety of techniques to demonstrate the feasibility of producing several product forms such as near net shape castings, forgings and sheet. Effect of metal removal and finishing methods on surface condition of gamma alloys were studied. Task II consisted of comprehensive physical and mechanical property measurements on the selected alloys. Included was an evaluation of the influence of simulated service exposure on surface stability and properties.

3. ALLOY AND PROCESS SELECTION - ALPHA-TWO ALLOY

It was found during the various studies conducted under Contract F33615-75-C-1167 that the optimum combination of room temperature tensile ductility and elevated temperature creep-rupture capability could be realized in alloys from the ternary $Ti-Al-Nb$ system. Additionally, it appeared that substitution of some vanadium for niobium would be desirable as it would result in a lighter alloy due to the difference in density between vanadium and niobium. An additional benefit could be in a lower cost alloy since $Ti-V$ alloys are more readily available in master alloy form. Based on a wide-ranging alloy development program conducted during these earlier studies, it was concluded that the optimum composition range was 25* percent aluminum, 10-12 percent niobium and 2-4 percent vanadium.

Since none of the more ductile $Ti-Al-Nb-V$ compositions have met the desired goal of achieving tensile properties of beta processed $Ti-6Al-2Sn-4Zr-2Mo$ combined with the stress-rupture strength of Inconel 713C⁽⁴⁾, additional modification was needed. The effect of substituting molybdenum, a more potent beta stabilizer, for some vanadium was investigated in this program. Procedures for the melting of Ti_3Al compositions have been developed to the extent that large ingots, weighing 245 kg (700 pounds) have been routinely produced with no cracking or macrosegregation problems.

*All compositions are in atomic % unless otherwise stated.

While heat treatment of Ti_3Al base alloys can be used to produce quite large variations in properties, the best ductility at low temperatures and the best creep-rupture capability is produced by a beta solution treatment. The cooling rate from the beta phase field has also been shown to be of crucial importance. By controlling the rate to give a fine Widmanstatten structure, the best property balance is achieved. In addition, molten salt quenching (and holding) at 815C (1500F) has been utilized to obtain the required structures⁽⁴⁾.

For the alloy characterization effort, an isothermally forged pancake was procured. Secondary studies included evaluation of sheet material and forging of a compressor blade component.

4. ALLOY AND PROCESS SELECTION - GAMMA ALLOYS

Recent TiAl alloy studies have concentrated almost exclusively on the Ti-48Al-1V composition and minor modifications of this base. Vanadium has been shown to improve intermediate temperature ductility but does not seem to have significant effect on room temperature ductility or stress-rupture properties. Additions of 0.1-0.2% carbon have been found to be extremely potent in raising the creep-rupture capability of Ti-48Al-1V by as much as a factor of 6:1 at 0.2% C. Unfortunately, the higher carbon level causes some loss in room temperature ductility. While maintaining the Ti-48Al-1V-.1C alloy as the basic gamma composition, it was decided to investigate some slight modifications, i.e. lowering the aluminum content by 1% to improve tensile strength and adding additional vanadium and molybdenum to lower the beta transus and thus increase the variety of structures that can be produced.

Melting and processing options for large ingots of TiAl alloys are more restricted than for Ti_3Al , but fair success has been achieved in the past 1-2 years. Although some segregation and porosity problems exist in ingots, major cracking problems appear to be solved. Isothermal forging remains the single practice for successfully producing TiAl parts from ingots, although recent evidence indicates that extrusion may become a viable process.

Heat treatment effects in gamma alloys have only become clear over the last two years⁽³⁾. Prior to that, most development in the laboratory had been conducted using as-forged material to screen the large number of compositions produced. Documentation of the microstructural changes observed has been previously reported for the Ti-48Al-1V system solution treated over the range of 982-1425C (1800-2600F)⁽⁴⁾.

After forging to produce a recrystallized structure, material heat treated in the temperature range 982-1260C (1800-2300F) exhibits microstructures that are predominantly equiaxed gamma phase with a small amount of isolated alpha-two phase particles. The alpha-two becomes more readily observable as the grain size coarsens. The average grain size increases from an average diameter of 2.7×10^{-4} mm to 1.25×10^{-1} mm over this range. From 1315-1370C (2400-2500F), the appearance changes because the beta phase, present at the solution temperature, transforms during cooling. This produces a lamellar structure of γ and α_2 in these grains. At 1425C (2600F) and above, the beta transus is exceeded and the resulting gamma/alpha-two microstructure is fully lamellar upon cooling. The addition of carbon or changing the relative amounts of aluminum or beta stabilizers such as vanadium or molybdenum will have an effect on the beta transformation temperatures of alloys. These elements will influence the temperature of phase transitions but not their nature, at least for low concentrations.

Based on previously reported test data⁽⁴⁾ and other internally generated results, it had been concluded that a microstructure consisting of about 30 percent of the transformed (lamellar) phase gives the best balance of properties, i.e. high temperature creep resistance with acceptable tensile strength and ductility. A fully acicular microstructure exhibits the best creep resistance but very low RT and 260C (500F) tensile ductility, while a coarse equiaxed gamma/alpha-two structure has relatively low tensile strength and creep resistance with only a small improvement in tensile ductility.

The TiAl ingots were isothermally forged into pancake shapes to provide the majority of test material. A limited number of cast and cast + hot isostatically pressed components were also produced. This latter effort was coordinated with a current ManTech program (F33615-79-C-2091) in which TiAl alloy castings will be produced by Howmet, Ti-Cast Division.

Recognizing that the manufacture of any component requires certain metal removal or surface finishing operations, an evaluation of the machinability of the aluminide alloys using several common machining methods was conducted. Methods evaluated included turning, grinding and milling. Since methods for these types of processing had already been established for the Ti_3Al type alloys⁽⁹⁾, the current effort concentrated on the $TiAl$ alloy. Parametric studies were conducted, resulting in recommendations for the most effective ways of machining this class of materials. Evaluation consisted of metallographic cross-section examinations of samples in both the as-machined and service-exposed conditions and were used to define the parameters that result in no surface damage. Surface improvement methods, such as peening, were also included in this study.

SECTION III
EXPERIMENTAL DETAILS

1. TASK I - MATERIAL PROCUREMENT AND PROCESSING

a. Large Ingots and Forgings

Four gamma alloy compositions and one alpha-two alloy were selected for use in this program. The ingot stock was double melted, using the vacuum consumable electrode method, by RMI, Niles, Ohio; chemical compositions and other details are given in Table 1. Both top and bottom sections of all ingots were removed for chemistry samples by RMI, causing some light cracking on the cut faces and exposing pipe on the top face (Figure 1). Radiographic examination revealed that the center of the ingots had sound-appearing sections 15-20 cm (6"-8") long. These were removed by abrasive sectioning and lathe turned to true the ends and clean the as-cast surfaces to produce forging multiples (Figure 2). As experience has shown that most of the shrinkage porosity in aluminide ingots is related to the pipe, it was decided not to hot isostatically press the ingots.

All five ingot sections were forged into 4.4 cm (1.75") thick by 35 cm (14") diameter pancakes using the 3000 ton isothermal press at Wyman-Gordon Company, Worcester, Massachusetts. Forging parameters are given in Table 2. The gamma alloy ingots showed varying degrees of edge cracking (Figures 3-6) with the Ti-48Al-1V composition showing the least. The alpha-two composition exhibited essentially no cracking (Figure 7).

The forgings were sectioned into two pieces, and smaller sections from the halves were used for a heat treatment study to determine the beta transus for each composition. These values are given in Table 3. The larger sections were heat treated as follows:

- alpha-two: 1150C (2100F)/1/salt quench to 815C (1500F)/.5 air cool
- gamma: beta-24C (beta-75F)/1 hour/argon cool

Physical and mechanical property specimens were machined from the heat treated sections for Task II testing. Specimen configurations are shown in Figures 8, 9 and 10. All physical (thermal) property testing was performed by Southern Research Institute, Birmingham, Alabama.

TABLE 1

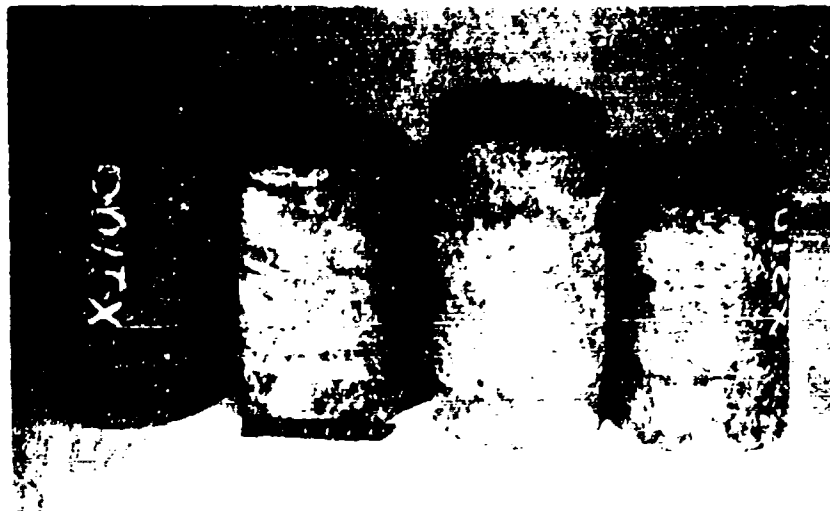
Actual and Aim Compositions in Weight % (Atomic %) of Titanium Aluminide Ingots Procured for Contract F33615-80-C-5163

Serial Number	Approximate Size, cm (in)		Approx. Weight kg(lb)	Al	Nb	V	Mo	C	O ₂	N ₂	Fe
	Dia.	Length									
21007	20 (8.0)	27 (10.5)	37.2 (82)	aim 14.0(25.0)	20.0(10.0) 19.5	3.2(3.0) 3.2	2.0(1.0) 1.95	-	0.06 max	-	-
				actual* 14.05					0.061		
21008	20 (8.0)	36 (14.25)	45.4 (100)	aim 32.0(47.0)	4.7(2.0) 4.7	2.6(2.0) 2.5	2.4(1.0) 2.3	-	0.06 max	-	-
				actual* 32.7					0.061		
21009	20 (8.0)	32.4 (12.75)	39.1 (86)	aim 33.2(47.0)	-	2.7(2.0) 2.7	-	-	0.06 max	-	-
				actual* 33.9					0.042		
21010	20 (8.0)	29.2 (11.5)	35.5 (78)	aim 33.2(47.0)	-	2.7(2.0) 2.75	-	-	0.06 max	-	-
				actual* 33.9					0.045		
21011	20 (8.0)	31.8 (12.5)	45.4 (100)	aim 34.0(48.0)	-	1.5(1.0) 1.22	-	-	0.06 max	-	-
				actual* 34.2					0.044		

*Average of ingot top and bottom analyses.



a

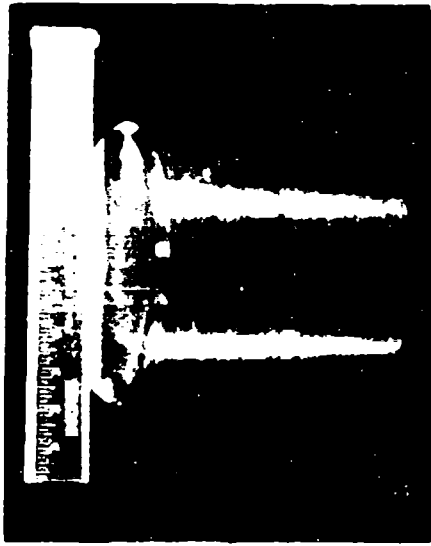


b

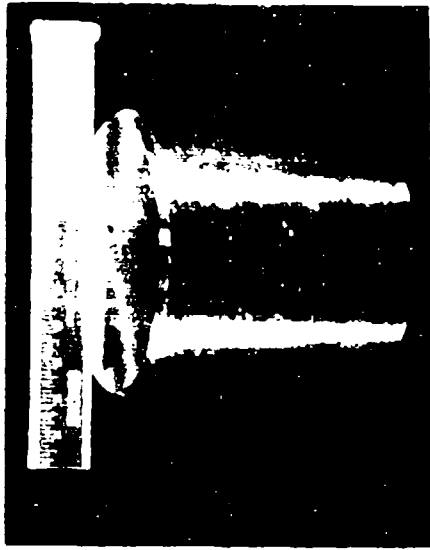
Figure 1. As-received titanium aluminide ingots supplied by RMI. (a) S/N 20007; (b) left to right, S/N 20008, S/N 20009, S/N 20010, S/N 20011.



(a)



(b)



(c)



(d)



(e)

Figure 2. Pancake forging preforms machined from RMI titanium aluminide ingots
a) S/N 2007; b) S/N 2008; c) S/N 2009; d) S/N 2010; e) S/N 2011.
Note fairly extensive porosity on gamma alloy ingots (b-e) compared to
the alpha-two alloy (a).

TABLE 2

Forging Parameters Measured During
Isothermal Pressing of Titanium Aluminide
Alloys for Contract F33615-80-C-5163

<u>Heat</u>	<u>Forging Serial No.</u>	<u>Temperature °C (°F)</u>	<u>Forging Parameters</u>		
			<u>Strain Rate cm/cm/sec/(in/in/min)</u>	<u>Breakthrough Pressure, Kg (ton)</u>	<u>Final Pressure, Kg (ton)</u>
21007	18	1120 (2050)	.0017 (.100)	2.63 x 10 ⁵ (290)	4.27 x 10 ⁵ (470)
21008	16	1120 (2050)	.0017 (.100)	9.25 x 10 ⁵ (1018)	1.1 x 10 ⁶ (1217)
21009	17	1120 (2050)	.0017 (.100)	9.81 x 10 ⁵ (1080)	1.31 x 10 ⁶ (1438)
21010	15	1120 (2050)	.0019 (.114)	9.32 x 10 ⁵ (1025)	1.68 x 10 ⁶ (1850)
21011	19	1120 (2050)	.0017 (.100)	8.54 x 10 ⁵ (940)	1.56 x 10 ⁶ (1715)

TABLE 3

Transus Temperatures of the Titanium
Aluminide Alloys for Contract F33615-80-C-5163

<u>Heat</u>	<u>Composition, a/o</u>	<u>Beta Transus Range, °C (°F)</u>	<u>Forging S/N</u>
21007	Ti-25Al-10Nb-3V-1Mo	1065-1093 (1950-2000)	18
21008	Ti-47Al-2Nb-2V-1Mo	1204-1230 (2200-2250)	16
21009	Ti-47Al-2V	1204-1230 (2200-2250)	17
21010	Ti-47Al-2V-.1C	1260-1290 (2300-2350)	15
21011	Ti-48Al-1V-.1C	1315-1340 (2400-2450)	19

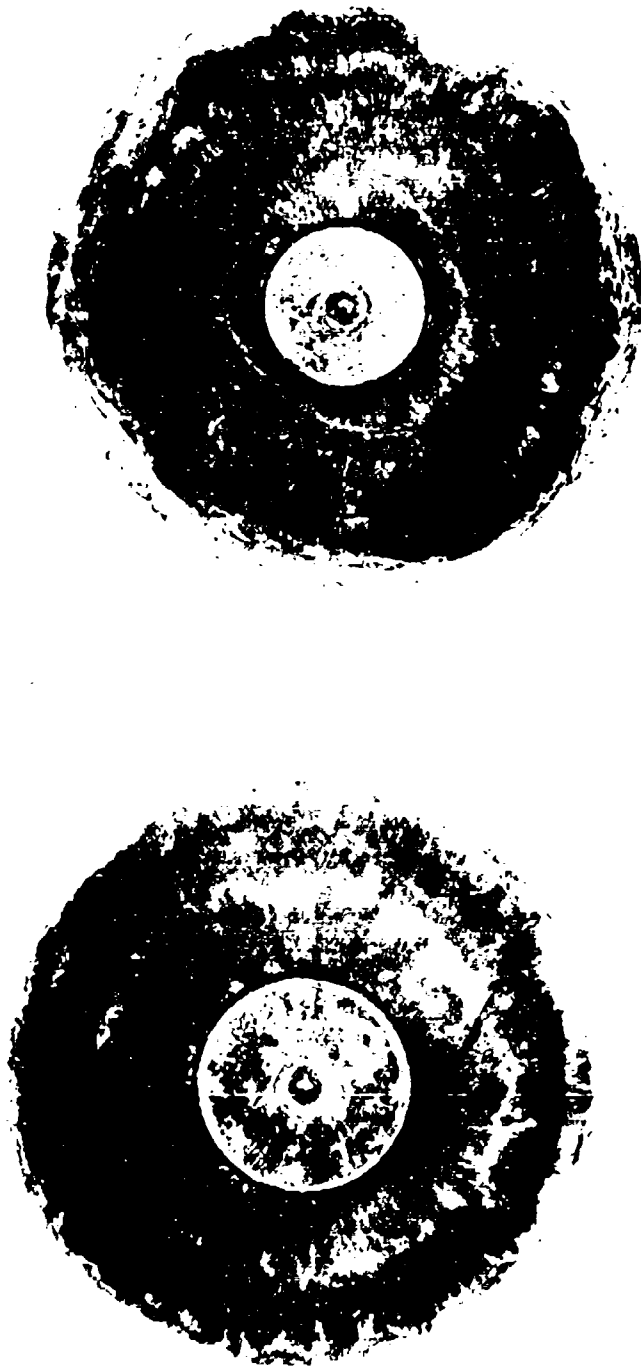


Figure 3. Top and bottom views of as-forged Ti-47Al-2V-2Nb-1Mo alloy pancake.

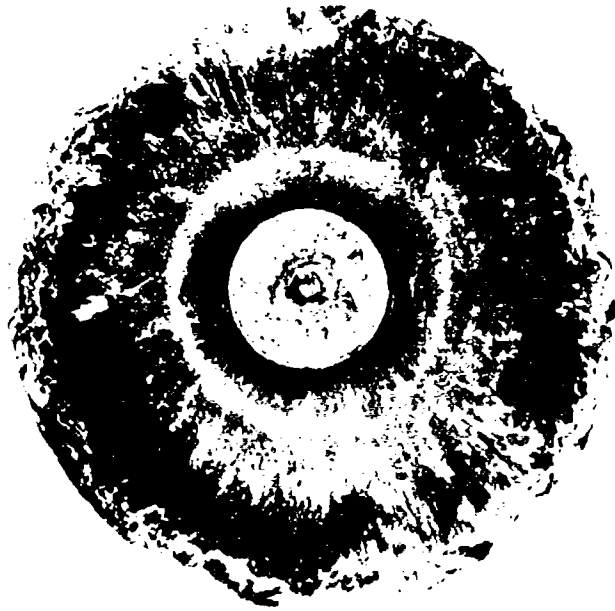


Figure 4. Top and bottom views of as-forged Ti-47Al-2V alloy pancake.

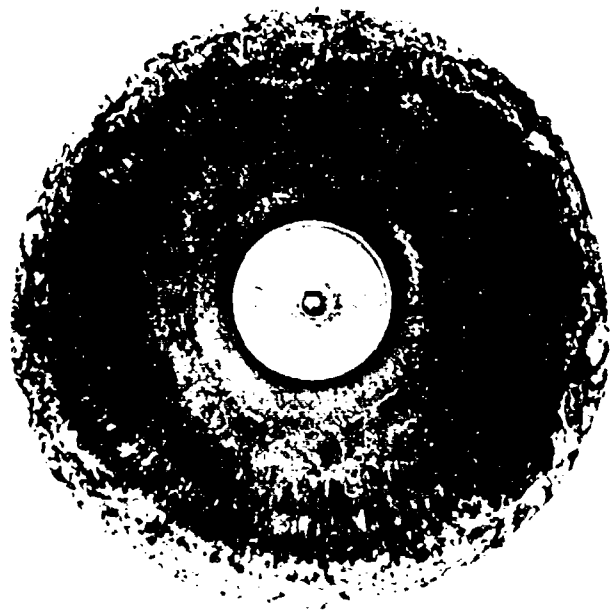


Figure 5. Top and bottom views of as-forged Ti-4Al-2V-.1C pancake.

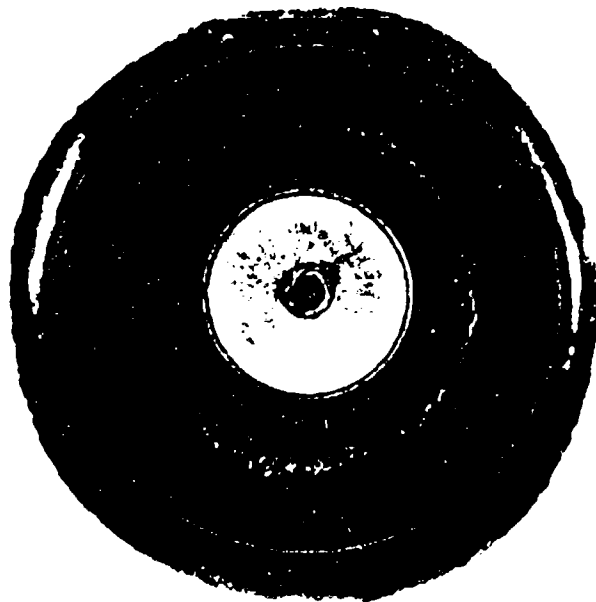
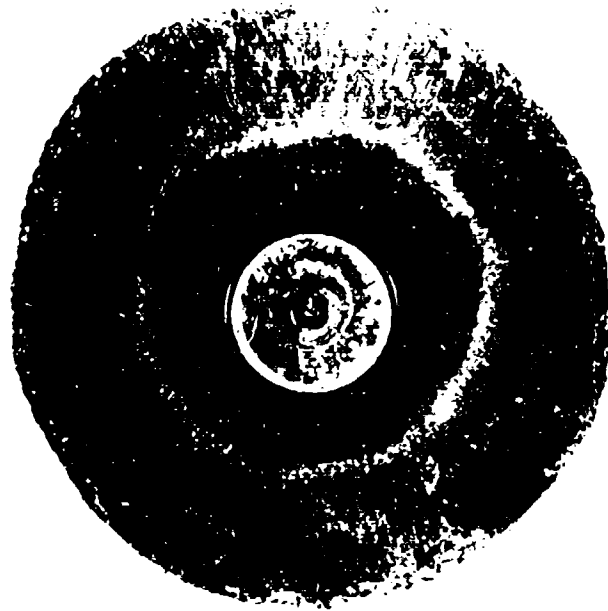


Figure 6. Top and bottom views of as-forged Ti-48Al-1V-.1C alloy pancake. Note better die fill and less cracking.



Figure 7. Top and bottom views of as-forged Ti-25Al-10Nb-3V-1Mo alloy pancake.

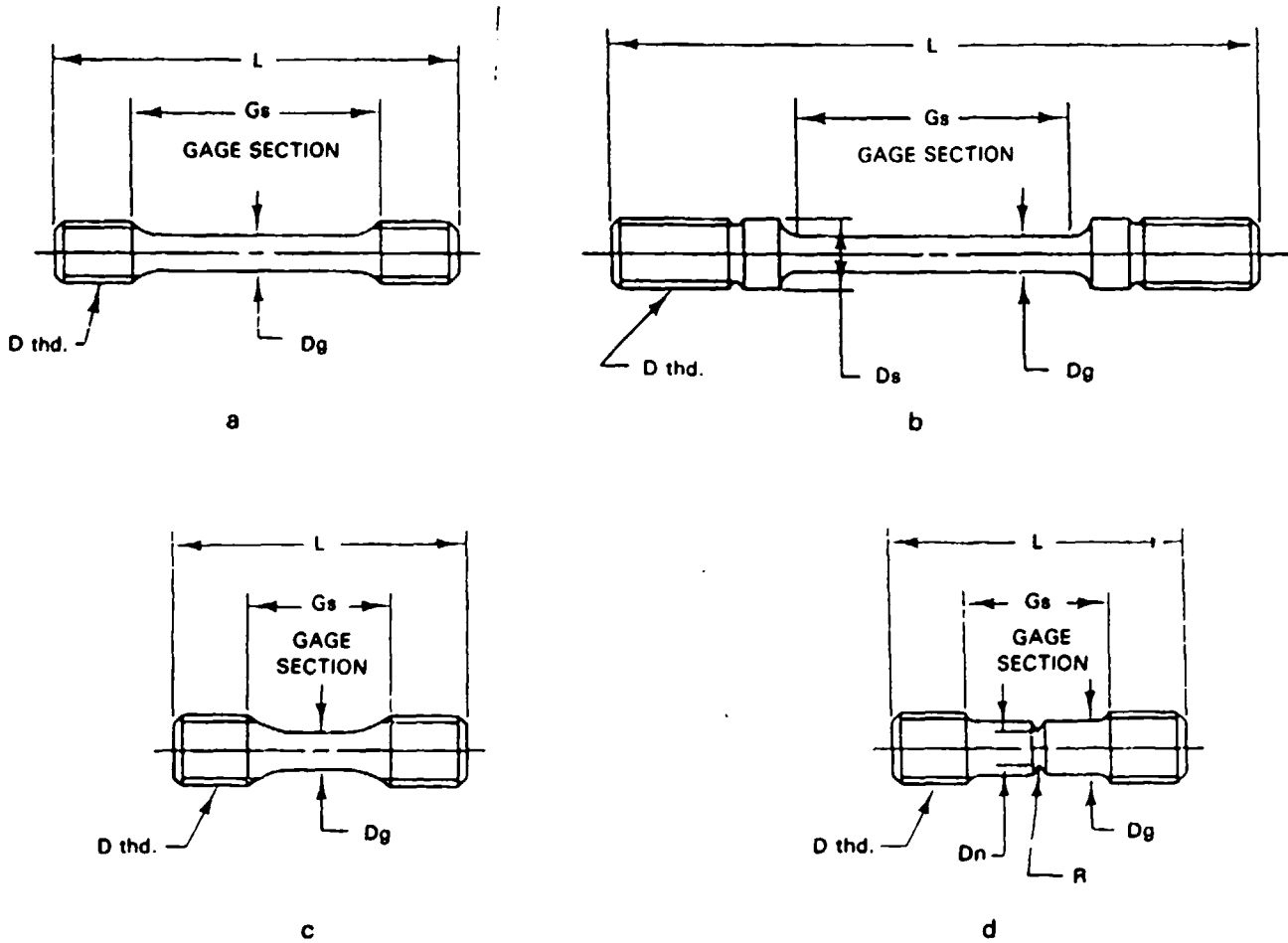


Fig.	Specimen Type	Specimen Dimensions, mm (in.)					
		L	GS	DS	DG	DN	φ Thd.**
a	Tensile	71.1(2.80)	43.2(1.70)	—	6.4(.250)	—	.4375 × 14
b	Creep	76.5(3.010)	25.4(1.00)	6.2(.242)	3.2(.125)	—	.250 × 28
c	Smooth LCF	60.8(2.00)	24.8(.970)	—	6.4(.250)	—	.5 × 20
d	Notched LCF* (Kt = 2.0)	60.8(2.00)	24.8(.970)	—	9.1(.357)	6.4(.250)	.5 × 20

*Notch radius .92 mm (.0365")
 ** All threads UNJF/inches

Figure 8 Specimens used to measure tensile, creep and low cycle fatigue capability of titanium aluminide alloys

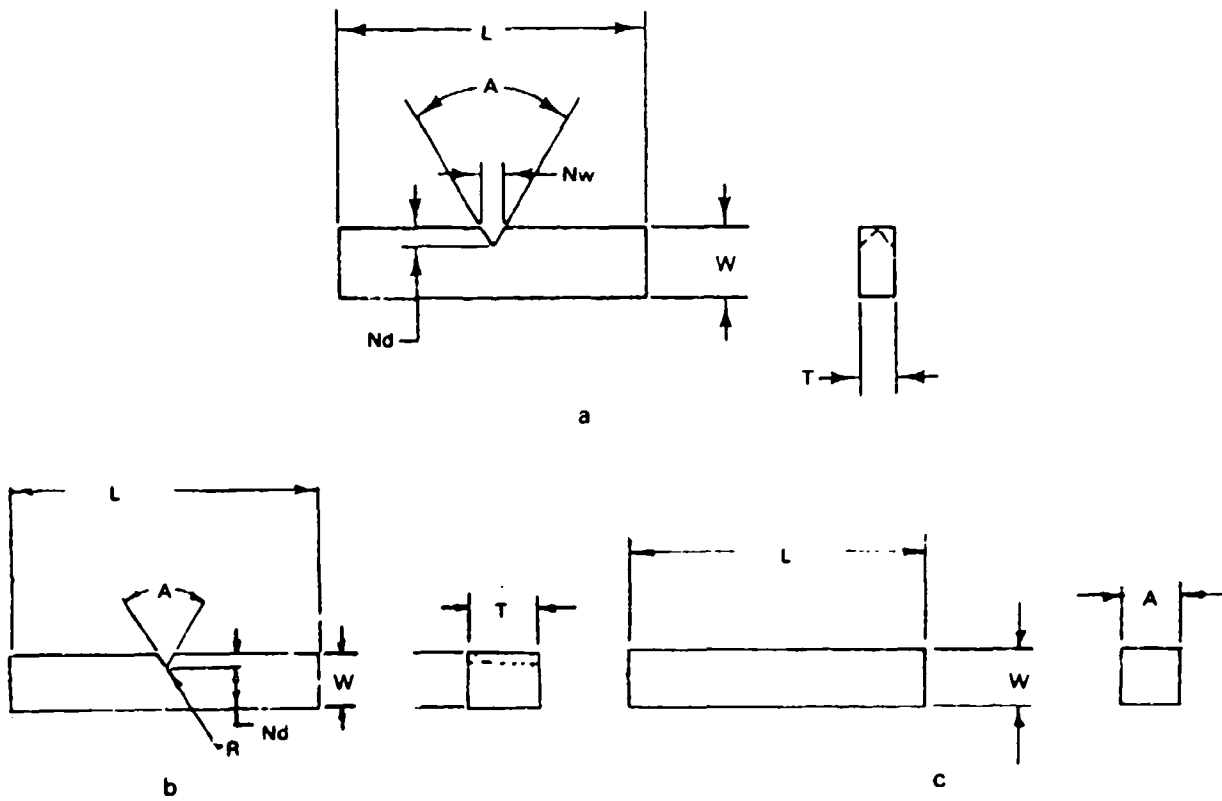


Fig.	Specimen Type	Specimen Dimensions, mm (in.)						
		<u>L</u>	<u>W</u>	<u>Nw</u>	<u>Nd</u>	<u>A</u>	<u>T</u>	<u>R</u>
a	Fracture Toughness	55.1(2.17)	12.7(.5)	3.5(.139)	3.05(.120)	60°	6.4(.210)	-
b	Notched Impact	55(2.165)	10(.394)	3.5(.139)	2.0(.080)	60°	10(.394)	.25(.01)
c	Smooth Impact	55(2.165)	10(.394)	-	-	-	10(.394)	-

Figure 9 Specimens used for impact and fracture toughness evaluation of titanium aluminide alloys

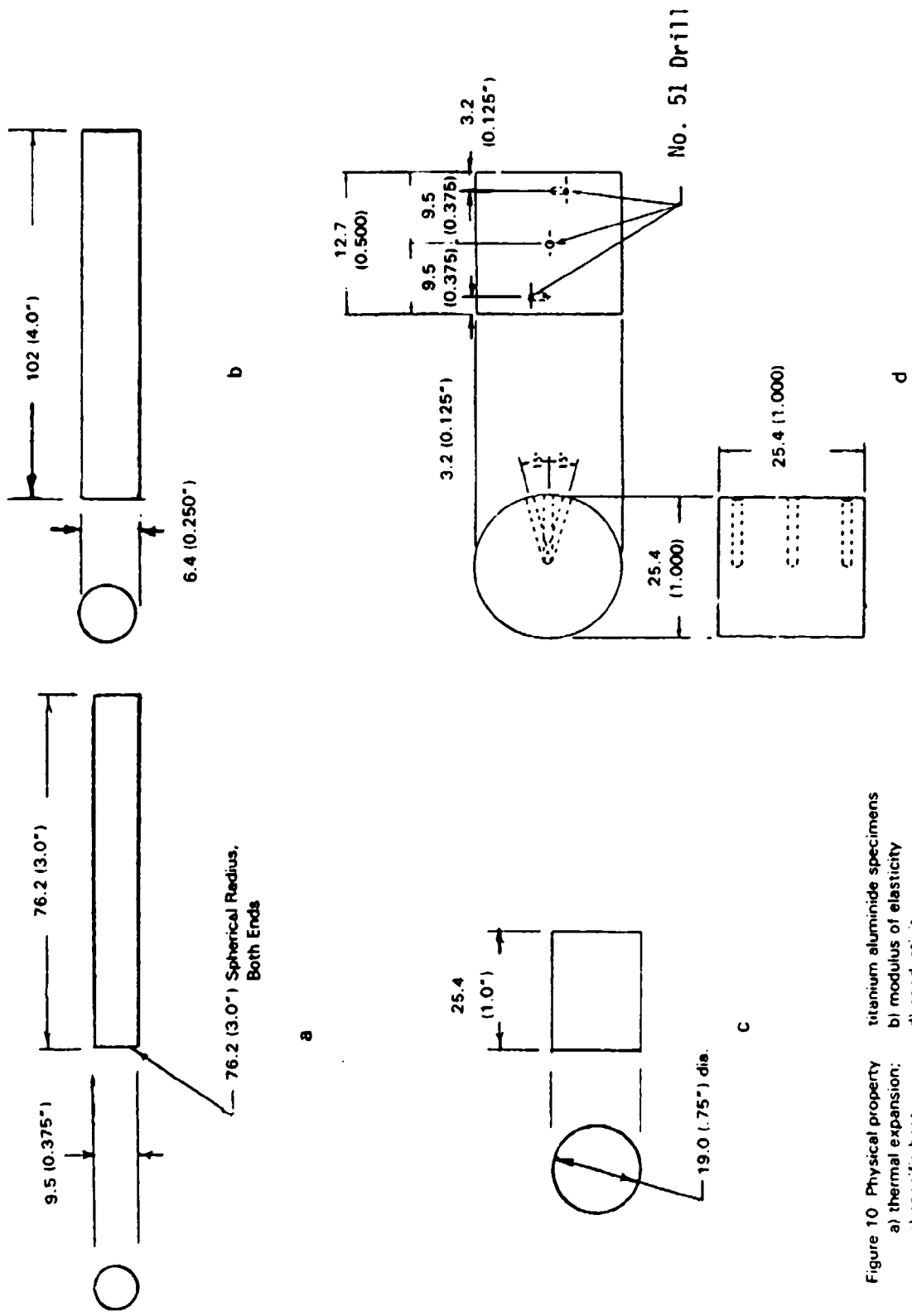


Figure 10 Physical property titanium aluminate specimens
 a) thermal expansion; b) modulus of elasticity
 c) specific heat; d) conductivity
 Dimensions in mm (in.)

SECTION IV
RESULTS AND DISCUSSION

1. INTRODUCTION

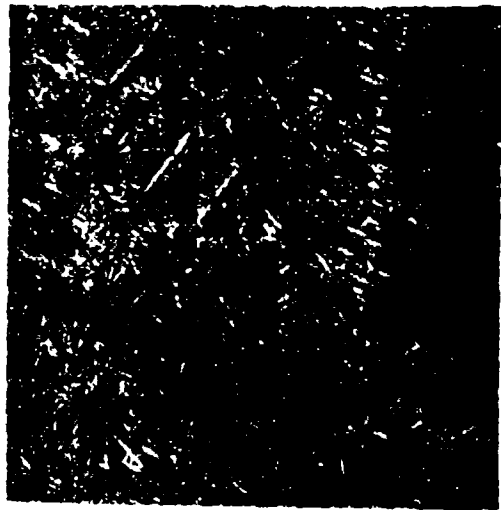
This section will be divided into three major subsections to facilitate discussion. The first two sections will present alloy characterization data for alpha-two and gamma alloys, respectively. A third section describes the various processing, machining and component fabrication trials.

2. MATERIAL CHARACTERIZATION - ALPHA-TWO ALLOY

Since there was only one alpha-two alloy composition, no screening tests were necessary. Metallographic examination of a radial section of the forging revealed a structure of predominantly equiaxed grains with an average grain size about 1.5 mm x 2.5 mm (0.060" x 0.100"). The extreme periphery and a banded region about mid-radius consisted of elongated grains about 2.5 mm x 7.5 mm (0.100" x 0.300"). The microstructure within the grains was uniform in all areas and consisted of a Widmanstatten array of fine beta/alpha-two platelets (Figure 11). This was the aim microstructure and this forging is the thickest to date in which the fine structure was achieved throughout the section due to the isothermal transformation in the salt bath (Section III).

Tensile properties are given in Table 4. It can be seen that strength is good for a large forging at and above 260C (500F) and equals or exceeds the properties of beta processed Ti-6Al-2Sn-4Zr-2Mo. The room temperature ductility is not as high as desired, but in view of the high strength, could be considered acceptable.

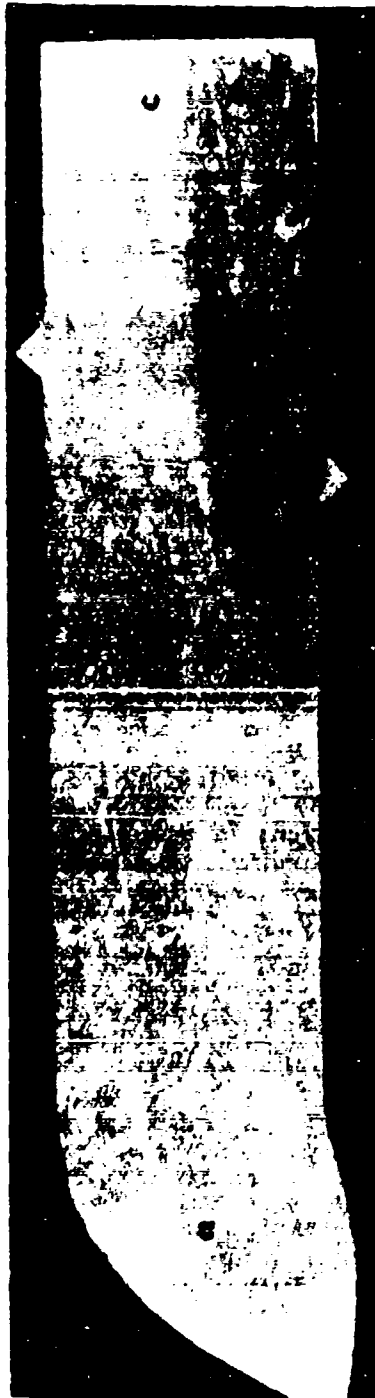
Creep-rupture tests were conducted at 650C/372 MPa (1200F/55 ksi) and 593C/413 MPa (1100F/60 ksi). Times to various elongations and rupture are given in Table 5. The 650C/372 MPa (1200F/55 ksi) condition has been a standard comparison point throughout the alpha-two studies in the past, and the goal was to achieve a minimum of 100 hours to rupture. Most potentially useful Ti-Al-Nb-(V) alloys previously studied have not met this goal. The two specimens tested at the above conditions exhibited rupture lives of 222 hours and >501 hours (extrapolation predicted 620 hours).



a

b

c



d

a) ~IX
Mag: b, c, d) 500X

Figure 11. Macro and microstructure of the forged and heat treated Ti-25Al-10Nb-3V-1Mo pancake forging (a). The rim, mid-radius and center microstructures are in b, c and d, respectively.

TABLE 4Tensile Properties of Isothermally Beta Forged
and Heat Treated Ti-25Al-10Nb-3V-1Mo Alloy

<u>Specimen Number</u>	<u>Test Temp. °C (°F)</u>	<u>0.2% Yield Str. MPa (ksi)</u>	<u>Ult. Tens. Str. MPa (Ksi)</u>	<u>%EL</u>	<u>%RA</u>
2588	RT	825 (119.7)	1047 (151.0)	2.2	1.7
2590	260 (500)	831 (120.5)	1058 (153.5)	9.2	14.1
2591	427 (800)	729 (105.7)	950 (137.7)	12.1	16.9
2592	538 (1000)	647 (93.8)	967 (140.3)	9.2	13.0
2593	650 (1200)	640 (92.7)	835 (121.1)	9.1	14.3

TABLE 5Creep-Rupture Properties of Isothermally Beta
Forged and Heat Treated Ti-25Al-10Nb-3V-1Mo Alloy

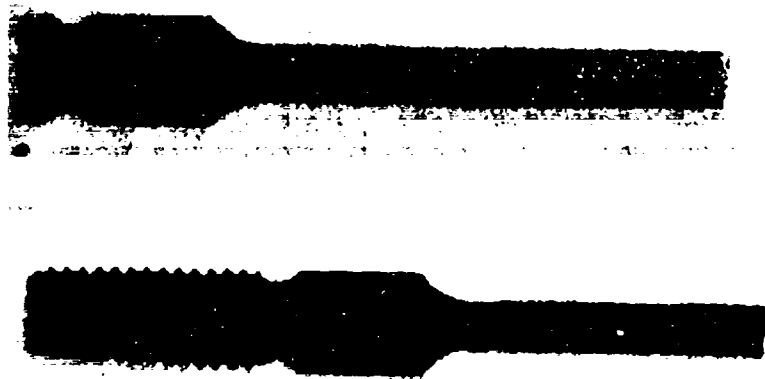
<u>Specimen Number</u>	<u>Test Conditions °C/MPa (°F/ksi)</u>	<u>Time in Hours To</u>			
		<u>0.2% EL</u>	<u>0.5% EL</u>	<u>1.0% EL</u>	<u>Rupture</u>
2594	650/380 (1200/55)	2.8	31.1	184.5	>501.6 ⁽¹⁾
2595	650/380 (1200/55)	1.4	12.0	66.3	222.8
2596	593/413 (1100/60)	27.0	405.6	>501.6	>501.6 ⁽¹⁾

(1) Test terminated, did not rupture.

A metallographic examination of the two specimens was conducted to determine if an explanation for the scatter could be found. Microstructurally, the specimens were identical, but it was noticed that the longer life specimens had been machined from a coarser, elongated grain region of the forging (Figure 12).

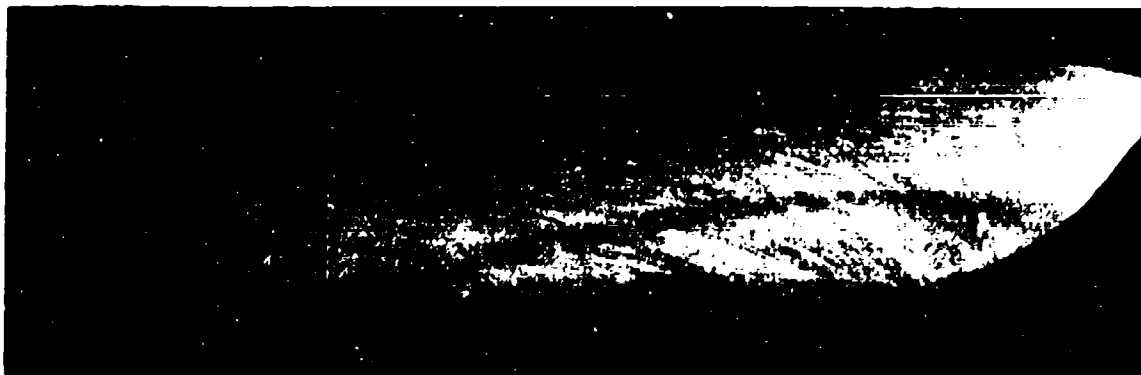
Based on these results, it was now considered that the coarse, non-uniform grain size observed may have contributed to the lower tensile ductility observed, the higher creep-rupture capability and some of the subsequent scatter in other properties. At the outset of the program, it was felt that the nature of the Widmanstatten platelet array was the key microstructural feature affecting properties and as a result, the beta grain size effect was not anticipated and no special effort to control it was made. To determine if the grain size grew during beta annealing, an as-forged radial section was examined. This revealed the presence of extremely elongated grains oriented with the long axis in the radial direction showing the flow pattern resulting from the isothermal forging operation (Figure 13). Comparisons of the two sections showed that many of the elongated grains recrystallized during the beta anneal and formed a wide range of equiaxed grain sizes. However, in certain areas near the edge of the forging, the elongated grains did not recrystallize, and there was little apparent change in structure after the heat treatment.

For comparison, as-forged and heat treated sections of a Ti-25Al-10Nb-4V (V-5810) pancake forging from an earlier study⁽⁴⁾ were re-examined. The heat treatment and forging temperature were identical to this study, but the V-5810 ingot had been redundantly upset and redrawn on a conventional forging press prior to conventionally forging into a slightly smaller pancake configuration on open dies. This additional working broke up the cast structure resulting in a much finer uniform grain size in the as-forged and heat treated condition (Figure 14). It can be concluded that a fine grain, worked structure is not "blown" by subsequent beta annealing of a Ti-Al-Nb-V alloy. In retrospect, it was probably a mistake to isothermally forge the ingot in one step without some previous redundant working.



Mag: 2.5X

Figure 12. Microstructure of various titanium aluminide creep specimens tested at 650C/372 MPa (1200F/55 ksi).
Top - Ti-25Al-10Nb-3V-1Mo est. 620 hours to rupture
Bottom - Ti-25Al-10Nb-3V-1Mo 222 hours to rupture



Mag: 0.7X

Figure 13. Macrostructure of as-forged Ti-25Al-10Nb-3V-1Mo alloy pancake forging. This was forged on isothermal dies at 1120C (2050F) in one step from a cast ingot.



Mag: 0.7X

Figure 14. Macrostructure of Ti-25Al-10Nb-4V pancake forging from a previous program⁽⁴⁾. Top - as-conventionally upset and forged at 1120C (2050F); bottom - heat treated 1150C (2100F)/1/ + salt quench to 815C (1500F)/.5/AC.

The stability of the alloy was evaluated by exposing machined tensile and creep-rupture specimens for 500 hours at 565C (1050F) + 100 hours at 675C (1250F) in air. Post-exposure tensile and creep properties are given in Tables 6 and 7. Creep life showed a significant increase, but RT and 260C (500F) tensile specimens failed in the threads at low loads, indicating that notch brittleness had been increased by the treatment. At 427C (800F) and above, specimens failed in the gage, but the ultimate strength and ductility were considerably lower than the unexposed specimens. Yield strength after exposure was about 140 MPa (20 ksi) higher at the 538C and 650C (1000F and 1200F) temperatures indicating that some metallurgical changes had occurred. Additional evaluation of the tensile specimens revealed:

- Hardness of the exposed specimens was about 40-100 DPH points higher than comparable baseline specimens after exposure (Figure 15).
- A hardened alpha case type surface layer about 0.02 mm (0.001") thick was formed (Figure 16).
- Optical examination of the fracture surfaces of exposed and unexposed specimens revealed cleavage across entire beta grains in exposed specimens (Figure 17a, c). At higher magnification using the SEM, surfaces of exposed and unexposed specimens appeared virtually identical (Figure 17b, d). No cleavage was apparent, but rather a semi-ductile tearing, not unlike conventional titanium alloy specimens with similar microstructures.

In an attempt to gain further insight into the reasons for the changes in properties observed after exposure, a limited transmission microscopy study was undertaken. Thin foils were prepared from the gage section of unexposed and exposed tensile specimens for examination. The fineness of the structure was something of a problem in obtaining definitive diffraction contrast and selected area analysis. It was also clear that more background work on the system would have been of considerable assistance in the present study in distinguishing between various features observed.

The general structure of the material in both conditions is rather similar to a conventional alpha beta titanium alloy in the beta processed condition. Figures 18a and 18b show the general features of phase arrangement, plates of the ordered alpha-two phase being enclosed by envelopes of the beta phase. We may also note that only a few plates have a common orientation in a given

TABLE 6

Effect of Thermal Exposure⁽¹⁾ on Tensile
Properties of Isothermally Beta Forged
and Heat Treated Ti-25Al-10Nb-3V-1Mo Alloy

<u>Specimen Number</u>	<u>Test Temp. °C (°F)</u>	<u>0.2% Yield Str. MPa (ksi)</u>	<u>Ultimate Tens. Str. MPa (ksi)</u>	<u>%Elongation</u>	<u>%Reduction of Area</u>
2933	RT	-	555 (80.5)	Thread Failure	-
2934	RT	-	445 (64.5)	Thread Failure	-
2935	260 (500)	-	483 (70.0)	Thread Failure	-
2936	427 (800)	827 (120.0)	857 (124.3)	6.9	7.4
2937	538 (1000)	826 (119.8)	842 (122.1)	4.6	9.2
2938	650 (1200)	838 (121.6)	860 (124.8)	1.4	-

TABLE 7

Effect of Thermal Exposure⁽¹⁾ on Creep-Rupture
Properties of Isothermally Beta Forged and
Heat Treated Ti-25Al-10Nb-3V-1Mo Alloy

<u>Specimen Number</u>	<u>Test Conditions °C/MPa (°F/ksi)</u>	<u>Time in Hours To</u>			
		<u>0.2% EL</u>	<u>0.5% EL</u>	<u>1.0% EL</u>	<u>Rupture</u>
2930	650/380 (1200/55)	15.1	128.1	450.1	> 503.9 ⁽²⁾
2931	650/380 (1200/55)	22.3	168.9	540.0 ⁽³⁾	> 500.1 ⁽²⁾
2932	650/414 (1200/60)	10.5	82.0	320.0	> 506.1 ⁽²⁾

(1) Exposure conditions: 565C (1050F)/500 hours + 675C (1250F)/100 hours

(2) Test terminated, did not rupture

(3) Extrapolated

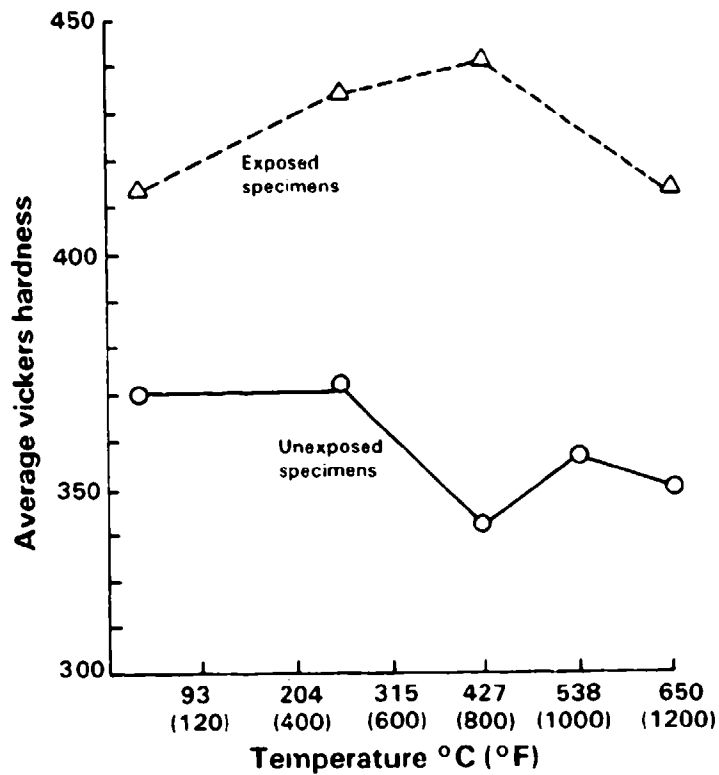


Figure 15. Effect of thermal exposure on hardness of Ti-25Al-10Nb-3V-1Mo tensile specimens.

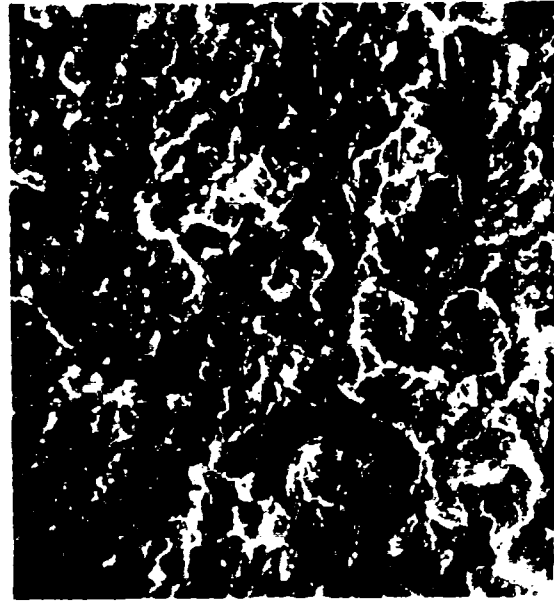


Mag: 500X

Figure 16. Surface of exposed Ti-25Al-10Nb-3V-1Mo alloy tensile specimen showing alpha case contamination (brackets) which has a hardness DPH 700-800.



a



b



c



d

Mag: a) 12.5X; b) 600X
b) 7.5X; d) 400X

Figure 17. SEM fractographs of tested Ti-25Al-10Nb-3V-1Mo tensile specimens. a, b) specimen 2594, not exposed; c, d) specimen 2933 exposed. Note thread failure and brittle-appearing cleavage facets in this specimen. At high magnification, the fracture mode is similar.



Figure 18. General microstructure of Ti-25Al-10Nb-3V-1Mo alloy thin foils cut from tensile specimens. a) specimen 2594, not exposed; b) specimen 2933, exposed.

area so that the coupled growth that would lead to a colony structure is restricted. The general darkening of the beta phase in the exposed specimen can also be seen but is illustrated more clearly in Figures 19a and 19b. The beta phase in the unexposed material tends to occur as rather featureless single phase lathes. After exposure, precipitation of a second phase in the form of thin plates occurs within the beta phase. Attempts to find any changes in the alpha two phase did not reveal any obvious features that differed between the two conditions but rather complex dislocation structures were evident in this phase after either treatment. The local chemical compositions of the phases were also evaluated using the EDAX system and the results for the alpha and beta phases in the unexposed sample are shown in Figure 20. The enrichment of the alpha two phase in aluminum and the beta phase in niobium and vanadium is as expected, paralleling the partitioning in conventional alpha beta alloys. No change in phase composition was observed after exposure.

It is concluded on the basis of these observations that the increase in yield strength is due to the formation of a precipitate within the beta phase. The exact nature of this phase was not established, but it would be anticipated that an (ordered?) alpha phase would form. Specific reasons for the marked reduction in tensile ductility are also not clearly understood but are consistent with the tendency to poor ductility at higher strength levels, and the coarse grain size of the alloy no doubt exacerbated this tendency. To reduce or eliminate this problem, a process cycle is needed that not only produces a fine grain size but also yields a beta phase that is stable at the exposure/service temperature.

Impact tests were initially planned for RT, 150C (300F), 260C (500F), 427C (800F), 538C (1000F) and 650C (1200F) on smooth bar specimens. However, in view of the relatively high impact strength at the lower temperatures, it was decided to notch the remaining three bars and repeat the tests. Smooth impact strength increased threefold between 150C (300F) and 260C (500F) indicating that a ductile-brittle transition point lay between these temperatures (Table 8). The notch sensitivity of the alloy was plainly apparent from this

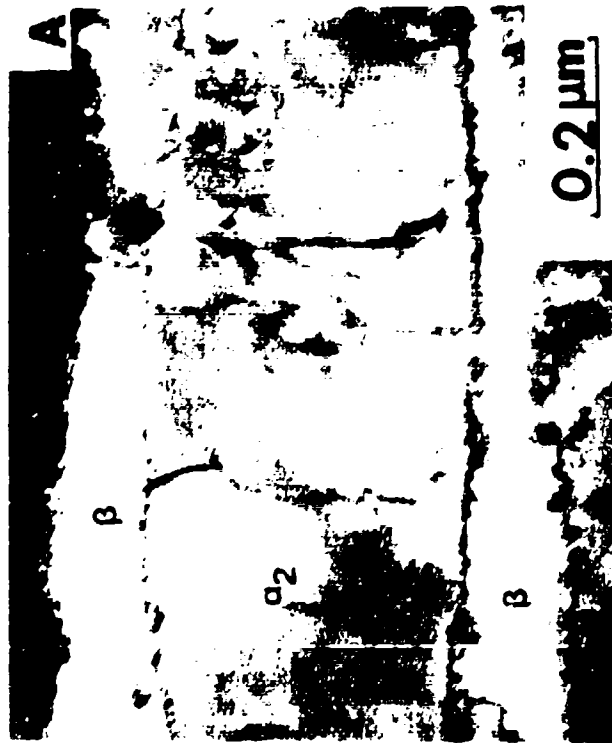


Figure 19. Enlarged view of Figure 18 showing the relatively "clean" beta phase in the unexposed Ti-25Al-10Nb-3V-1Mo specimen 2588 (a) and the darkened beta phase with heavy precipitation after exposure in specimen 2933 (b).

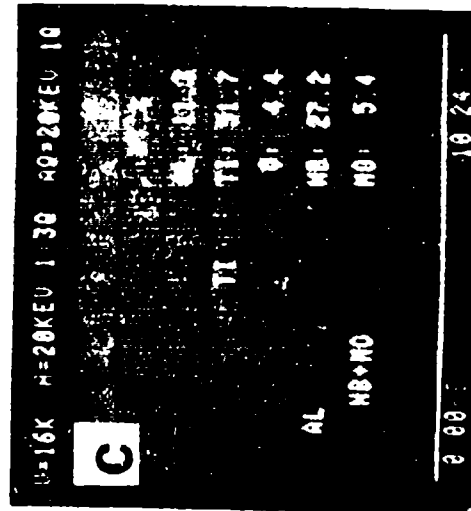
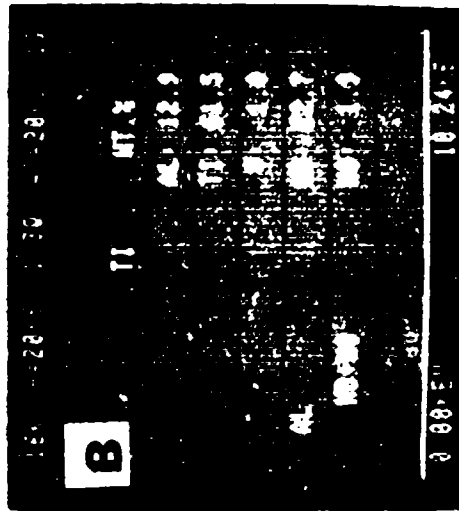


Figure 20. General microstructure of the unexposed Ti-25Al-10Nb-3V-1Mo tensile specimen 2588 showing spectrum and composition of alpha- two phase (b) and beta phase (c).

second set of impact results. Notched values ranged from 2.2-3.2 Joules (1.6-2.4 ft.-lbs.) over the range compared to 28.5-139.0 Joules (21-102.5 ft.-lbs.) for smooth. These values indicate that the alloy is quite notch brittle. But fracture toughness tests, performed over the temperature range of RT-427C (800F) in three point bending, showed numbers ranging from 13.5 MPa \sqrt{m} (12.3 ksi \sqrt{in}) to 49.0 MPa \sqrt{m} (44.5 ksi \sqrt{in}) (Table 9). These data seem to indicate a lesser degree of notch sensitivity than the impact results.

Smooth low cycle fatigue test specimens were run in axial tension-release loading at a frequency of 1 Hertz (60 cpm) and R = 0.1. Originally, it was planned to run five specimens at 260C (500F) and five at 650C (1200F). The first three specimens run at 260C (500F) failed in the threads even though peening of threads was instituted after the first failure. Subsequent specimens were tested at 650C (1200F), and prior to running, the gage diameter was reduced from 6.4 mm (0.25") to 5.1 mm (0.20"). Specimens which exceeded 10^5 cycles were uploaded to a higher stress to cause failure. The 650C (1200F) test data are given in Table 10 and shown graphically in Figure 21. The data form a fairly smooth curve with a 10^5 cycle stress capability of 634 MPa (92 ksi).

In view of the thread fractures encountered with the smooth specimens at 260C (500F), it was decided to initiate testing of the notched ($K_t = 2.0$) specimens at 650C (1200F). Due to the large variability of lives, additional check tests were performed which resulted in all specimens but one being utilized. The large amount of scatter encountered was disturbing, and metallographic examination of all specimens was conducted to identify reasons for the scatter. Grain size was shown to be a major contributor, and if the data are plotted as a function of this parameter, the relationship shown in Figure 22 is obtained. It can be seen that there is at least a 35 MPa (5 ksi) difference in the 10^5 cycle runout stress between equiaxed and coarse elongated grain specimens. Also, the notched runout stress is about 175-210 MPa (25-30 ksi) lower than smooth at 650C (1200F). An example of the extremes in grain size and the resultant effect on fatigue life is shown in Figure 23. The one remaining specimen tested at 260C (500F) showed reasonable life but failed in the threads.

TABLE 8

Smooth and Notched Charpy Impact Strength
of Isothermally Beta Forged and Heat
Treated Ti-25Al-10Nb-3V-1Mo Alloy

<u>Specimen Number</u>	<u>Specimen Type</u>	<u>Test Temp. °C (°F)</u>	<u>Impact Strength Joule (ft-lbs)</u>
2603	Smooth	RT	28.5 (21.0)
2604	↓	149 (300)	50.1 (37.0)
2605		260 (500)	139.0 (102.5)
2606	Notched	RT	2.2 (1.6)
2607	↓	149 (300)	3.1 (2.3)
2608		260 (500)	3.2 (2.4)

TABLE 9

Fracture Toughness of Isothermally Beta
Forged and Heat Treated Ti-25Al-10Nb-3V-1Mo
Precracked Slow Bend Specimens

<u>Specimen Number</u>	<u>Test Temp. °C (°F)</u>	<u>K_{1C}</u>	
		<u>MPa√m</u>	<u>ksi√in.</u>
2828	RT	13.5	12.3
2829	149 (300)	17.0	15.4
2830	260 (500)	18.0	16.4
2832	315 (600)	31.0	30.1
2831	427 (800)	49.0	44.5

TABLE 10

Smooth Low Cycle Fatigue Properties
of Isothermally Beta Forged and
Heat Treated Ti-25Al-10Nb-3V-1Mo Alloy

Specimen Number	Test Temp. °C (°F)	Stress Range MPa (ksi)	Cycles to Rupture
2683	260 (500)	0-620 (0-90)	81,900 (THDS)
2684	260 (500)	0-689 (0-100)	30,500 (THDS)
2685	650 (1200)	0-730 (0-106)	18,800
2686	260 (500)	0-689 (0-100)	5,900 (THDS)
2687	650 (1200)	0-448 (0-65)	>136,700
	650 (1200)	0-668 (0-97)	20,000
2688 ⁽¹⁾	650 (1200)	0-551 (0-80)	600 (THDS)
2689 ⁽¹⁾	650 (1200)	0-551 (0-80)	4,100 (THDS)
2690	650 (1200)	0-875 (0-127)	600
2691	650 (1200)	0-758 (0-110)	900
2692	650 (1200)	0-606 (0-88)	>122,000
		0-655 (0-95)	11,500

(1) Points not plotted in Figure 21 as failure was due to flaws in threads.

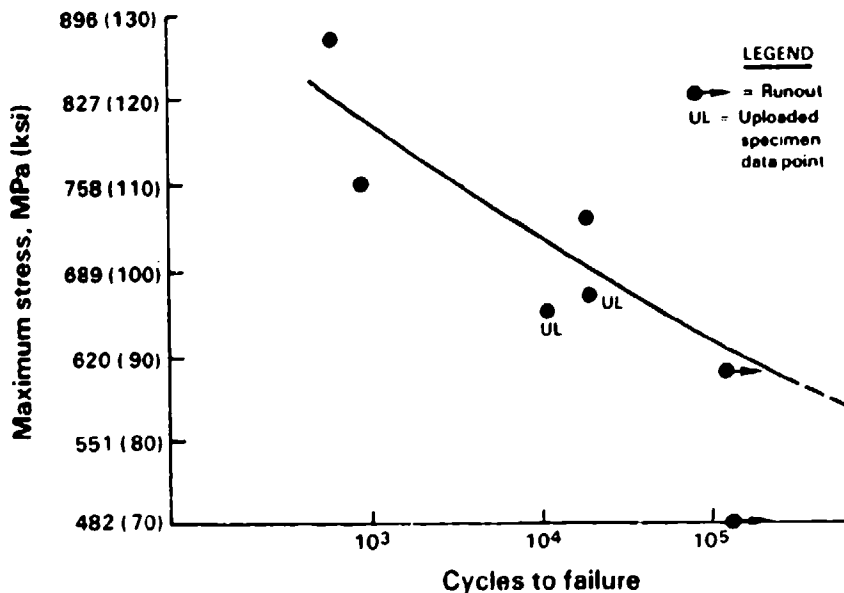


Figure 21. S/N curve for smooth Ti-25Al-10Nb-3V-1Mo alloy specimens tested at 650C (1200F).

TABLE 11

Notched ($K_t = 2.0$) Low Cycle Fatigue
 Properties of Isothermally Beta
 Forged and Heat Treated Ti-25Al-10Nb-3V-1Mo Alloy

Specimen Number	Test Temp. °F (°C)	Nominal Stress Range, MPa (ksi)	Cycles to Rupture
2693	260 (500)	0-482 (0-70)	55,100 (THD)
2694	650 (1200)	0-413 (0-60)	600
2695	650 (1200)	0-396 (0-57.5)	>130,000
		0-413 (0-60)	14,700
2696	650 (1200)	0-380 (0-55)	>598,000
		0-413 (0-60)	>357,000
		0-448 (0-65)	103,100
2697	650 (1200)	0-396 (0-57.5)	12,600
2698	650 (1200)	0-413 (0-60)	200
2699	650 (1200)	0-276 (0-40)	>101,600
		0-413 (0-60)	600
2700	650 (1200)	0-344 (0-50)	>124,000
		0-448 (0-65)	299,800
2701	650 (1200)	0-380 (0-55)*	>100,400
2702	650 (1200)	0-396 (0-57.5)	>124,000
		0-482 (0-70)	900

*Failed on uploading to 448 MPa (65 ksi).

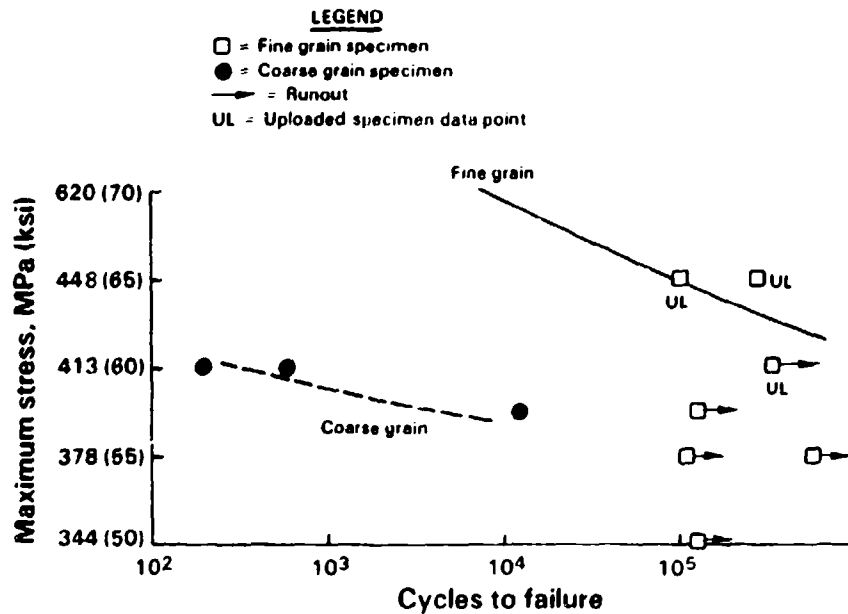
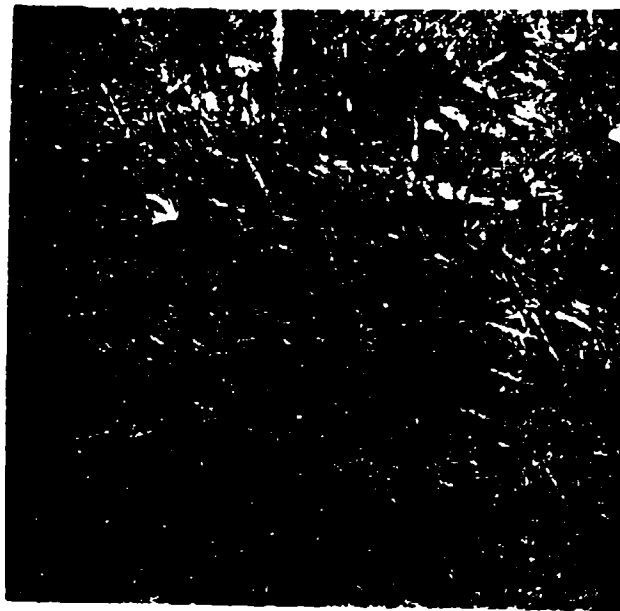


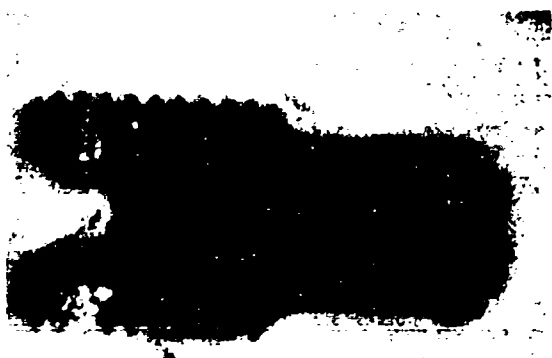
Figure 22. S/N curves for notched Ti-25Al-10Nb-3V-1Mo specimens tested at 650C (1200F) based on grain size measurements.



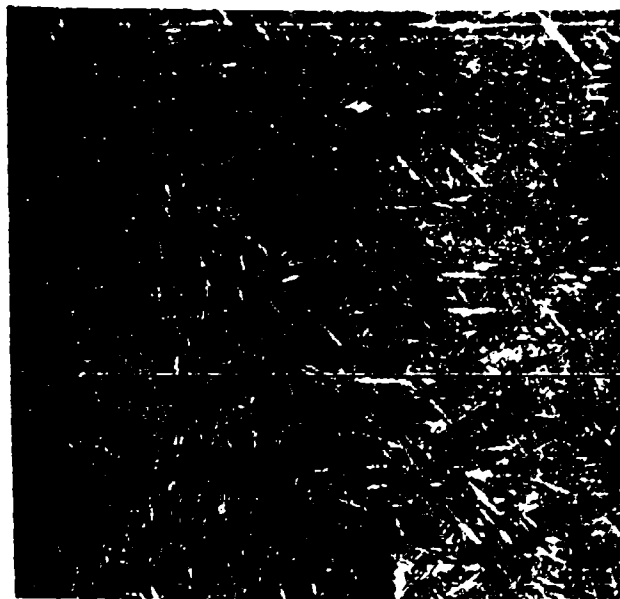
a



b



c



d

Mag: a,c) 2.6X
b,d) 500X

Figure 23. Selected notched Ti-25Al-10Nb-3V-1Mo LCF specimens showing extremes in grain size but similar microstructures. a, b) S/N 2644, 600 cycles to failure at 0-413 MPa/0-60 ksi; c, d) S/N 2696, 100, 300 cycles to failure at the same condition.

Young's modulus of the Ti-25Al-10Nb-3V-1Mo alloy was determined using a rod 100 cm (4") long by 6.4 cm (0.25") diameter tested in a dynamic vibration mode. The data are listed in Table 12 and plotted vs. temperature in Figure 24. The modulus ranged from 12.5×10^6 KPa (18.2×10^6 psi) at room temperature to 111.6×10^6 KPa (16.2×10^6 psi) at 650C (1200F). While the room temperature modulus of this alloy is within the range of most conventional alloys such as Ti-6Al-4V, Ti-8Al-1Mo-1V, etc., it should be noted that the drop in modulus up to 650C (1200F) was much less than any conventional alloy.

The thermal conductivity of the Ti-25Al-10Nb-3V-1Mo alloy was determined using the comparative rod apparatus method. In this method, the specimen is placed between two reference samples of known thermal conductivity. Reference material is selected with thermal conductivity near that of the specimen being evaluated, in this case type 316 stainless steel. Heat flow was induced axially through the reference-specimen-reference stack, and the temperature differences are monitored by thermocouples mounted in small holes drilled in the references and specimen. Once the temperature differences are known, the Fourier conduction rate equation for one-dimensional heat flow was used to solve for the thermal conductivity of the specimen.

The thermal conductivity of the Ti-25Al-10Nb-3V-1Mo alloy was shown to vary linearly as a function of temperature within the range of 68C (154F) to 660C (1220F). The thermal conductivity varied from 7.18 Watt/meter-Kelvin (49.9 Btu-inch/hour-foot²-F) to 13.3 Watt/meter-Kelvin (92.4 Btu-inch/hour-foot²-F). A graph of the thermal conductivity versus temperature is shown in Figure 25. The conductivity of duplicate specimens was well within the five percent tolerance of the comparative rod apparatus.

The specific heat at constant pressure (heat capacity) was measured in an adiabatic calorimeter. In such a device, a heated specimen is dropped into a thermally guarded cup and the temperature rise of the cup monitored. The resulting temperature rise will, by the first law of thermodynamics, define an enthalpy change for the specimen. The enthalpy changes for various initial temperatures of the specimen are, by definition, the specific heat of the material.

TABLE 12

Dynamic Modulus of Isothermally Beta Forged and Heat Treated Ti-25Al-10Nb-3V-1Mo Alloy

Test Temp. °C (°F)	Young's Modulus	
	KPa x 10 ⁶	PSI x 10 ⁶
RT	125.3	18.2
93 (200)	124.0	18.0
204 (400)	121.9	17.7
315 (600)	119.9	17.4
427 (800)	116.4	16.9
538 (1000)	113.7	16.5
650 (1200)	111.6	16.2

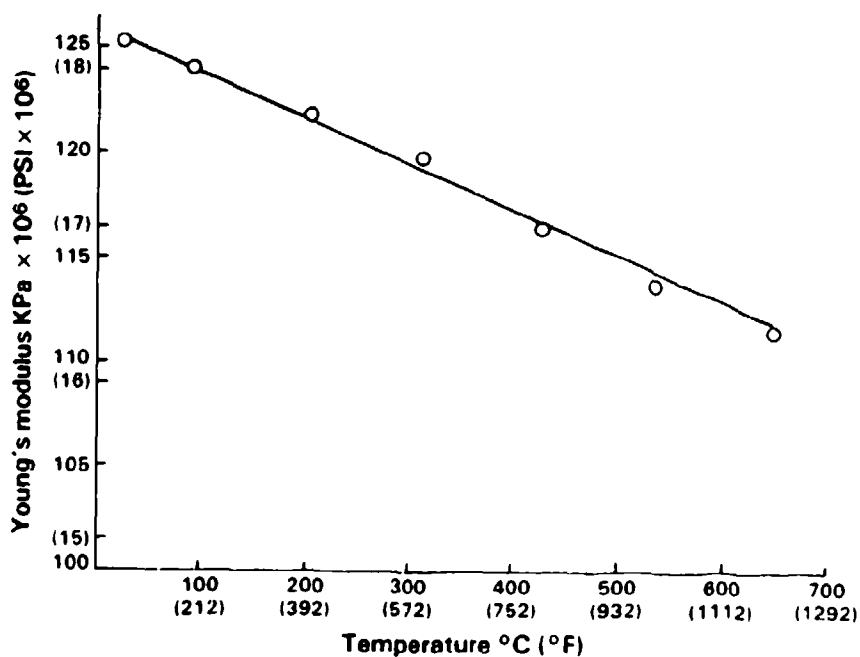


Figure 24. Young's modulus of Ti-25Al-10Nb-3V-1Mo alloy specimens versus temperature.

The specific heat (heat capacity) of the Ti-25Al-10Nb-3V-1Mo alloy was measured within the range of 82C (180F) to 651C (1204F). In this range, the specific heat varied from a low value of 473 Joule/Kg-K (0.113 Btu/lb.-F) at 82C (180F), increased to a maximum value of 628 Joule/Kg-K (0.150 Btu/lb.-F) at 593C (1000F) and then decreased to a value of 594 Joule/Kg-K (0.142 Btu/lb.-F) at 651C (1204F). The equation,

$$C_p = 0.088 + 1.487 \times 10^{-4} T - 8.708 \times 10^{-8} T^2 \dots\dots(1)$$

where C_p is the specific heat and T is the temperature in degrees Fahrenheit, will very accurately predict the value of the specific heat over the aforementioned temperature range. Equation 1) is the derivative of the enthalpy equation given by,

$$h = 0.088 T + 7.436 \times 10^{-5} T^2 - 2.907 \times 10^{-8} T^3 \dots\dots(2)$$

where h is the enthalpy (Btu/lb.), and T is the temperature in degrees Fahrenheit. Equation 2) was obtained by at least squares, polynomial regression curve fit of data. Figure 26 shows the graphical representation of the enthalpy data. Figure 27 shows the specific heat.

Thermal expansion measurements were made on a quartz tube type dilatometer. In such a device, the specimen is set with one end at the bottom of the tube while the other end is free to expand and push against a quartz rod which in turn pushes against a dial gage calibrated to 0.00254 mm (0.0001 inches). Thermocouples are used to measure the temperature of the specimen. Readings are taken from the dial gage and recorded as a function of temperature. A furnace completely surrounds the specimen to allow for uniform heating.

The thermal expansion of the aluminide alloy was shown to vary linearly over the temperature range 25C (75F) to 650C (1200F). A graph of thermal expansion versus temperature is shown in Figure 28.

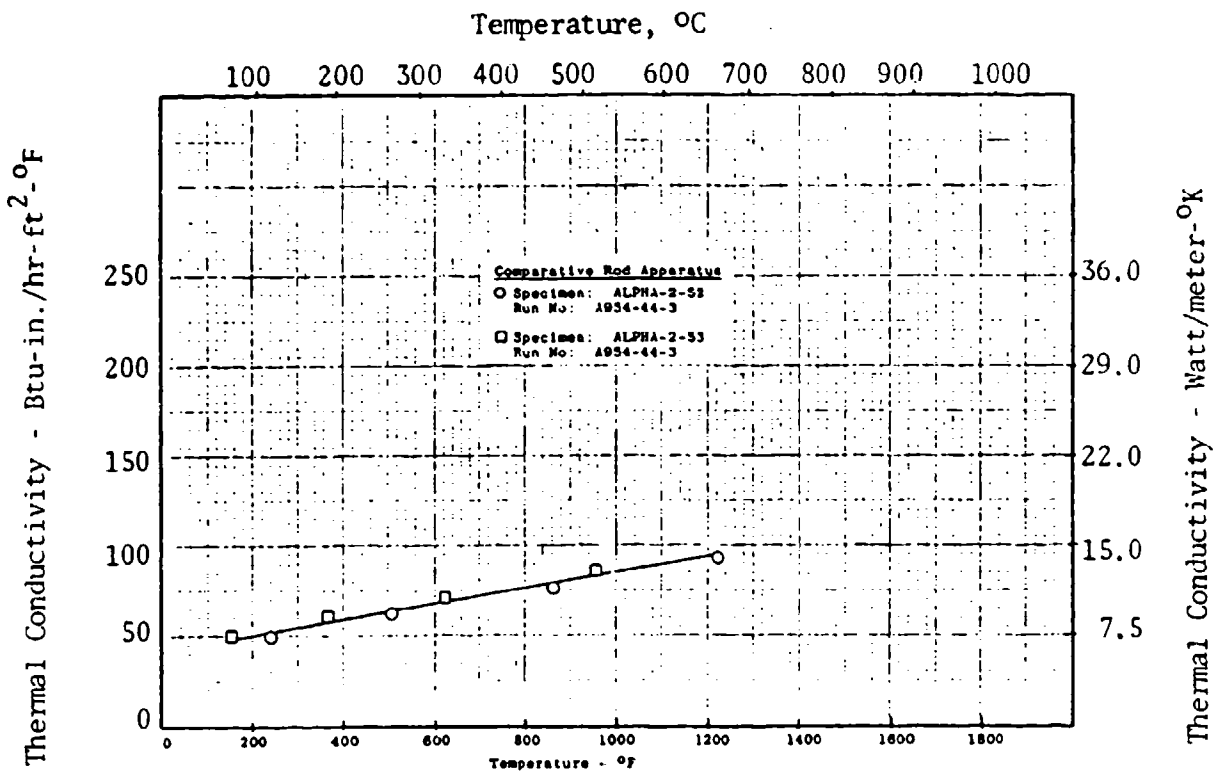


Figure 25. Thermal conductivity of the Ti-25Al-10Nb-3V-1Mo alloy.

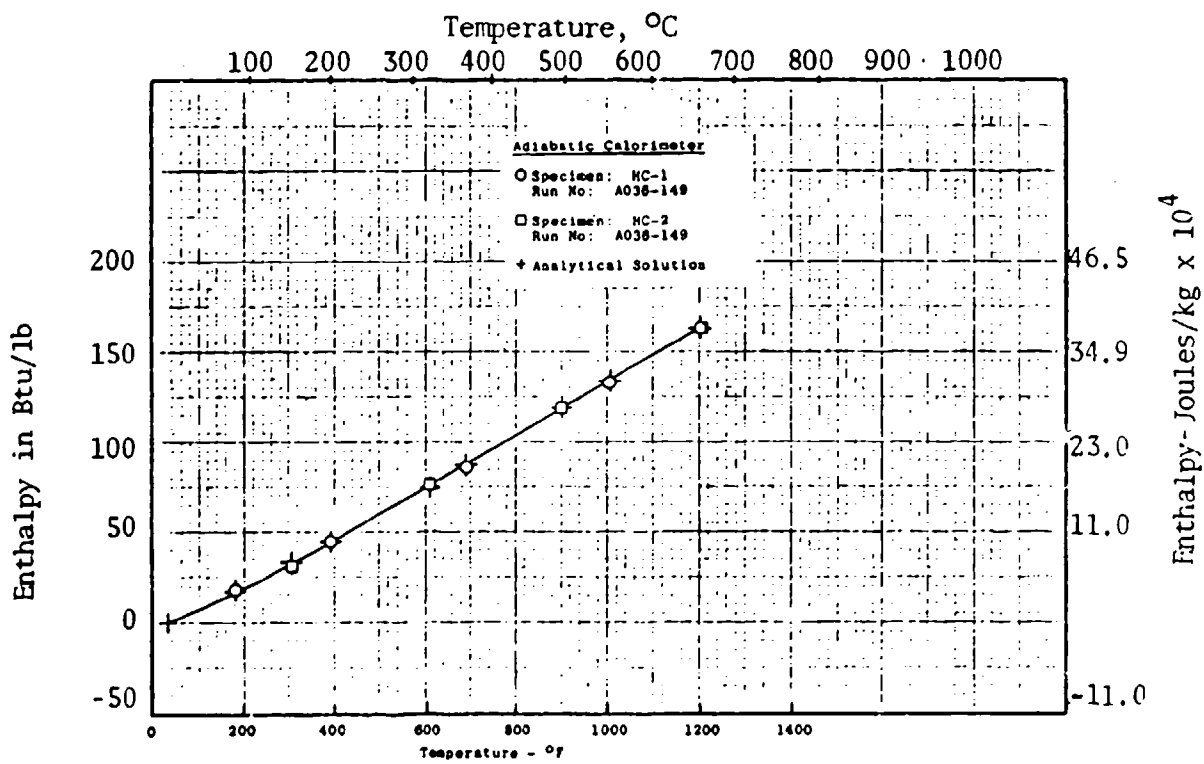


Figure 26. Enthalpy of the Ti-25Al-10Nb-3V-1Mo alloy.

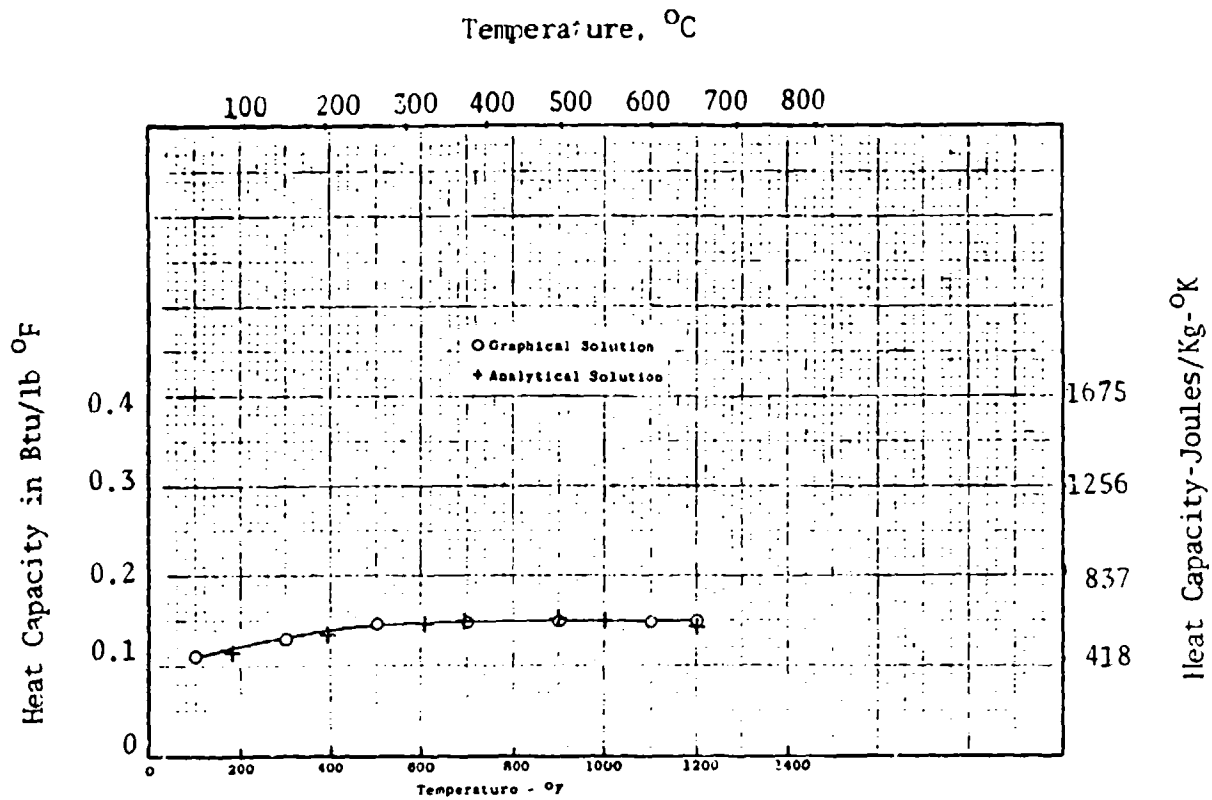


Figure 27. Heat capacity of the Ti-25Al-10Nb-3V-1Mo alloy.

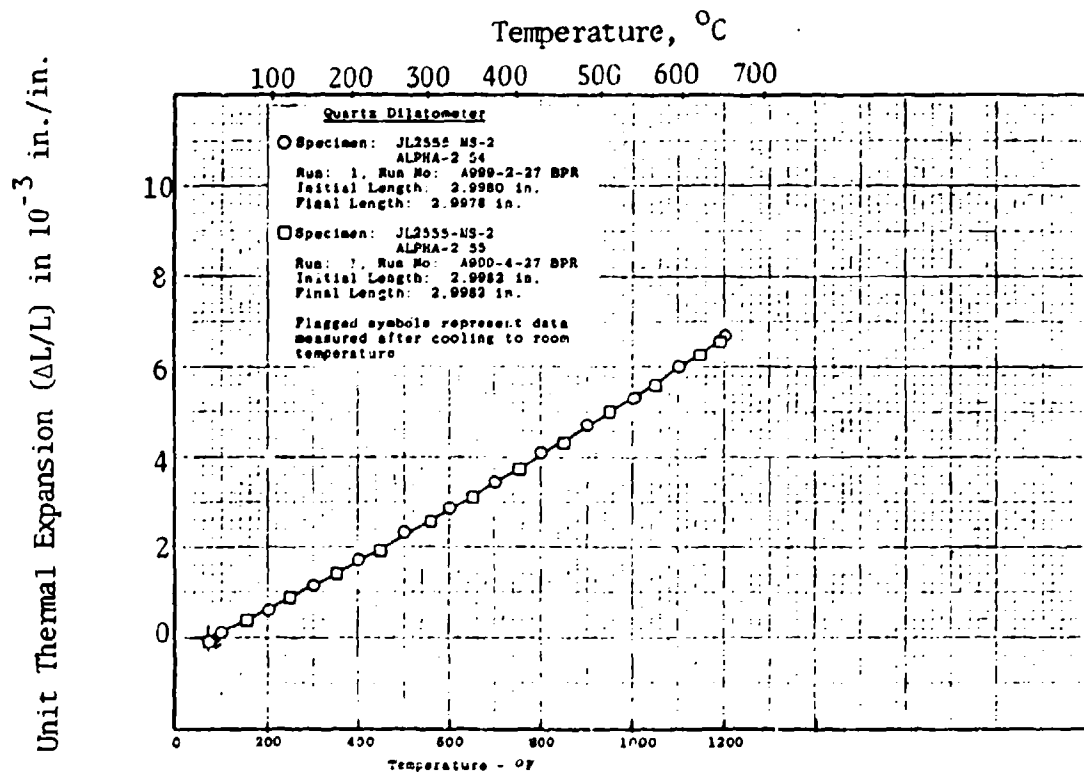


Figure 28. Thermal expansion of the Ti-25Al-10Nb-3V-1Mo alloy.

3. MATERIAL CHARACTERIZATION - GAMMA ALLOYS 1-4

a. Screening Tests

Since four gamma alloys were included in the program, a small scale test program was performed to select one alloy before proceeding to low cycle fatigue, toughness, impact and physical property testing. Tensile tests at RT, 260C (500F) and 650C (1200F) and stress-rupture tests at 760C/276 MPa (1400F/40 ksi) and 815C/172 MPa (1500F/25 ksi) were used to screen alloys.

The results obtained in this precursor program are given in Table 13. Major test problems were encountered as eight of the sixteen tensile specimens broke in the threads during testing, especially at the lower test temperatures. The Ti-48Al-1V-.1C alloy exhibited only one thread failure, but ductility of this alloy was about half of that previously measured for a similar alloy in an earlier program⁽⁴⁾. Metallographic examination of the specimens revealed the presence of considerable internal porosity in the Ti-47Al-2V, Ti-47Al-2V-.1C and a smaller amount in the Ti-47Al-2V-2Nb-1Mo alloy (Figure 29). Although no porosity was detected in the Ti-48Al-1V-.1C alloy, some external tearing and grinding cracks were present on the threads of the specimens near the failure site (Figure 30). Stress-rupture data showed that the Ti-47Al-2V-.1C alloy had the highest rupture lives, and the Ti-48Al-1V-.1C and Ti-47Al-2Nb-2V-1Mo compositions were about equal in capability. No problems that could be traced to porosity or cracks were found in these tests.

It is virtually certain that the porosity was formed during casting and not healed during subsequent processing, indicating the decision not to hot isostatic press the ingot section was probably a mistake. Since the Ti-48Al-1V-.1C alloy had the lowest breakthrough stress, lowest strength and greatest flow characteristics, sealing of porosity would be more likely during forging than for the lower aluminum content alloys.

Based on the tensile and stress-rupture results, the Ti-48Al-1V-.1C system still appeared to be the best overall gamma alloy of the group as the others offered no substantial advantages over this composition which has been characterized previously.

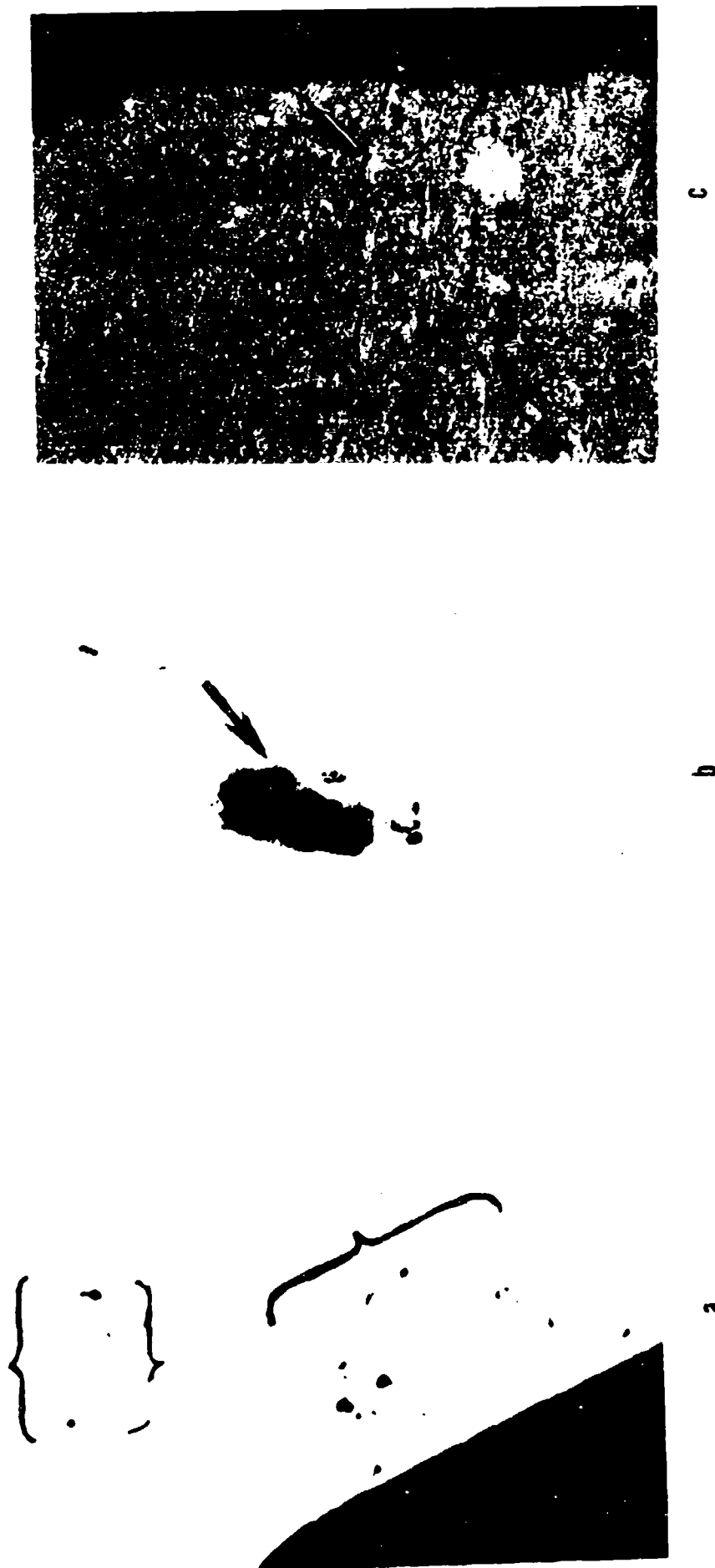
TABLE 13

Tensile and Stress-Rupture Properties of Forged and Heat Treated Gamma Alloy Pancake Forgings

Alloy/Heat Treatment	OC(°F)	Test Temp. °C (°F)	0.2% YS MPa (ksi)	UTS MPa (ksi)	%EL	Broke in Threads	%RA	Stress-Rupture Test Conditions °C/MPa (°F/ksi)	Hours to Rupture (3)	%EL	%RA
21008 (Ti-47Al-2Nb-2V-1Nb) 1204 (2200)/1/argon cool	RT			321(46.5)		Broke in Threads		760/276(1400/40)	45.0	11.2	16.6
	RT	260 (500)	447(64.9)	447(64.9)		Broke in Threads		815/172(1500/25)	67.7(56.0)	35.4	55.8
	650 (1200)	476(69.1)	616(89.3)	616(89.3)	1.7	1.9(S)					
21009 (Ti-47Al-2V) 1190 (2175)/1/argon cool	RT			604(87.6)	0.3		0	815/276(1500/40)	(4) 4.5(4.0)	37.0	58.8
	RT	260 (500)	600(87.0)	607(88.0)	0.5		0.7(S)	815/172(1500/25)	50.9(43.2)	68.5	73.0
	650 (1200)	446(64.7)	625(90.5)	625(90.5)	1.9	1.8(S)					
21010 (Ti-47Al-2V-.1C) 1190 (2175)/1/argon cool	RT			358(51.9)		Broke in Threads		760/276(1400/40)	70.0(66.1)	42.1	51.4
	RT	260 (500)	495(72.0)	505(73.3)		Broke in Threads		815/172(1500/25)	109.3(104.0)	52.9	58.0
	650 (1200)	408(59.2)	510(74.0)	510(74.0)	0.5	0.7					
21011 (Ti-48Al-1V-.1C) 1260 (2300)/1/argon cool	RT			385(55.7)		Broke in Threads		760/276(1400/40)	36.0(35.1)	46.1	63.5
	RT	260 (500)	430(62.4)	457(66.3)	0.5	0.4		815/172(1500/25)	60.0(59.9)	45.6	65.6
	650(1200)	353(51.2)	465(67.4)	465(67.4)	1.7	2.3					

(4) Should have been run at 760C (1400F)
(5) Broke in threads

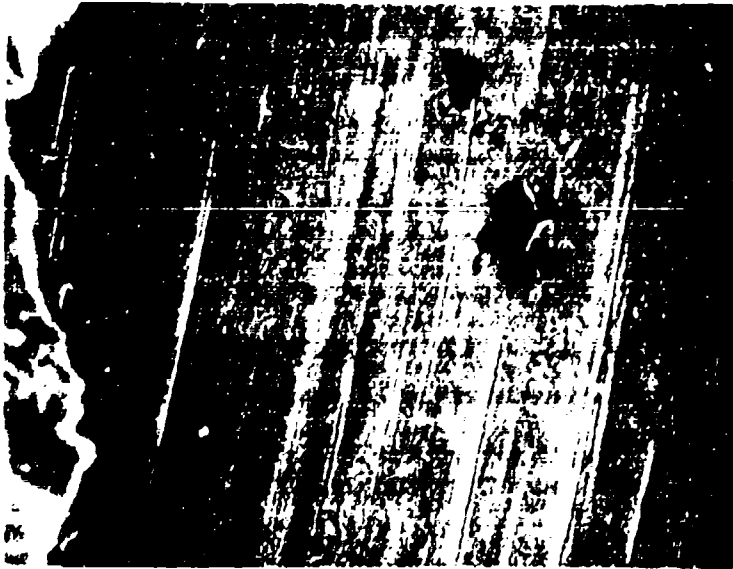
- (1) 0.1% yield strength
- (2) 0.05% yield strength
- (3) Due to extensive elongation, most specimens interrupted at times shown in parenthesis and were restarted.



Mag: 100X

Figure 29. Cross section of tested gamma alloy titanium aluminide tensile specimens showing internal porosity (arrow, brackets).

- a) Ti-47Al-2V-.1C
- b) Ti-47Al-2V
- c) Ti-47Al-2V-2Nb-1Mo



a



b

a) 400X
Mag: b) 100X

Figure 30. Grinding cracks and porosity on thread surface of a Ti-48Al-IV-.1C tensile specimen. Right, a cross section of a thread root on the same specimen revealing a root crack.

Steps were subsequently taken to improve the overall quality of the remaining Ti-48Al-1V-.1C specimens and prevent thread failures as follows:

- Hot isostatic pressing was employed on the remainder of the Ti-48Al-1V-.1C pancake forging in order to seal possible internal porosity. Conditions were 1220C/172 MPa/3 hours (2225F/25 ksi/3 hours).
- The hot isostatically pressed forging was reheat-treated at 1260C (2300F), argon cooled and an 815C (1500F) aging step was added.
- Extra precautions were taken during thread machining including more generous root radii, slower and lighter grinding passes and glass bead peening of fatigue specimen threads. Gage diameters of the tensile and smooth low cycle fatigue specimens were reduced by 1.27 mm (0.050") while maintaining the same thread size.

b. Material Characterization - Ti-48Al-1V-.1C

Tensile properties of reHIP'ed and heat treated Ti-48Al-1V-.1C are given in Table 14. No thread failures occurred and RT tensile ductility was improved over that measured during the screening trials. Elevated temperature properties were approximately the same.

The values were almost equal to those previously reported⁽⁴⁾ for the same alloy heat treated in a similar manner. In this earlier study, the room temperature and 650C (1200F) ductilities were higher; however, that forging was isothermally pressed in a two step operation with the final reduction conducted at 1065C (1950F). The slightly greater reduction and lower finish temperature may have contributed to the better properties due to the increased amount of working and more uniform grain size.

Stress-rupture lives at 825C/172 MPa (1500F/25 ksi) were 60.7 and 86.4 hours compared to 100-200 hours previously measured for Ti-48Al-1V or Ti-48Al-1V-.1C⁽⁴⁾ (Figure 15). Two reasons for this may be advanced; the difference in working schedule noted above and the use of a solution temperature about 27C (50F) higher in the earlier study which resulted in a microstructure containing more acicular transformed phase. Such a structure can be inferred to have a greater creep-rupture capability (Figure 31). (A fully acicular structure would have a life of 500-600 hours under the same test conditions.)

TABLE 14

Tensile Properties of Isothermally Forged + HIP
+ Heat Treated Ti-48Al-1V-.1C Alloy (1)

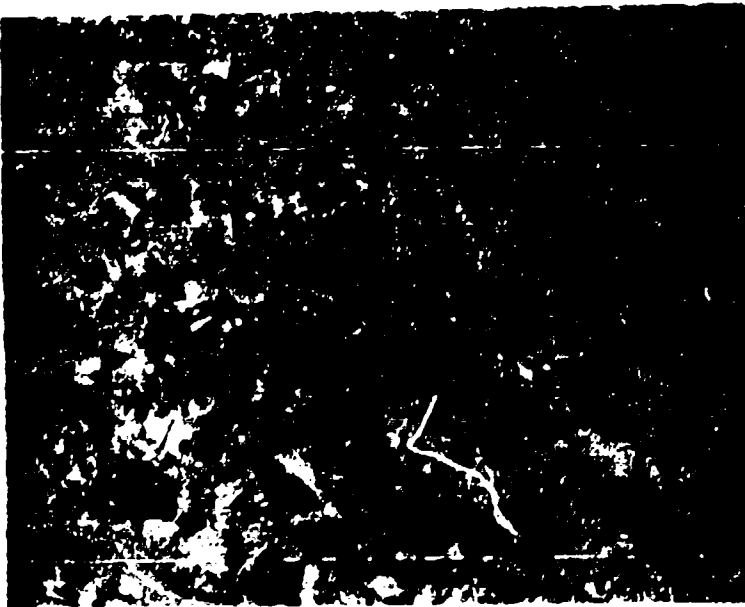
<u>Specimen Number</u>	<u>Test Temp. °C (°F)</u>	<u>0.2% Yield Str. MPa (ksi)</u>	<u>Ult. Tens. Str. MPa (Ksi)</u>	<u>%EL</u>	<u>%RA</u>
3535	RT	392 (56.8)	406 (58.9)	1.4	1.5
3536	260 (500)	296 (42.9)	430 (62.4)	2.0	2.1
3537	427 (800)	-	487 (70.7)	2.7	2.3
3538	538 (1000)	247 (35.8)	384 (55.7)	2.7	2.0
3539	650 (1200)	283 (41.1)	428 (62.1)	2.6	4.9
3540	760 (1400)	320 (46.4)	470 (68.2)	10.8	14.0

TABLE 15

Stress-Rupture Properties of Isothermally
Forged + HIP + Heat Treated Ti-48Al-1V-.1C Alloy(1)

<u>Specimen Number</u>	<u>Test Conditions °C/MPa (°F/ksi)</u>	<u>Hours to Rupture</u>	<u>%EL</u>	<u>%RA</u>
3722	815/172 (1500/25)	86.4	39.1	48.0
3723	815/172 (1500/25)	60.7	44.1	77.8

(1) HIP 1220C/172 MPa/3 hours (2225F/15 ksi/3 hours)
Heat treatment 1260C (2300F)/1/argon cool +
815C (1500F)/8 hours/AC



a



b

Mag: 100X

Figure 31. Microstructures of Ti-48Al-1V-.1C creep specimens showing relative amounts of acicular phase present. a) specimens from previous study solution treated at 1287C (2350F); b) current specimen 3723 solution treated at 1260C (2300F).

Tensile and creep-rupture specimens were thermally exposed in a static air environment for 500 hours at 675C (1250F) plus 100 hours at 730C (1350F) to determine the effect of exposure on properties. Properties were virtually unchanged as shown in Tables 16 and 17. Metallographic examination of a tested tensile and stress-rupture specimen revealed no hardened alpha case present but a thin, gray oxide film similar to that observed on some nickel-based superalloys (Figure 32).

Smooth bar impact data for Ti-48Al-1V-.1C are given in Table 18. Compared to the alpha two alloy, the values are closer to notched properties of that system and show little increase in strength as test temperature increases up to 760C (1400F). In view of the low smooth bar data, notched impact testing was not conducted. In designing a component for the Ti-48Al-1V-.1C system, this lack of impact strength could be a major consideration.

Fracture toughness testing was conducted using three point bend specimens as before. The initial attempt to fatigue precrack the notched specimens was unsuccessful in that cracks did not originate at the notch but rather as a result of galling at the sharp edge of the specimen where it was gripped. By deepening the notch and chamfering the edges of the specimen, successful precracking was performed, but only three specimens remained for testing. Measurements were made at RT, 260C (500F) and 427C (800F) as shown in Table 19. The room temperature fracture toughness value was reported as 12.3 MPa \sqrt{m} (11.5 ksi \sqrt{in}), which was higher than expected for the alloy in view of the results obtained for the Ti-25Al-10Nb-3Mo-1V alloy and considering the low impact strength of the Ti-48Al-1V-.1C itself. Values of 7.8-7.9 MPa \sqrt{m} (8.6-8.7 ksi \sqrt{in}) have been reported for a wrought powder Ti-48Al-2Nb-1W alloy⁽⁵⁾, so perhaps the results are not exceptional. A careful review of the test procedures and calculations revealed no errors, and the precrack was within the prescribed ASTM E-399 limits for the type of specimen. The values of 16.5 MPa \sqrt{m} (15 ksi \sqrt{in}) and 25.1 MPa \sqrt{m} (22.8 ksi \sqrt{in}) at 260C (500F) and 427C (800F) seem reasonable.

TABLE 16

Effect of Thermal Exposure⁽¹⁾ on
Tensile Properties of Isothermally
Forged + HIP + Heat Treated
Ti-48Al-1V-.1C Alloy

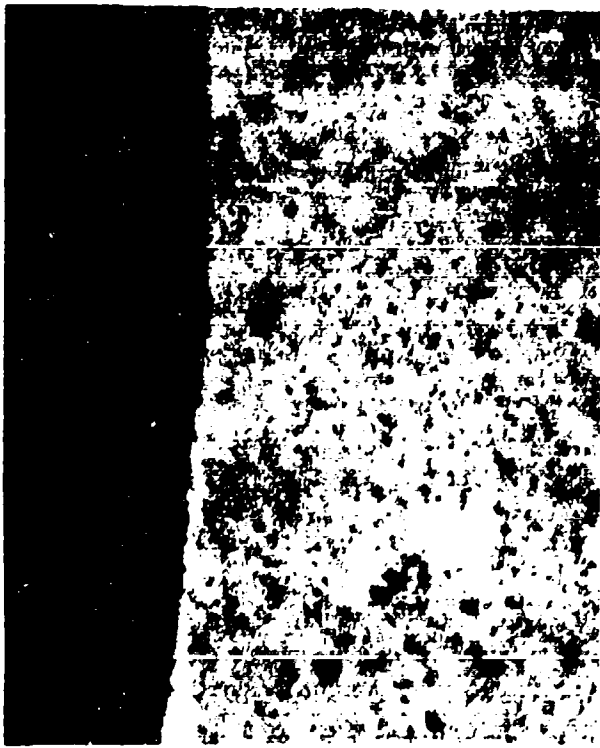
<u>Specimen Number</u>	<u>Test Temp. °C (°F)</u>	<u>0.2% Yield Str. MPa (Ksi)</u>	<u>Ult. Tens. Str. MPa (Ksi)</u>	<u>%EL</u>	<u>%RA</u>
3734	RT	394 (57.1)	447 (64.8)	1.1	1.2
3735	260 (500)	276 (40.0)	467 (67.7)	2.3	2.6
3736	427 (800)	344 (49.9)	440 (63.8)	1.6	1.5
3737	650 (1200)	336 (48.7)	461 (66.8)	2.4	2.5
3738	815 (1500)	292 (42.3)	423 (61.3)	11.9	10.9

TABLE 17

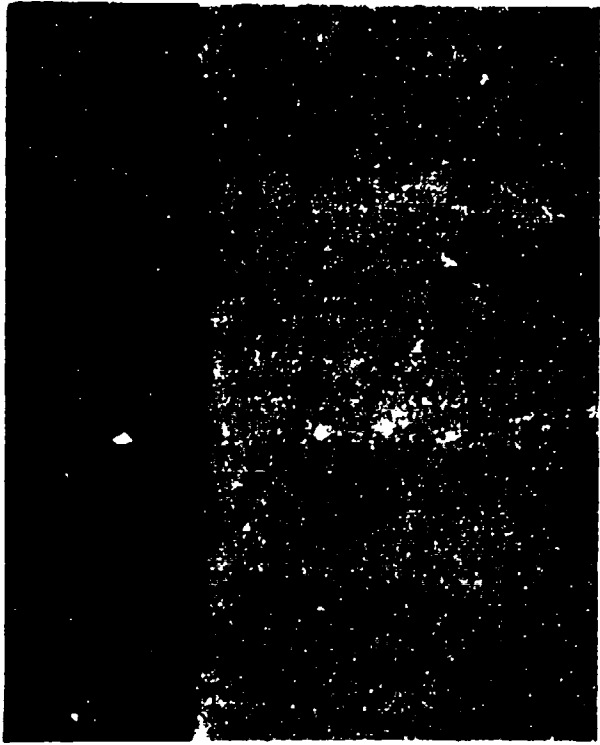
Effect of Thermal Exposure⁽¹⁾ on the
Creep-Rupture Properties of Isothermally Forged +
HIP + Heat Treated Ti-48Al-1V-.1C Alloy

<u>Specimen Number</u>	<u>Test Conditions °C/MPa (°F/Ksi)</u>	<u>Hours to Rupture</u>	<u>%EL</u>	<u>%RA</u>
3724	815/172 (1500/25)	62.8	41.8	89.3
3725	815/172 (1500/25)	69.1	44.5	67.1

(1) Exposure Conditions: 675C (1250F)/500 hours + 730C (1350F)/
100 hours using fully machined specimens
with the surface left in the "as-exposed"
condition for testing.



a



b

a) 200X
Mag: b) 500X

Figure 32. Continuous oxide layer formed on Ti-48Al-1V-.1C alloy specimens after a thermal exposure of 500 hours at 675C (1250F) plus 100 hours at 730C (1350F) (brackets).

TABLE 18

Smooth Impact Properties of Isothermally
Forged + HIP + Heat Treated Ti-48Al-1V-.1C Alloy

<u>Specimen Number</u>	<u>Test Temp. °C (°F)</u>	<u>Impact Strength, Joules (Ft.-Lbs.)</u>
3552	RT	1.4 (1.0)
3553	260 (500)	3.3 (2.4)
3555	538 (1000)	3.3 (2.4)
3554	650 (1200)	3.8 (2.8)
3556	650 (1200)	3.5 (2.6)
3557	760 (1400)	3.3 (2.4)

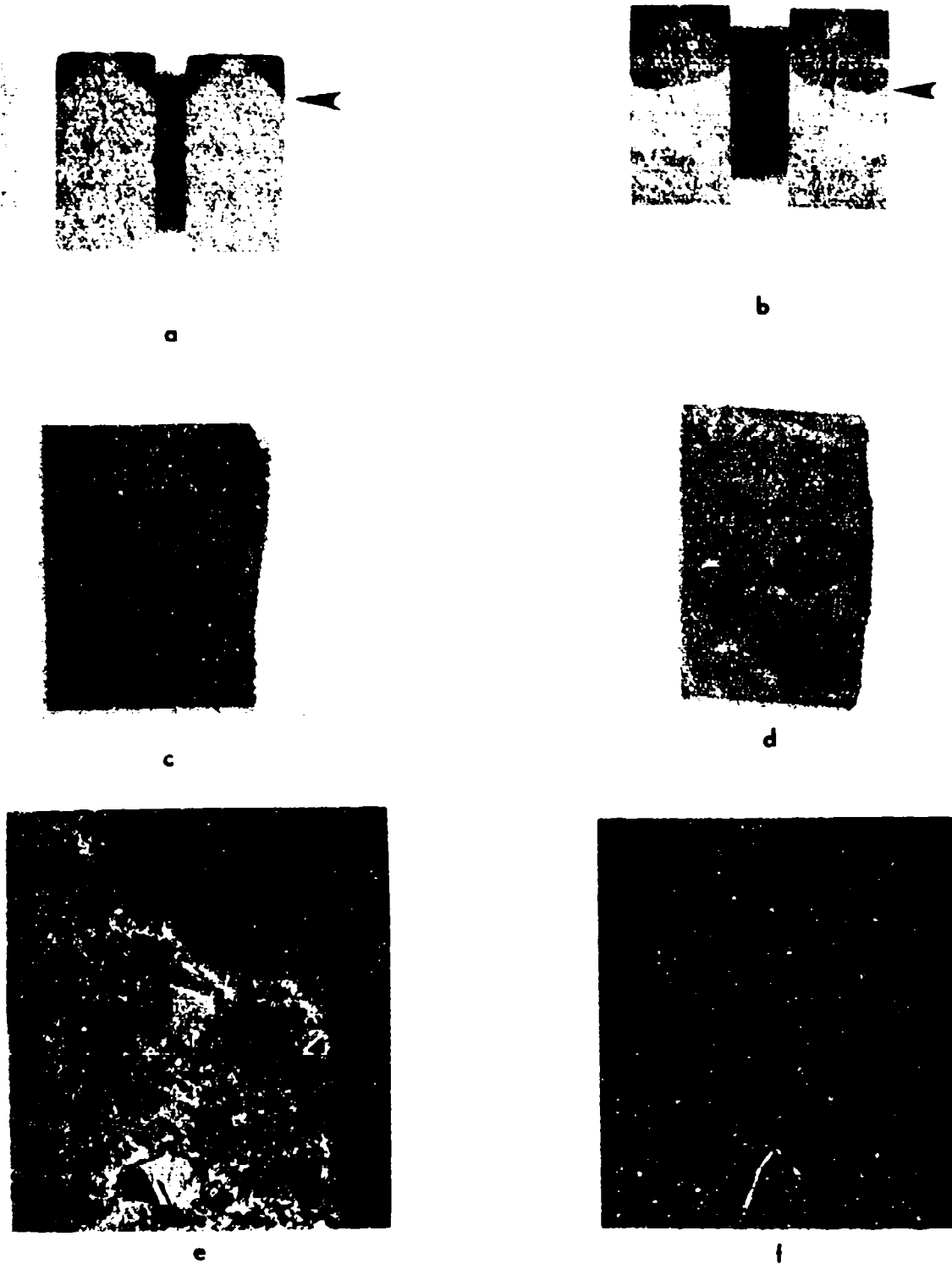
TABLE 19

Fracture Toughness of Isothermally Forged +
HIP + Heat Treated Ti-48Al-1V-.1C Alloy
Precracked Slow Bend Specimens

<u>Specimen Number</u>	<u>Test Temp. °C (°F)</u>	<u>K_{1C}</u>	
		<u>MPa√m</u>	<u>ksi√in.</u>
3889	RT	12.3	11.5
3890	260 (500)	16.5	15.0
3892	437 (800)	25.1	22.8

Visual and metallographic examination of a selected toughness specimen showed fundamental differences when compared with the Ti-25Al-10Nb-3V-1Mo alloy (Figure 33a, b). The alpha two specimen had a flat fracture surface with no shear lips and revealed relatively coarse equiaxed and elongated grains. The gamma alloy specimen had very small shear lips and a slightly banded appearance resulting from the alternating regions of fine grains with regions of somewhat coarser grains. A cross section of the two specimens revealed that the crack path was a mixture of transgranular and intergranular in both alloys, but tended to be more jagged and tortuous in the gamma alloy (Figure 33c, d, e, f) while the smooth, large grains in the alpha two specimen possibly provided an easier path for crack propagation. Thus, it is possible that the high toughness of the Ti-48Al-1V-.1C alloy might be explained by a combination of low yield strength and the particular banded microstructure reminiscent of the "necklace" structure observed in some nickel-base alloys.

Smooth low cycle fatigue specimens were run in an axial tension-release loading mode at a frequency of 1 Hertz (60 cpm); ten of the smooth specimen type were machined, and it was originally planned to test five at 650C (1200F) and five at 815C (1500F). However, when a specimen exceeded 200,000 cycles at a given load, the stress was increased to a higher load to cause failure; therefore, there are more data points than specimens. No thread failures occurred. The test data are presented in Table 20 and plotted graphically in Figure 34. At the 815C (1500F) test temperature, the data form a typical smooth S/N curve with a good fit for all points and little scatter apparent. Runout stress at 10^5 cycles was about 330 MPa (48 ksi). Specimens tested at 650C (1200F) exhibited more scatter in results, and it was not possible to determine a reasonable S/N curve. Fracture surfaces were analyzed by scanning electron microscope (SEM) and metallographic sectioning, and the results indicated some reasons for the wide range of values found. Specimens which had longer lives under similar conditions exhibited more of the very fine grain in transformed structure regions while the shorter life specimens had larger areas of coarse gamma grains (Figure 35). Fracture mode was intergranular and cracks were found to initiate in coarse grain regions (Figure 36). A graphical presentation of the fine and coarse grained data is shown in Figure 34. It is apparent that grain size had an effect on LCF properties at the lower test temperature but at 815C (1500F) played little role even though the fracture mode at 815C (1500F) was also intergranular.



a,b) 2.6X
 c,d) 4X
 Mag: e,f) 100X

Figure 33. Fracture mode in precracked slow bend toughness specimens. Left column, Ti-48Al-1V-.1C; right column, Ti-25Al-10Nb-3V-1Mo. Note difference in grain size.

TABLE 20

Smooth Axial Low Cycle Fatigue⁽¹⁾ of
 Isothermally Forged + HIP + Heat Treated
 Ti-48Al-1V-.1C Alloy Specimens

Specimen Number	Test Temp. °C (°F)	Stress Range, MPa (ksi)	Cycles to Rupture
3744	650 (1200)	0-344 (0-50) 0-413 (0-60)	>346,100 400
3745	650 (1200)	0-380 (0-55)	1,400
3746	650 (1200)	0-362 (0-52.5) 0-413 (0-60)	>245,000 3,900
3747	650 (1200)	0-380 (0-55)	600
3748	650 (1200)	0-362 (0-52.5)	3,300
3749	650 (1200)	0-344 (0-50)	2,500
3750	815 (1500)	0-344 (0-50)	47,000
3751	815 (1500)	0-380 (0-55)	32,300
3752	815 (1500)	0-310 (0-45)	150,500
3753	815 (1500)	0-413 (0-60)	2,100

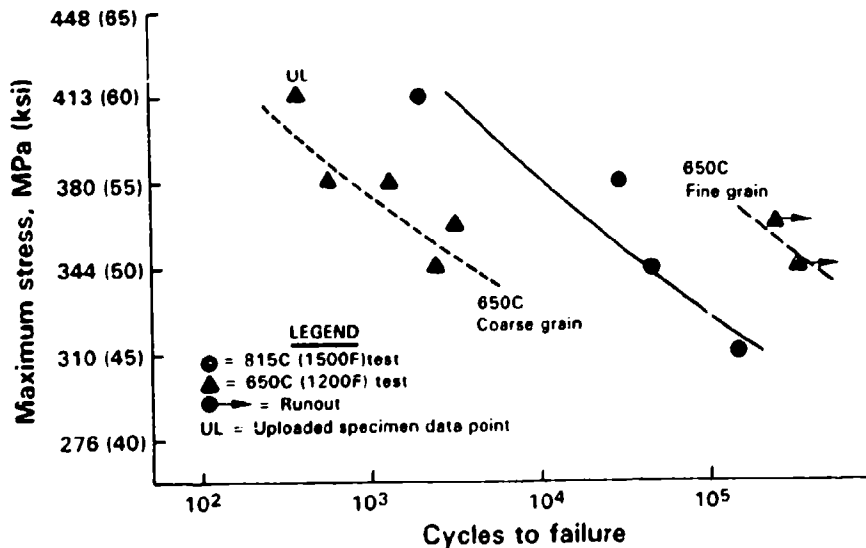
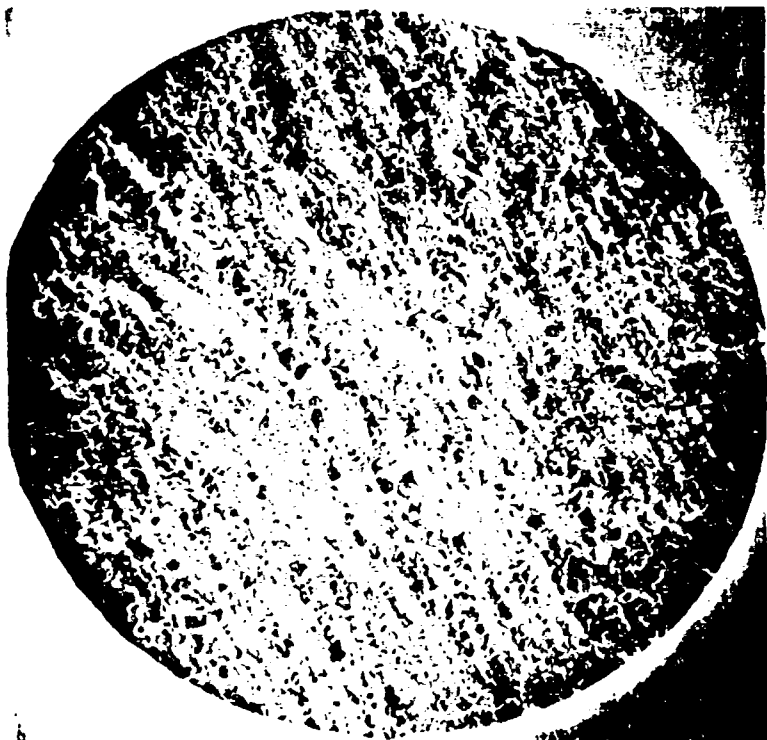


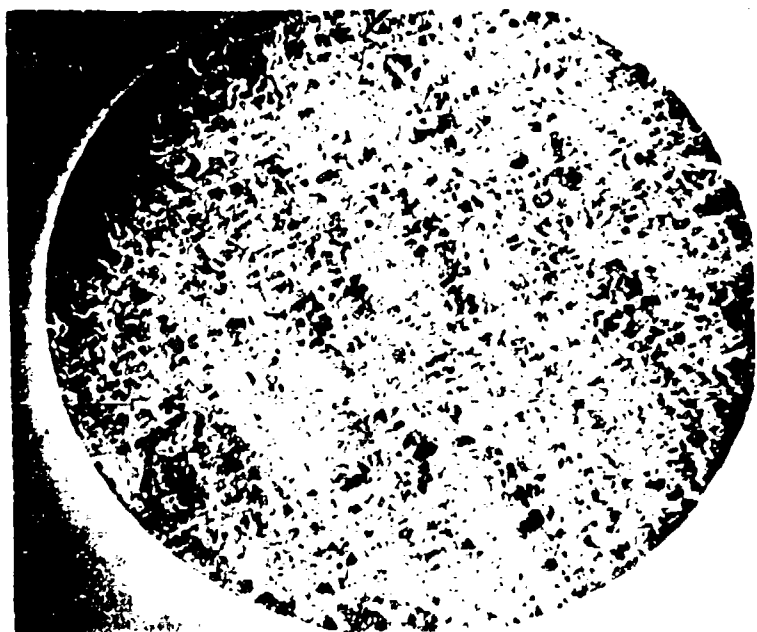
Figure 34. S/N curves for smooth Ti-48Al-1V-.1C LCF specimens drawn to show effect of grain size on 650C (1200F) life.



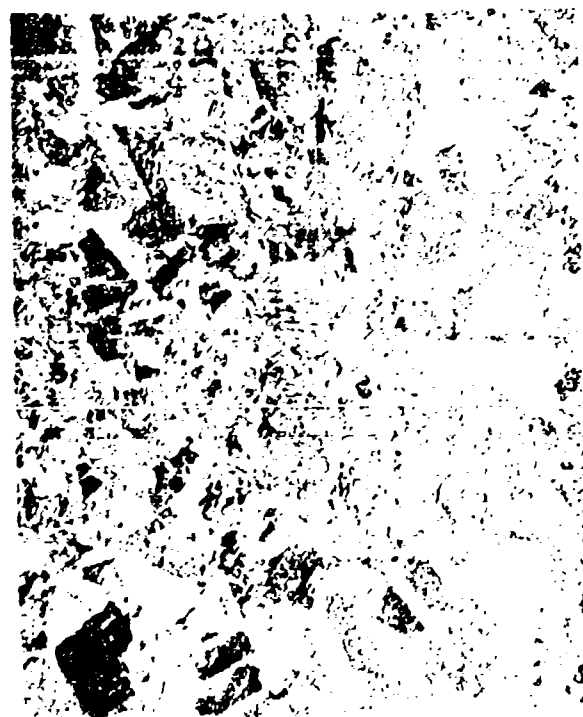
a



b



c



d

a, c) 183x
Mag: b, d) 100x

Figure 35. Fracture appearance and microstructures of smooth Ti-48Al-17.1F low cycle fatigue specimens tested at 650C (1200F) and 544MPa/50 ksi; a, c) specimen 3744 which ran 346,000 cycles; b, d) specimen 3749 which failed after 2399 cycles. Note fine grain regions in 3744.



a

b

c

a,b) 60X
Mag: c) 100X

Figure 36. Ti-48Al-1V-1C smooth LCF specimens tested at 650C. (1200F) and 344 MPa (50 ksi). Note origins in coarse grain areas in specimen 3744 a) and 3749 b). Fracture path c) is basically intergranular.

Ten notched ($K_t = 2.0$) Ti-48Al-1V-.1C specimens were machined to be tested at 650C (1200F) and 815C (1500F). The first specimen, intended for testing at 650C (1200F), broke during installation in the rig; the second was cycled at 0-413 MPa (0-60 ksi), and the test suspended at 349,000 cycles with no crack indications. In order to expedite testing and meet the program schedule, the mechanical test personnel were instructed to utilize higher stresses in order to achieve rupture lives in the normal low cycle fatigue regime of 10^3 - 10^5 cycles. Several test rigs became available about this time, allowing concurrent specimen testing, but the stresses selected* were too high, causing failure on loading or at less than 50 cycles. Thus, no real assessment of notch capability of the alloy at 1200F was obtained. Testing of notched specimens at 815C (1500F) was successful and these data are shown in Table 21 and plotted in Figure 37. 10^5 cycle runout stress was 310 MPa (45 ksi).

Young's modulus was measured dynamically over the range RT-815C (1500F) using a solid rod 100 mm (4") long x 6.2 mm (0.25") diameter. Test data are given in Table 22 and plotted graphically in Figure 38. The Ti-48Al-1V-.1C showed about a 40% increase in modulus compared to the Ti-25Al-10Nb-3V-1Mo alloy and is at least 50% higher than most conventional titanium alloys.

The thermal conductivity of the Ti-48Al-1V-.1C alloy was determined using the comparative rod apparatus method (CRA) as previously described. Results showed that the thermal conductivity of the Ti-48Al-1V-.1C alloy varied in a slightly non-linear fashion over the range of RT to 815C (1500F). The variation is from a low average value of 21.6 Watt/meter-K (150 Btu-in./hr.-ft.²-F) at 24C (75F) to a high average value of 28.1 Watt/meter-K (195 Btu-in./hr.-ft.²-F) at 815C (1500F). The thermal conductivity of the second specimen was slightly higher than the first but well within the five percent accuracy of the testing apparatus. Figure 39 is a graph of thermal conductivity versus temperature.

The specific heat (heat capacity) of the Ti-48Al-1V-.1C alloy was measured within the range of 93C (200F) to 815C (1500F). In this range, the specific heat varied from a low value of 649 Joules/Kg-K (0.155 Btu/lb.-F) at 93C (200F) to an average value of 733 Joules/Kg-K (0.175 Btu/lb.-F) at 815C (1500F). The equation,

*Selected stresses were 490 MPa (70 ksi), 455 MPa (65 ksi) and 437 MPa (62.5 ksi).

TABLE 21

Notched ($K_t = 2.0$) Axial Low Cycle Fatigue of
Isothermally Forged + HIP + Heat Treated
Ti-48Al-1V-.1C Alloy Specimens

<u>Specimen Number</u>	<u>Test Temp. °C (°F)</u>	<u>Nominal Stress Range, MPa (ksi)</u>	<u>Cycles to Rupture</u>
3625	815 (1500)	0-274 (0-40)	>234,000
	815 (1500)	0-291 (0-42.5)	8,900
3626	815 (1500)	0-344 (0-50)	15,300
3627	815 (1500)	0-310 (0-45)	93,800
3628	815 (1500)	0-327 (0-47.5)	17,300
3629	815 (1500)	0-317 (0-46)	82,500

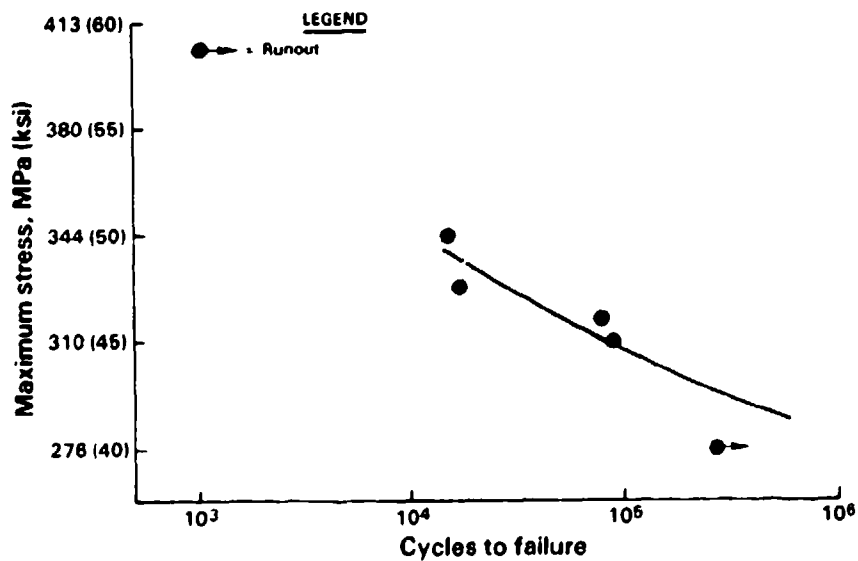


Figure 37. S/N curve for 815C (1500F) Ti-48Al-1V-.1C notched low cycle fatigue specimens.

TABLE 22

Dynamic Modulus of Isothermally Forged +
HIP + Heat Treated Ti-48Al-1V-.1C Alloy

Test Temp. °C (°F)	Elastic Modulus	
	KPa x 10 ⁶	PSI x 10 ⁶
RT	168.0	24.4
93 (200)	166.0	24.1
204 (400)	163.3	23.7
315 (600)	160.5	23.3
427 (800)	156.4	22.7
538 (1000)	153.0	22.2
650 (1200)	148.8	21.6
760 (1400)	146.0	21.2
815 (1500)	144.0	20.9

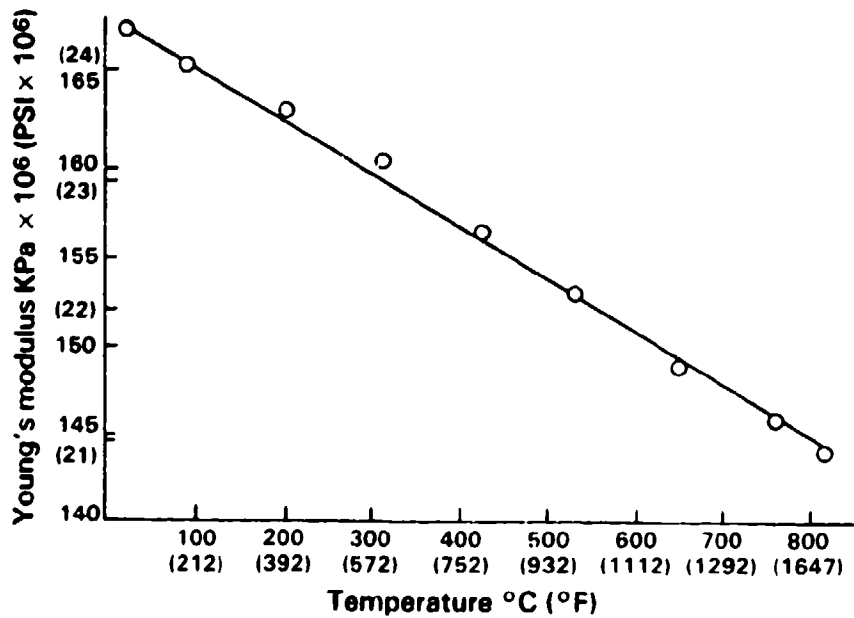


Figure 38. Young's modulus of the Ti-48Al-1V-.1C alloy.

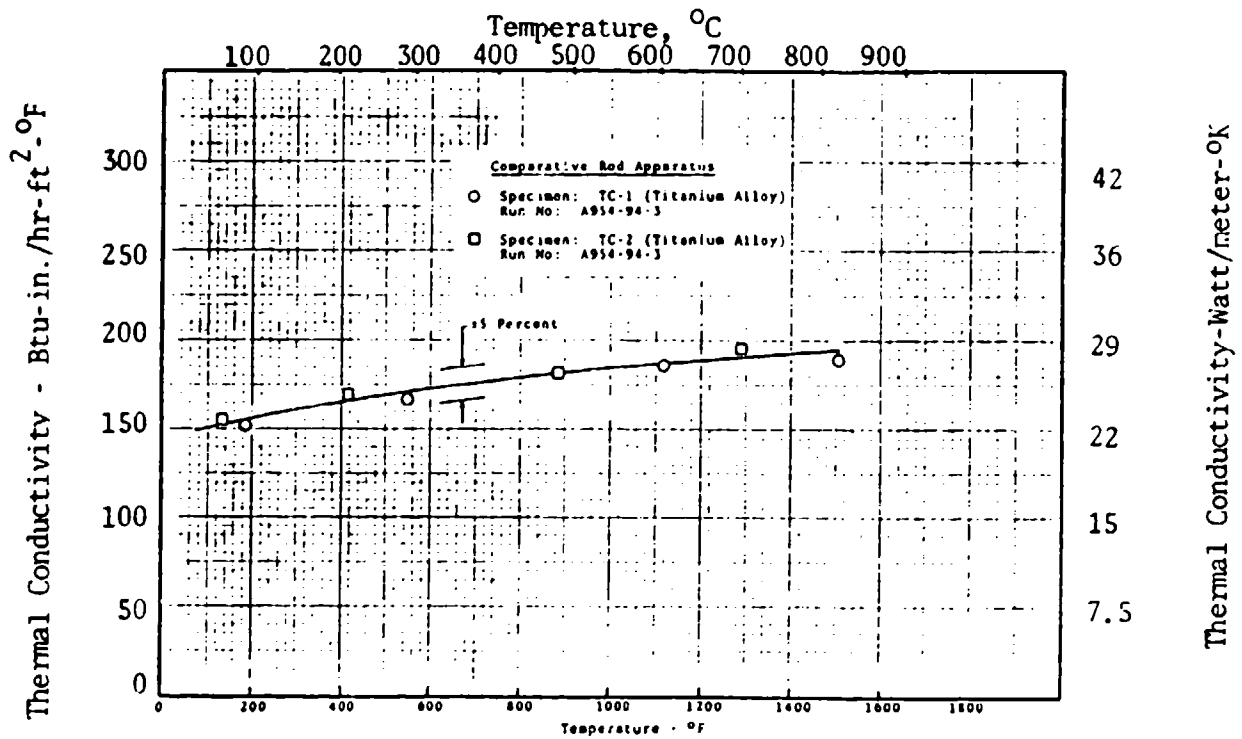


Figure 39. Thermal conductivity of the Ti-48Al-1V-.1C alloy.

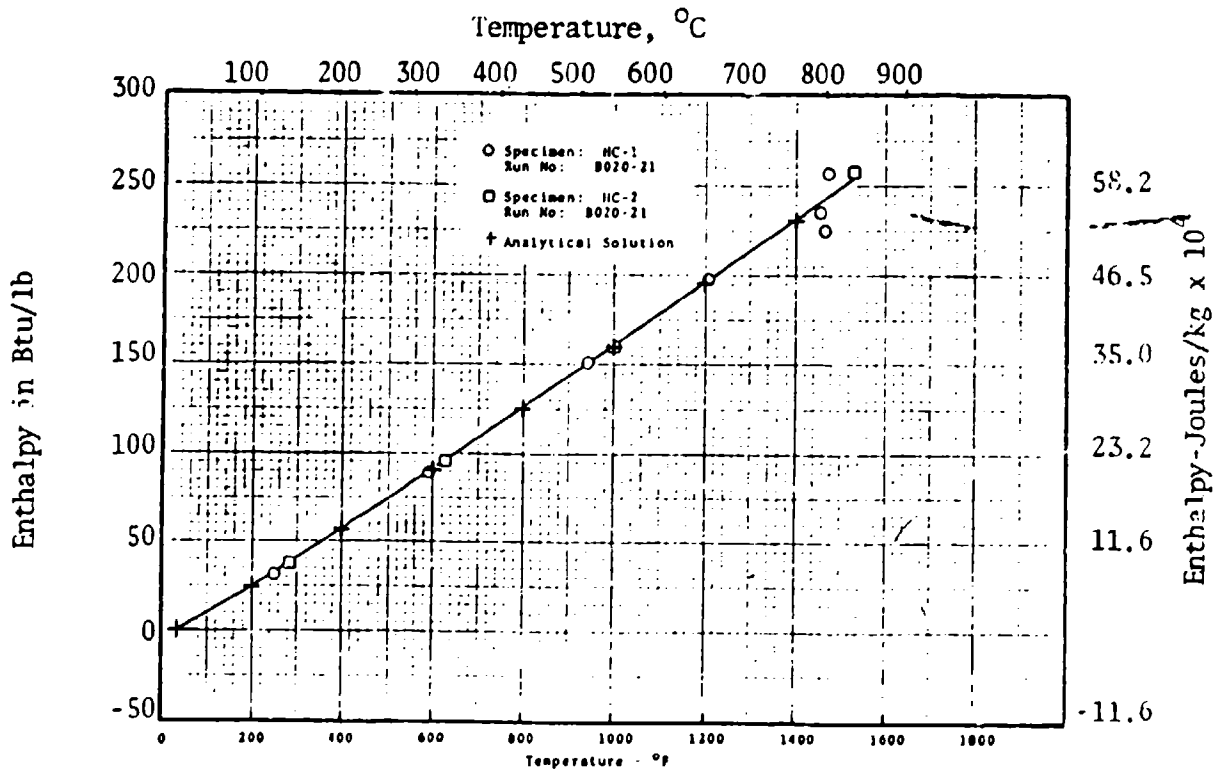


Figure 40. Enthalpy of the Ti-48Al-1V-.1C alloy.

$$1) c_p = 0.1748 - 0.2303 \times 10^{-4} T + 0.2581 \times 10^{-7} T^2$$

where c_p is the specific heat and T is the temperature in degrees Fahrenheit, will very accurately predict the value of the specific heat over the aforementioned temperature range. The specific heat equation is the derivative of the enthalpy equation obtained by a curve fit of the data shown in Figure 40. (The enthalpy showed some scattering at about 793C (1460F); this may be indicative of phase change in the material.) An average value of the scattered points was used to obtain the enthalpy equation.

$$2) h = 0.1748 T - 0.1151 \times 10^{-4} T^2 + 0.8603 \times 10^{-8} T^3$$

where h is the enthalpy (Btu/lb.) and T is the temperature in degrees Fahrenheit. Equation 2 was obtained by a least squares, polynomial regression curve fit of data. Figure 41 showed the graphical representation of the specific heat data. As can be seen, there is good correlation between the data and the curve fit.

The thermal expansion of the Ti-48Al-1V-.1C alloy was shown to vary linearly over the temperature range RT to 815C (1500F). A graph of thermal expansion versus temperature is shown in Figure 42.

4. PROCESSING STUDIES

The primary material characterization of Task I was supplemented by additional studies to gain experience on various processing techniques and product forms for both alloy types. Results of these investigations are as follows.

a. Net Shape Gamma Alloy Casting

One mold of approximately forty Ti-48Al-1V F100 compressor blade preforms were centrifugally cast by Howmet (Ti-Cast). The castings had excellent definition and fill as shown in Figure 43a. However, fluorescent penetrant examination revealed surface indications at the intersection of the airfoil convex side and blade root. Subsequent fractographic analysis revealed that the indications were surface connected porosity 0.25-0.5 mm (0.010"-0.020") deep (Figure 43b, c). Howmet considers that the porosity could be eliminated by a minor wax modification to increase the radius slightly. Radiographic examination of a sample as-cast blade revealed considerable centerline shrinkage, particularly in the airfoil section. This was verified by subsequent sectioning of the blade which showed the dendritic nature of the porosity (Figures 44 and 45).

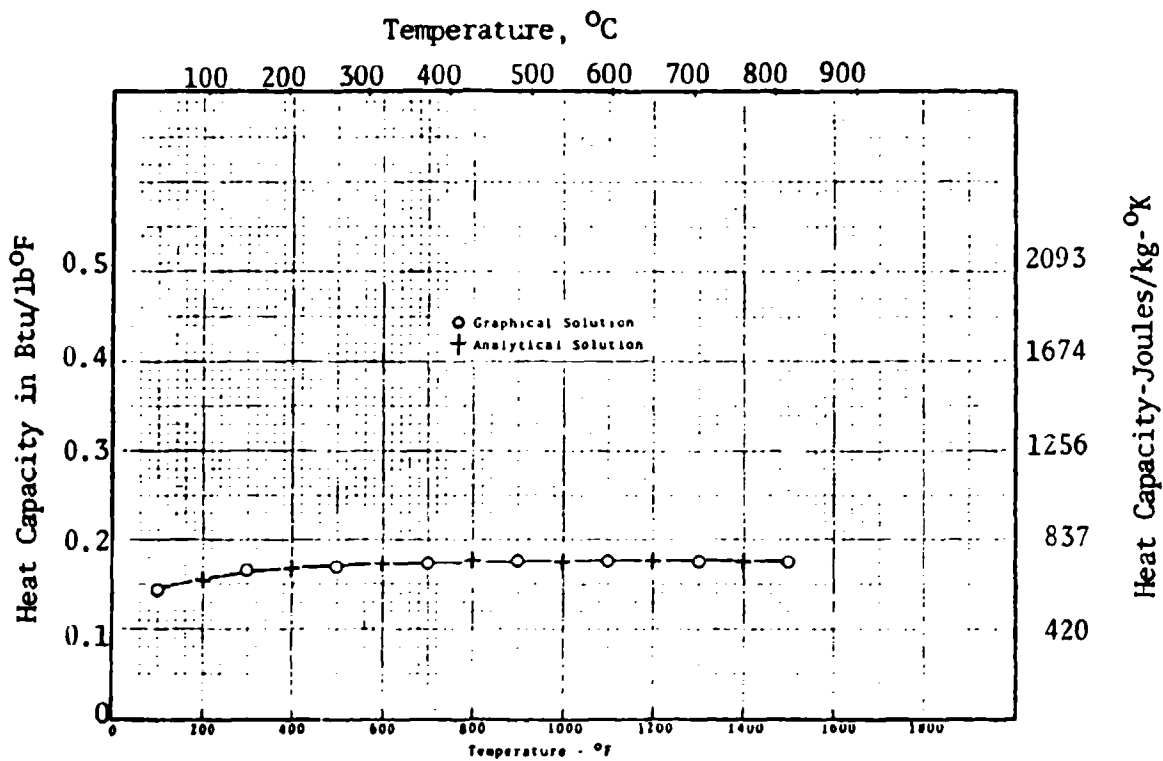


Figure 41. Heat capacity of the Ti-48Al-1V-.1C alloy.

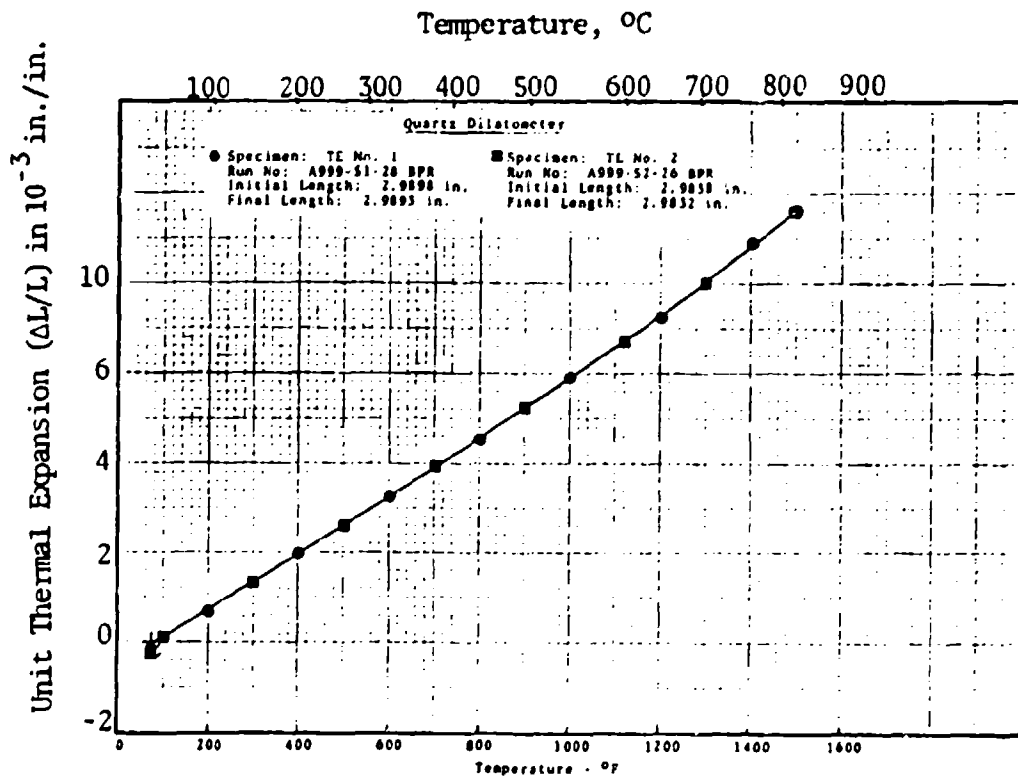


Figure 42. Thermal expansion of the Ti-48Al-1V-.1C alloy.

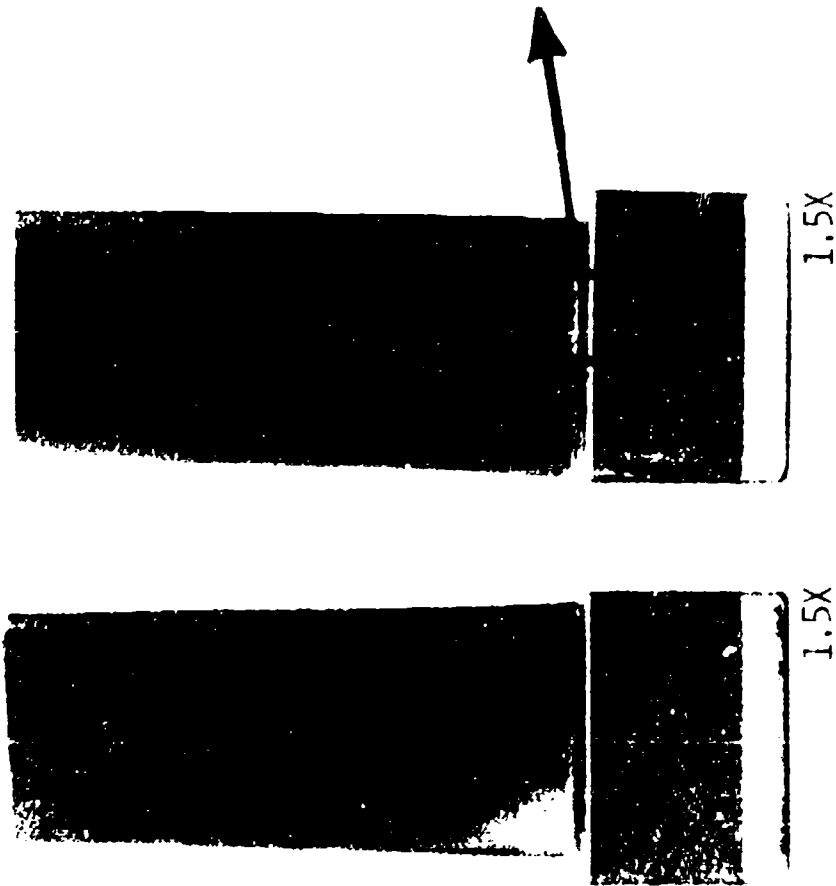


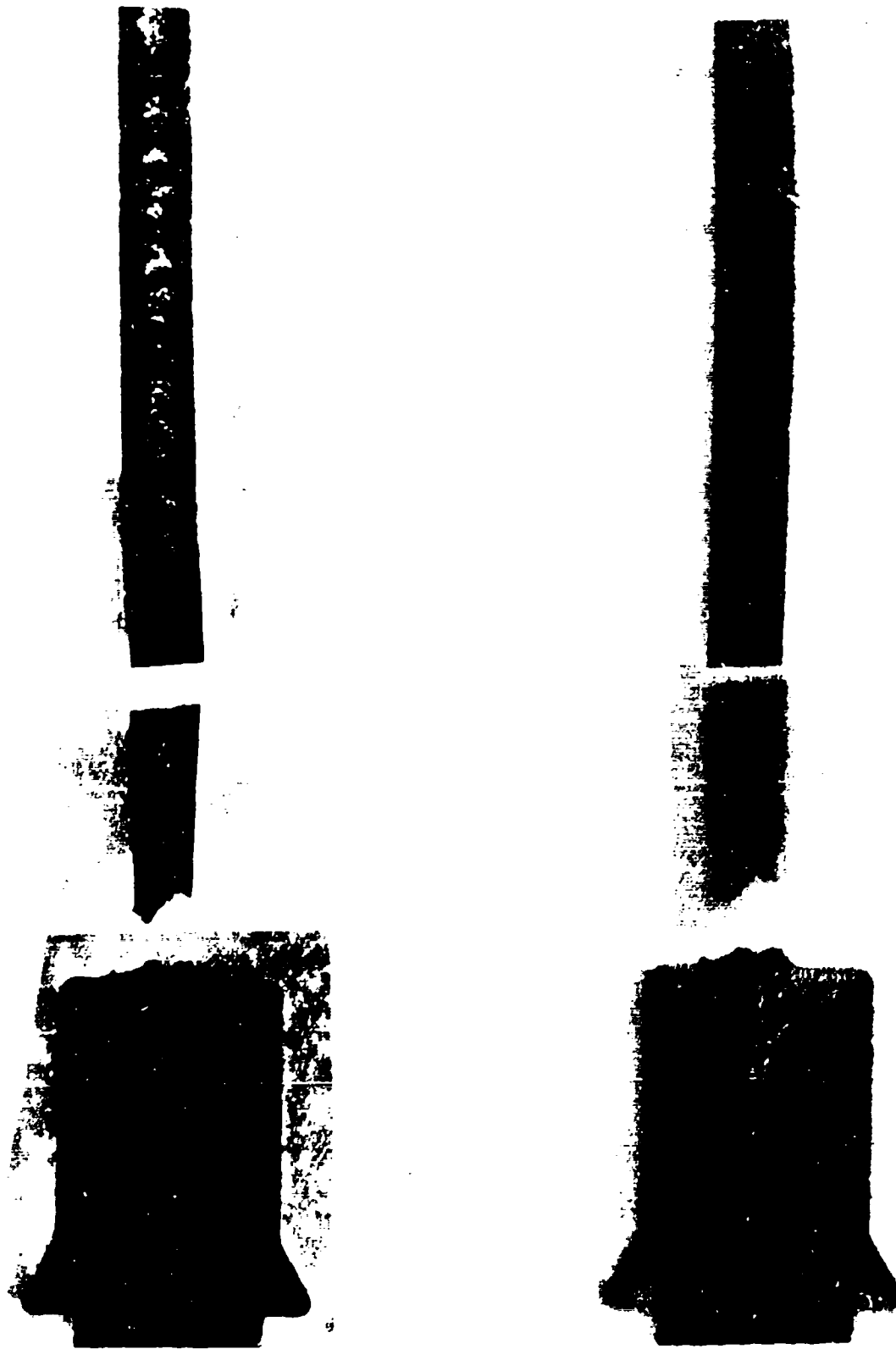
Figure 43. Cast Ti-48Al-IV F100 compressor blade preforms showing good fill and definition (a) but surface connected shrinkage porosity at the convex side airfoil platform interface (b, c).



b

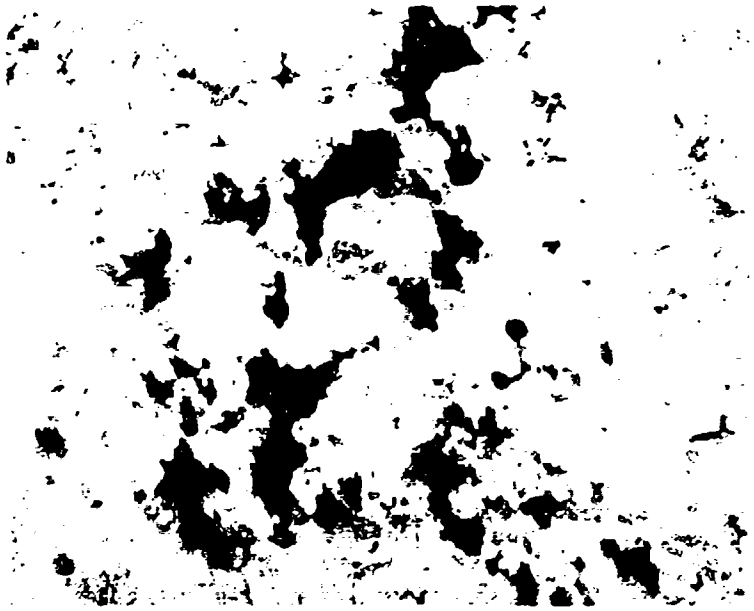


c



Mag: ~3X

Figure 44. Cross sections of as-cast Ti-48Al-1V compressor blade preform. Left, black light photo showing centerline shrink; right, normal light photo showing grain flow. (Note this blade was sectioned for fractographic analysis prior to these photos.)



Mag: 100X

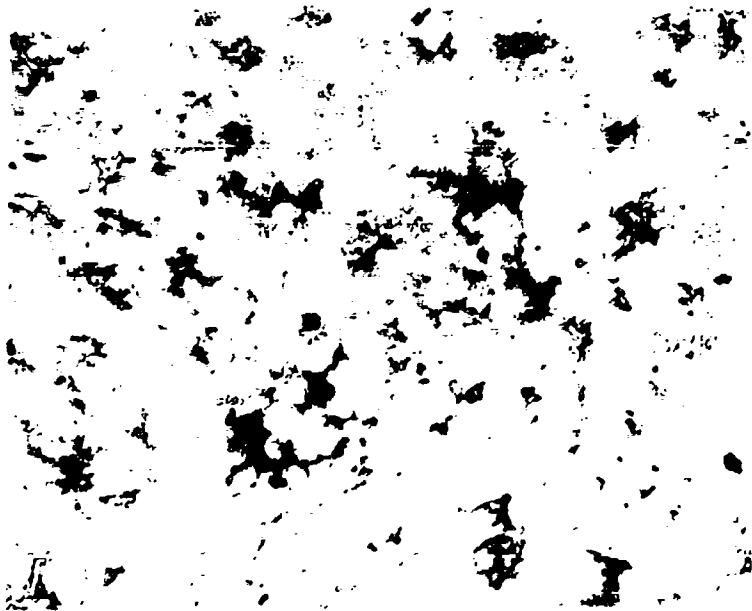


Figure 45. Typical dendritic appearance of centerline shrinkage in as-cast Ti-48Al-1V compressor blade preform.

In an attempt to eliminate this shrinkage, a blade was hot isostatically pressed (HIP) at 1190C/103 MPa/3 hours (2180F/15 ksi/3 hours). Radiographic examination after HIP revealed that all x-ray detectable porosity appeared to be healed, but metallographic studies revealed that a few small pores were still present (Figures 46 and 47). Subsequent experiments conducted by Howmet indicate that higher pressures in the 138-172 MPa (20-25 ksi) range and temperatures of 1200-1260C (2200-2300F) are needed to fully heal porosity in gamma alloys.

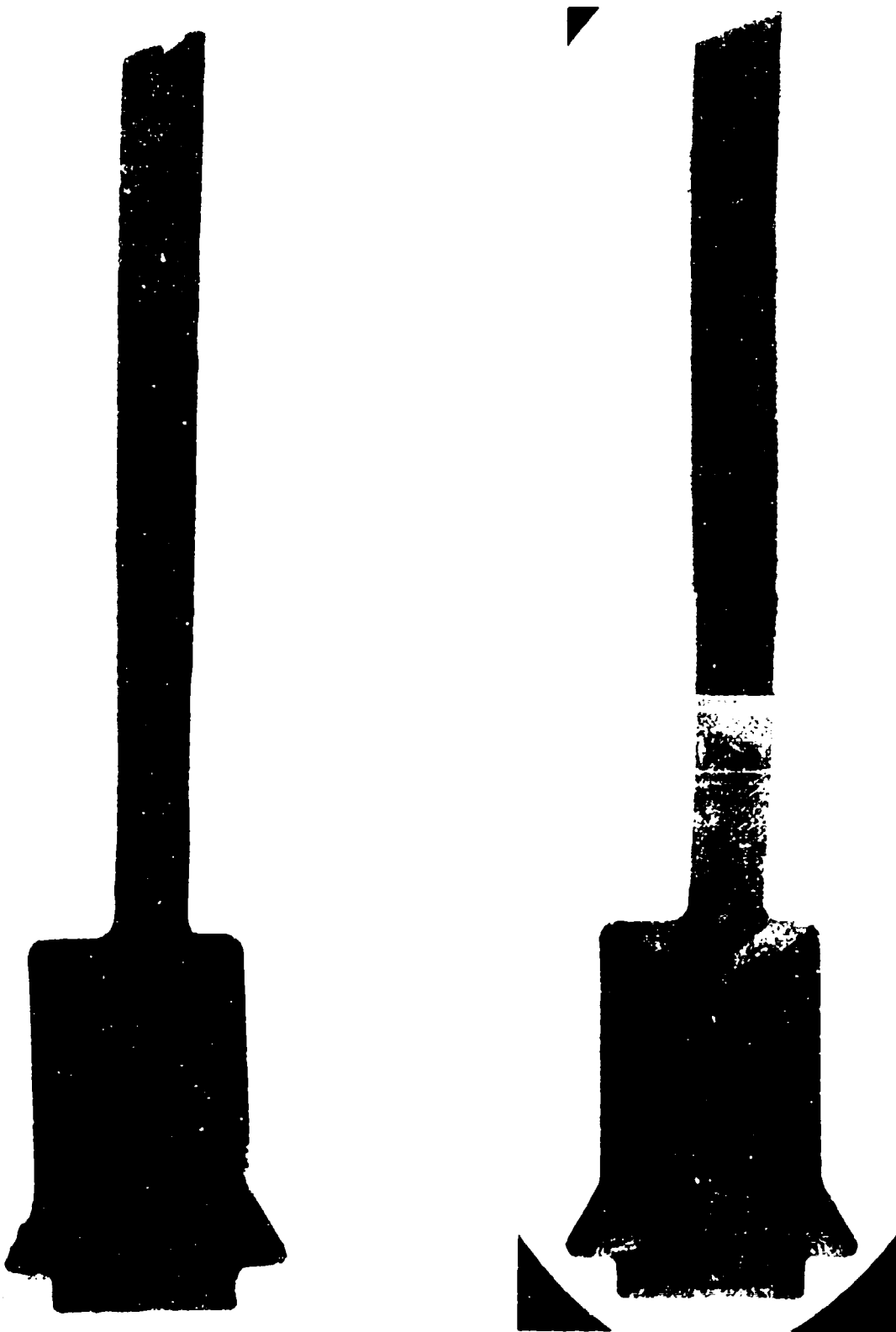
A current ManTech effort is underway to produce cast JT9D 5th stage turbine blade using the Ti-48Al-1V-.1C alloy⁽¹³⁾. A systematic HIP/heat treatment/mechanical property study is being conducted as part of this effort to more fully establish procedures for producing cast gamma alloy components. A full development effort was beyond the scope of the present program, but the results do indicate small gamma castings of acceptable quality can be produced.

b. Gamma Alloy Machinability

Forged and heat treated* Ti-48Al-1V alloy stock was used for machinability and peening experiments. Machining methods evaluated were milling, drilling, single point turning and grinding; peening trials utilized glass beads and steel shot at three intensity levels.

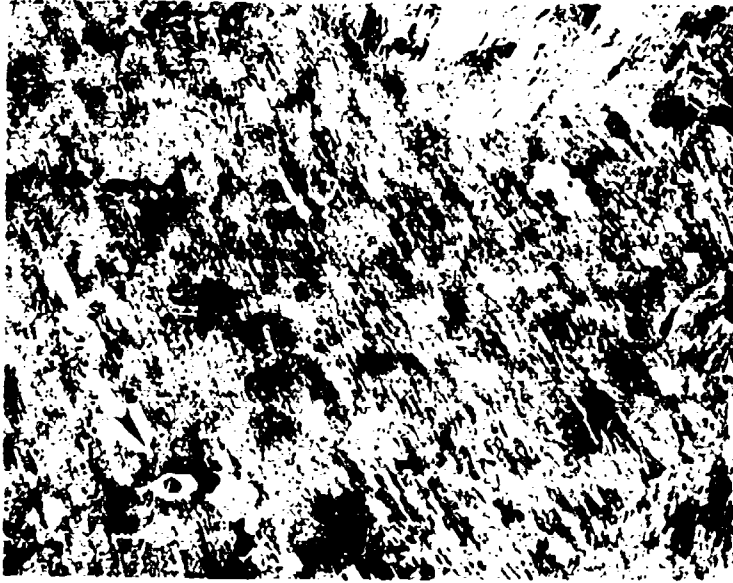
Due to limited material availability, hole drilling and lathe turning operations were performed on the same piece of stock resulting in the configuration shown in Figure 48. Twelve different turning variables and eight drilling parameters were evaluated. Fluorescent penetrant examination of the as-machined test specimen detected no crack indications. The machined test piece was subsequently sectioned longitudinally for metallographic examination in the as-machined condition, while the second half was thermally exposed for 24 hours at 650C (1200F) to determine if any surface recrystallization or thermal cracking occurred.

*1315C (2400F)/1/argon cool + 815C (1500F)/8/air cool



Mag: 5X

Figure 46. Cross sections of cast + HIP (1190C/103 MPa/3 hours, 2180F/15 ksi/3 hours) Ti-48Al-1V compressor blade preform. Left, black light photo, no indications present; right, natural light photo showing grain flow.



Mag: 100X

Figure 47. Microstructure of cast + HIP Ti-48Al-1V compressor blade preform showing residual unhealed porosity (arrows).

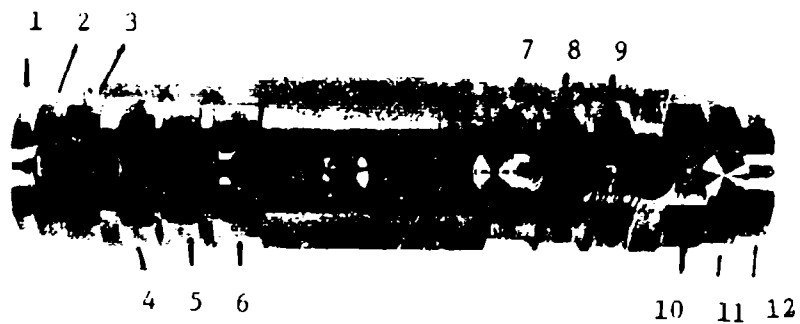


Figure 48. Ti-48Al-1V machinability specimen after lathe turning and hole drilling trials. Numbers correspond with specimen numbers in Tables 23 and 24.

Metallographic examination revealed that rotational speed was the critical factor in producing acceptable crack and/or recrystallization-free surfaces during lathe turning, while feed rate and depth of cut could be varied over a wide range. Of the two rotational speeds evaluated, 225 RPM produced crack-free surfaces with no subsequent recrystallization at all feed rates and depths of cut (Table 23). At 350 RPM, only light feed rates and low depth of cut produced acceptable surfaces. While other combinations of speeds and feeds may also prove acceptable, the parameters established provide a reasonable rate of material removal for most applications.

Hole drilling, on the other hand, was much more sensitive to cracking or thermal recrystallization and only one condition, 135 RPM, 3 thousandths/revolution feed rate was acceptable (Table 24). Higher speeds at the same or even half of the feed rate cracked and/or exhibited surface recrystallization. An alternative to mechanical drilling may be the use of an electrodischarge technique followed by honing to remove the remelt layer.

Milling trials were conducted on a rectangular bar with 23 cuts being made on three sides as shown in Figure 49. Fluorescent penetrant examination revealed three indications in cuts 1, 17 and 22, but subsequent metallographic examination found additional cracking in sections 13-16 and 18 and 20 (Table 25). No surface recrystallization was detected after 650C (1200F) 24 hour exposure in any specimen, but an additional crack occurred in cut number 1. Optimum milling speed conditions for the alloy was 660 RPM as a wide range of cut depths and feed rates resulted in acceptable, crack-free surfaces and rapid metal removal.

Sixteen grinding parameters were evaluated which are listed in Table 26. Fluorescent penetrant examination revealed considerable cracking on four of the specimens (Figure 50). Three of these were from the group ground with a 60 grit aluminum oxide wheel using a fast traverse speed with various cut rates and feed rates. A slow traverse speed using the same wheel resulted in a crack-free specimen. The remaining cracked specimen was ground using a 100 grit silicon carbide wheel with a heavy feed rate

TABLE 23

Effect of Lathe Turning*
Variables on the Machinability of
Forged and Heat Treated Ti-48Al-1V

<u>Specimen Number</u>	<u>Speed (RPM)</u>	<u>Feed Rate (Thousandths/Min.)</u>	<u>Depth of Cut (Thousandths)</u>	<u>Observations**</u>
1	350	1.8	.200	Surface cracks, no recrystallization
2	350	1.8	.100	No cracks or recrystallization
3	350	1.8	.050	Surface cracks, no recrystallization
4	225	1.8	.050	No cracking or recrystallization
5	225	1.8	.100	No cracking or recrystallization
6	225	1.8	.200	No cracking or recrystallization
7	225	0.9	.150	No cracking or recrystallization
8	225	0.9	.100	No cracking or recrystallization
9	225	0.9	.050	No cracking or recrystallization
10	350	0.9	.050	No cracking or recrystallization
11	350	0.9	.100	Surface cracks, no recrystallization
12	350	0.9	.200	Surface cracks, no recrystallization

*Single point carbide tool, no coolant

**Examined in the as-machined condition and after 650C (1200F)/24 hour exposure

TABLE 24

Effect of Drilling Variables*
on Machinability of Forged
and Heat Treated Ti-48Al-IV

<u>Specimen Number</u>	<u>Speed (RPM)</u>	<u>Feed (Thousandths/Rev.)</u>	<u>Observations**</u>
1	135	1.5	Cracks plus disturbed surface layer
2	210	1.5	Cracks plus disturbed surface layer
3	325	1.5	Cracks plus disturbed surface layer
4A	660	1.5	No cracks, some surface disturbance
5	1115	1.5	Heavy cracking, surface oxidized and disturbed
6	135	3.0	Very slight surface disturbed layer
7	210	3.0	Exit crack and surface disturbed layer
8	325	3.0	Heavy surface disturbance and cracking

*Carbide drill, cutting fluid, no coolant

**Examined in the as-machined condition and after 650C (1200F)/24 hour exposure

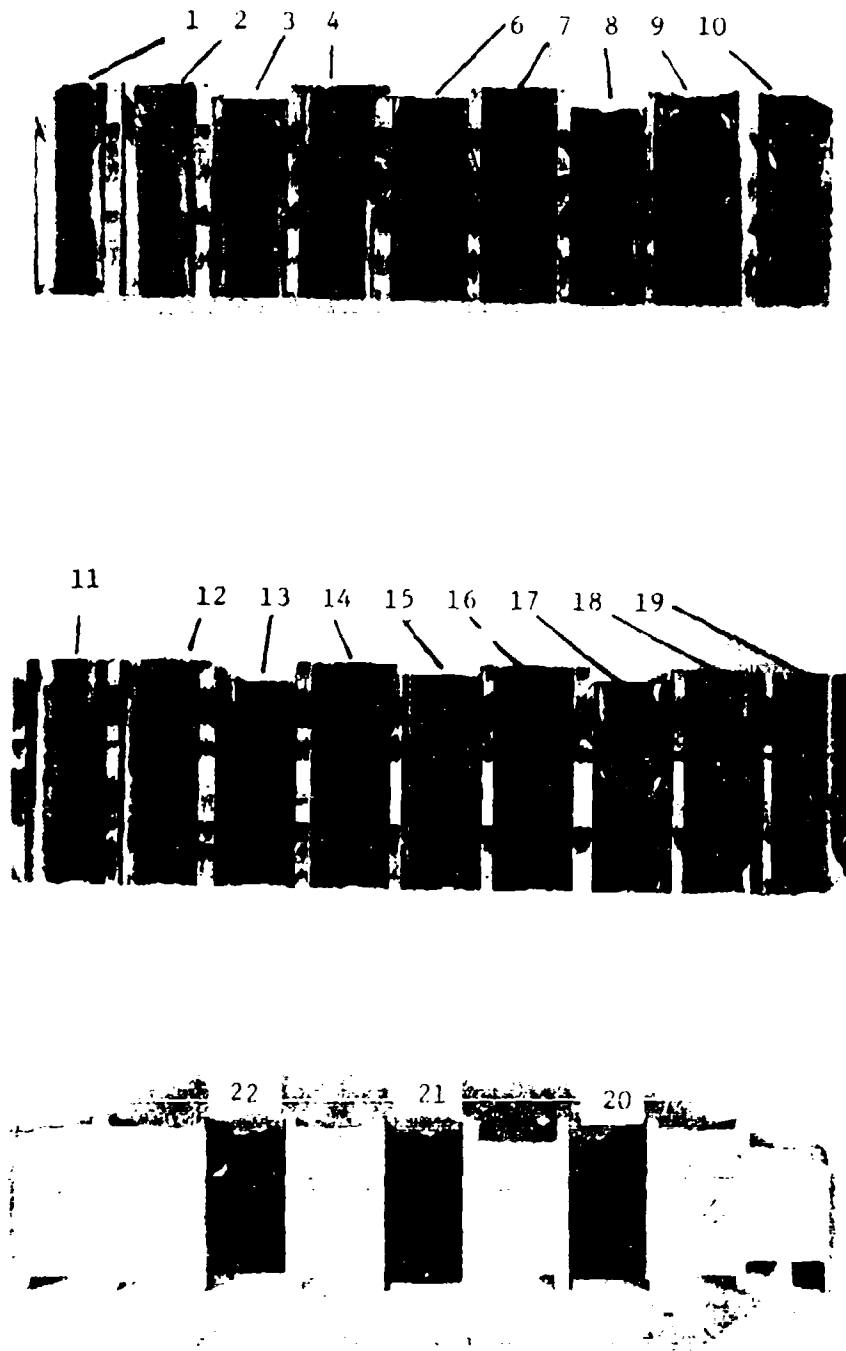


Figure 49. Ti-48Al-1V machinability specimen after milling trials. Numbers correspond with specimen numbers in Table 25.

TABLE 25

Effect of Milling Variables on*
the Machinability of Forged
and Heat Treated Ti-48Al-IV

<u>Specimen Number</u>	<u>Speed (RPM)</u>	<u>Feed Rate (Thousandths/Min.)</u>	<u>Depth of Cut (in.)</u>	<u>Observations**</u>
1	1115	2.0	.050	Surface cracked after thermal exposure
2	1115	1.625	.050	Surface cracked as-machined and after exposure
3	1115	1.25	.075	No cracking or surface disturbed layer
4	1115	1.625	.050	No cracking or surface disturbed layer
6	660	2.0	.075	No cracking or surface disturbed layer
7	660	1.625	.125	No cracking or surface disturbed layer
8	660	1.625	.100	No cracking or surface disturbed layer
9	660	2.0	.050	No cracking or surface disturbed layer
10	660	1.25	.150	No cracking or surface disturbed layer
11	325	1.25	.075	No cracking or surface disturbed layer
12	325	1.625	.050	No cracking or surface disturbed layer
13	325	0.75	.100	Surface cracked, no disturbed layer
14	325	0.75	.075	Surface cracked, no disturbed layer
15	325	1.25	.050	Surface cracked, no disturbed layer
16	325	0.562	.100	Surface cracked, no disturbed layer
17	210	0.75	.075	Surface cracked, no disturbed layer
18	210	0.562	.100	Surface cracked, no disturbed layer
19	210	0.562	.175	Chipping/spalling, no surface disturbed layer
20	135	0.75	.075	Light surface cracking, no surface disturbed layer
21	135	0.937	.050	No cracking or surface disturbed layer
22	135	0.562	.100	Light cracking, possible surface recrystallization

*Carbide cutter, no coolant

**Examined in the as-machined condition and after 650C (1200F)/24 hour exposure

TABLE 26

Effect of Grinding Variables*
on the Machinability of Forged
and Heat Treated Ti-48Al-1V

Specimen Number	Wheel Type	Feed Rate	Cut Depth	Traverse Speed	Wheel RPM	Observations**
LAL	C100J9V	.020"	.010"	Fast	2100	No cracking or surface disturbed layer
1BL	C100J9V	.020"	.006"	Fast	2100	No cracking or surface disturbed layer
L4S	C60J9V	.010-.020"	.004"	Slow	2100	No cracking or surface disturbed layer
1BS	C60J9V	.060"	.001"	Fast	2100	Surface cracks, no disturbed layer or recrystallization
2AL	A60I8V	.020"	.010"	Fast	2100	Surface cracks, no disturbed layer or recrystallization
2BL	A60I8V	.020"	.006"	Fast	2100	Surface cracks, no disturbed layer or recrystallization
3AS	A60I8V	.010-.020"	.004"	Slow	2100	No cracking or surface disturbed layer
3BS	A60I8V	.060"	.001"	Fast	2100	Surface cracks, no disturbed layer or recrystallization
5AL	A54I2V	.020"	.010"	Fast	2100	No cracking or surface disturbed layer
5BL	A54I2V	.020"	.006"	Fast	2100	No cracking or surface disturbed layer
4AS	A54I2V	.010-.020"	.004"	Slow	2100	No cracking or surface disturbed layer
4BS	A54I2V	.060"	.001"	Fast	2100	No cracking or surface disturbed layer but some chatter marks
4AL	A100G8V	.020"	.010"	Fast	2100	No cracking or surface disturbed layer
4BL	A100G8V	.020"	.006"	Fast	2100	No cracking, but some surface disturbance and recrystallization observed
2AS	A100G8V	.010-.020"	.004"	Slow	2100	No cracking but surface recrystallized layer
2BS	A100G8V	.060"	.001"	Fast	2100	No cracking or surface disturbed layer

*Wheel size: 10" diameter, water soluble coolant

**Examined in the as-machined condition and after 650C (1200F)/24 hour exposure

C100J9V Regular silicon carbide, 100 grit grain size, medium hardness and density, vitrified bond
 C60J9V AS above except 60 grit grain size
 A60I8V Regular aluminum oxide, 60 grit grain size, soft hardness, medium density, vitrified bond
 A54I2V Regular aluminum oxide, 54 grit grain size, soft hardness, high density, vitrified bond
 A100G8V Regular aluminum oxide, 100 grit grain size, soft hardness, medium density, vitrified bond

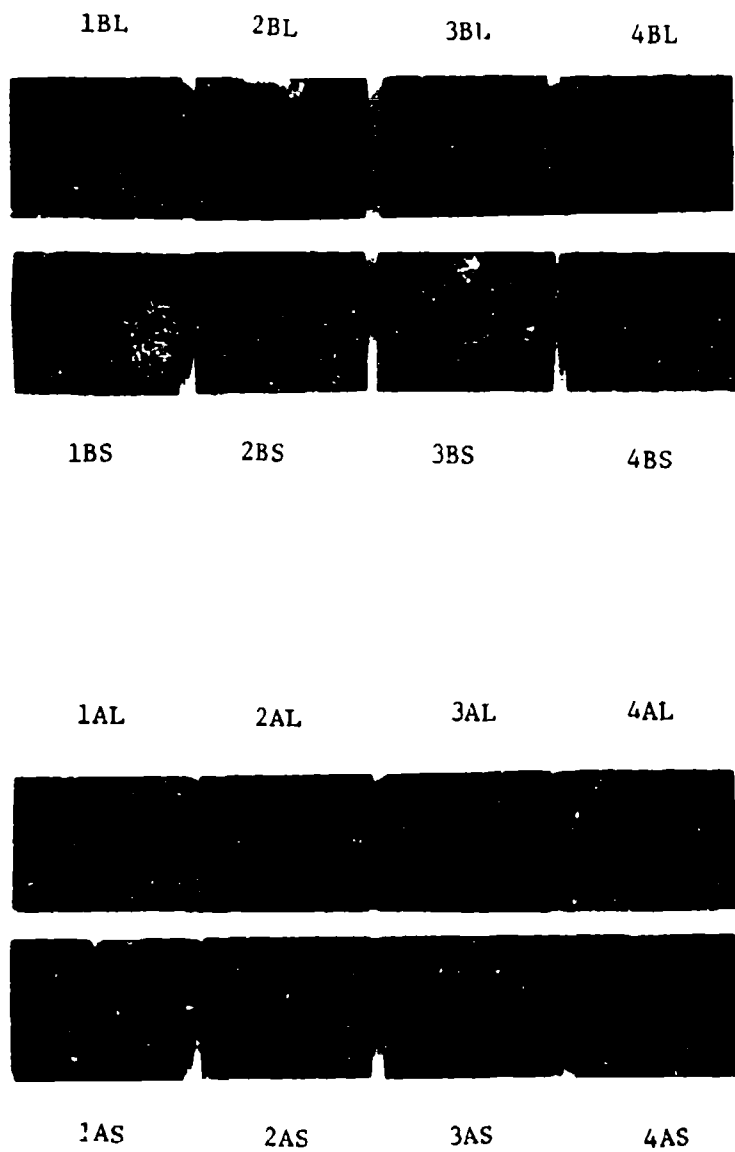


Figure 50. Black light photographs of Ti-48Al-1V grinding trial specimens after FPI examination. Note surface cracking on 2BL, 1BS, 3BS and 2AL.

but a light cut depth at high speed. No other cracks were found upon subsequent metallographic examination, however, two specimens ground with a 100 grit alumina wheel showed evidence of surface disturbance and/or recrystallization after thermal exposure. In general, the grinding results were encouraging as ten of the sixteen parameters resulted in smooth, crack-free surfaces.

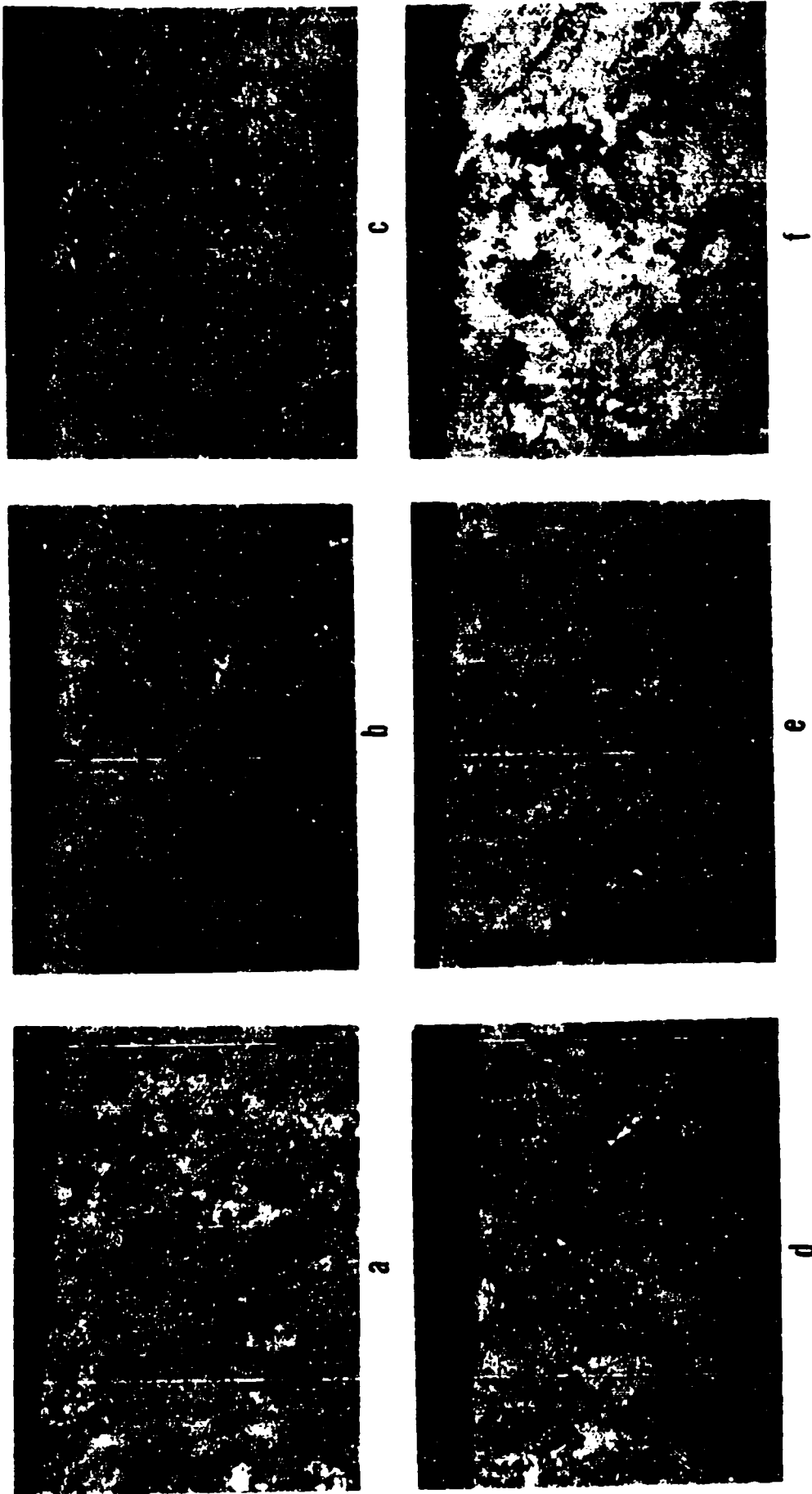
Other approaches such as electrodischarge machining and electrochemical milling techniques were not systematically evaluated here, but have been proven successful in machining of hundreds of specimens over the years with few problems. Thus, it is concluded that, although certain precautions are advisable, machinability of the gamma alloy should not be a barrier in its application to engine components.

Peening trials were conducted on ground (600 grit silicon carbide finish) blocks utilizing glass beads and steel shot at intensities of 6N, 11N and 6A, respectively. Residual surface stresses after peening were documented using an x-ray diffraction technique. Residual surface stresses were not significantly different for the three intensities. Average values were as follows:

6N glass -607 MPa (-88 ksi) compressive
11N glass -634 MPa (-92.5 ksi) compressive
6A steel -593 MPa (-86 ksi) compressive

These values are very similar to those obtained on conventional titanium alloys.

Metallographic examination of as-peened and peened + thermally exposed at 650C (1200F) for 24 hours was conducted. Examination of as-peened specimens revealed extensive surface cracking resulting from the 11N glass bead peen while none was detected on the 6N glass bead peened or 6A shot peened specimens. Peened specimens subsequently exposed at 650C (1200F) for 24 hours and re-examined showed no recrystallized layer; however, minor surface cracking was detected on the 6A shot peened specimen (Figure 51a-f). Since the residual surface stress imparted was about equal for all intensities, the 6N glass bead treatment is recommended. This will not produce as deep a hardened layer as the higher intensities, but should be acceptable for most components.



Mag: 100X

Figure 51. Effect of peening and subsequent thermal exposure on forged and heat treated Ti-48Al-IV. a) 6A peened; b) 6N peened; c) 6N peened plus thermal exposure; d) 6A peened plus thermal exposure; e) 6N peened plus thermal exposure; f) 6N peened plus thermal exposure plus thermal exposure.

c. Forged Alpha-Two Alloy Compressor Blade

To demonstrate the feasibility of producing a compressor blade forging using current manufacturing techniques, it was decided to fabricate a JT8D fifth stage blade using a screw press.

Conventionally rolled Ti-25Al-11Nb-2V bar was used from which billets 28.6 mm (1.125") diameter x 31.1 mm (1.225") high were machined. A preform was extruded to give the required shape at 1170C (2150F) in a steel die. Five extruded preforms were made before severe die galling was observed indicating lubrication problems. Two of the extrusions were selected to be upset forged into JT8D 5th stage compressor blades on the screw press. Forging temperature selected was 1170C (2150F), and the blades produced exhibited excellent die fill and no cracking. The preforms, extrusions and blades used in the production sequence are shown in Figure 52.

It is apparent that conventional production techniques used to produce Ti-6Al-4V alloy compressor blades can be applied to Ti-Al-Nb-V aluminide alloys with only minor adjustments. A die/lubricant development effort would be necessary due to the higher extrusion and forging temperatures which promote some tendency to galling.

d. Alpha-Two Alloy Sheet Stock

Ti-25Al-11Nb-2V sheet stock rolled from the same heat of barstock described in the preceding section was furnished by the Government Products Division of P&WA, who had originally procured it from TIMET, Henderson Technical Laboratories, Henderson, Nevada. The material was 1.3 mm (0.050" thick and in the annealed condition upon receipt. Due to the limited amount of available material, it was decided to use three point bend testing to evaluate the strength and ductility as had been done in earlier aluminide studies^(3,5).

The following conditions were evaluated:

- As-received, longitudinal and transverse
- Beta solution heat treated and aged, longitudinal and transverse
- Welded + direct age
- Welded + full beta solution and age

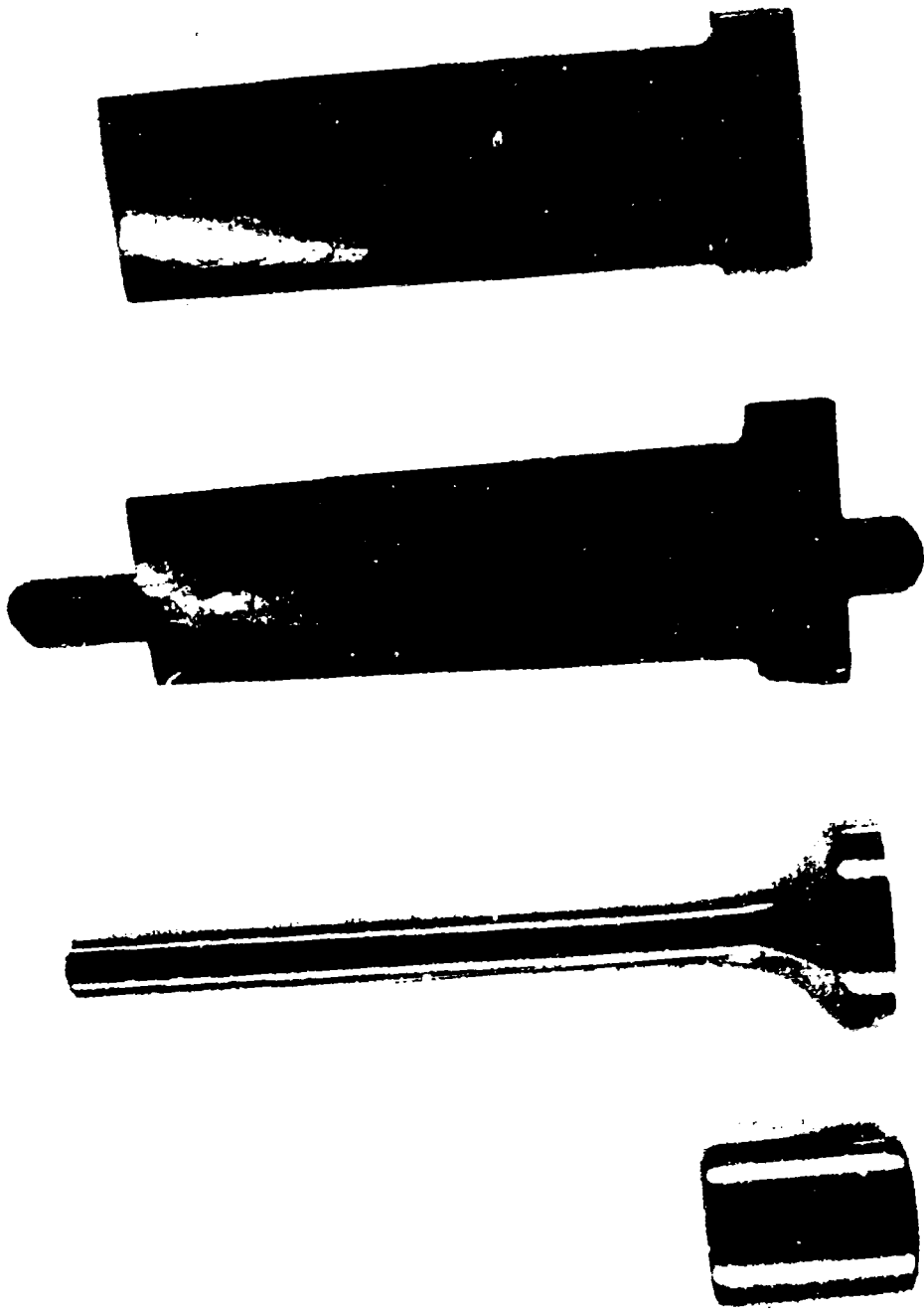
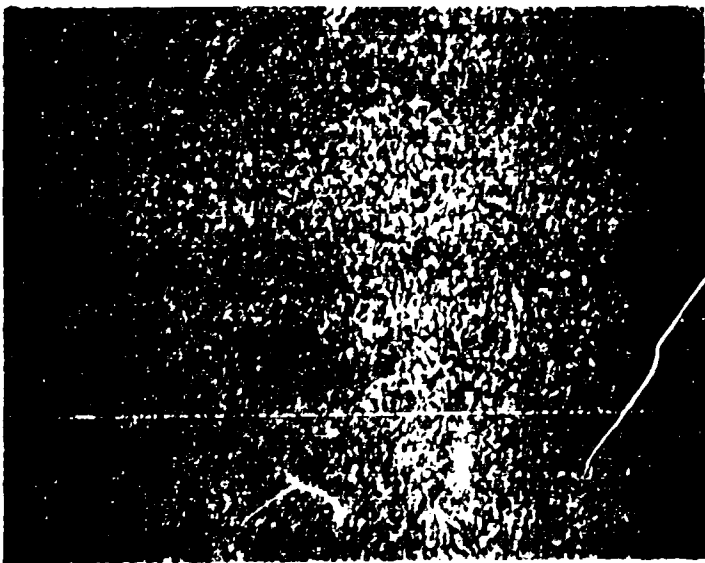


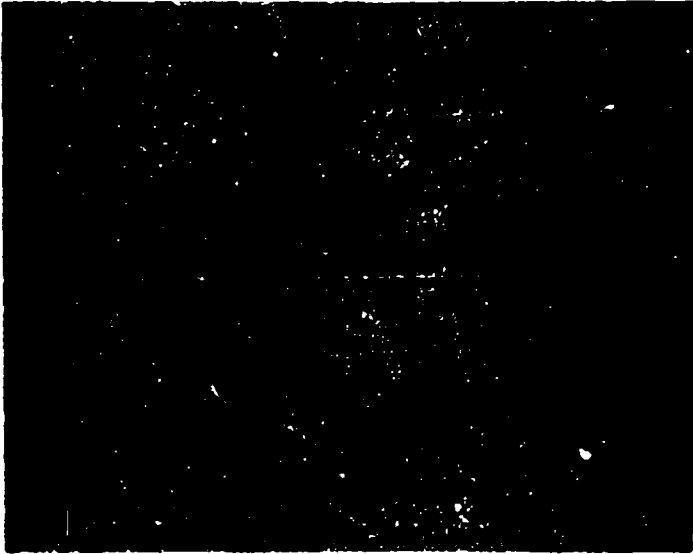
Figure 52. Process procedure for forging Ti-25Al-9Nb-2V compressor blade; left to right, billet, extruded preform, as-forged blade, trimmed blade for final machining.

Typical microstructures of the sheet after various processes are shown in Figure 53. Welding was performed by a manual tungsten inert gas (TIG) technique in an argon-filled dry box using AMS 4956 (Ti-6Al-4V) filler wire. Weld quality appeared excellent and no cracking or porosity was detected.

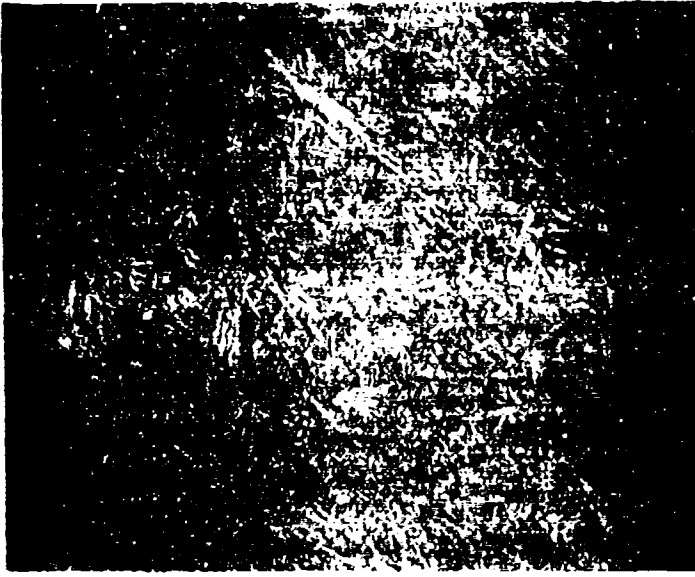
Bend testing was performed at room temperature and 260C (500F). Results showed a significant difference in strength and ductility between longitudinal (rolling direction) and transverse specimens (Table 27). The longitudinal specimens were 10-20% stronger than transverse specimens in the as-received condition and 40-50% stronger after solution treating and aging (STA). In general, strength was somewhat lower for STA material in either direction; however, the properties are comparable to data previously reported for specimens machined from forged and STA Ti-25Al-10Nb-4V pancakes⁽⁴⁾. Welded properties were about equivalent to transverse parent metal properties and there was little difference in between material direct aged or fully STA after welding.



a



b



c

Mag: 500X

Figure 53. Typical microstructure of Ti-25Al-9Nb-2V sheet. a) as-received, annealed; b) beta solution treated and age; c) welded area after full STA heat treatment.

TABLE 27

Bend Test Data for Alpha-Two
Sheet Specimens, V-5816, Ti-25Al-11Nb-2V

<u>Specimen Condition</u>	<u>Orientation</u>	<u>Test Temp. °C (°F)</u>	<u>Yield Str. MPa (ksi)</u>	<u>Max. Fiber Stress MPa (ksi)</u>	<u>%Ductility</u>
As-Rec'd. (1)	Longitudinal	RT	1336 (193.7)	1498 (217.2)	2.3
	Transverse	RT	1127 (163.5)	1227 (178.0)	>1.9(3)
	Longitudinal	260 (500)	1198 (173.7)	1350 (195.0)	>1.9(3)
	Transverse	260 (500)	1081 (156.8)	1194 (173.2)	>1.9
STA (2)	Longitudinal	RT	1251 (181.5)	1552 (225.1)	2.2
	Transverse	RT	762 (110.5)	857 (124.3)	>1.5(3)
	Longitudinal	260 (500)	998 (144.8)	1391 (201.7)	>2.4(3)
	Transverse	260 (500)	634 (92.0)	722 (104.7)	>1.2(3)
Welded (4) + 815C (1500F)/1/AC	-	RT	-	1100 (159.5)	1.1(3)
	-	260 (500)	-	1451 (210.5)	>1.7(3)
Welded + STA	-	RT	-	1109 (160.9)	1.2
	-	260 (500)	1189 (172.4)	1310 (190.0)	>1.7(3)

(1) As-received = 982C (1800F)/.5/AC

(2) STA = 1204C (2200F)/1/vacuum cool + 815C (1500F)/1/AC

(3) Specimens tested to limit of ram travel without cracking

(4) AMS 4956, Ti-6Al-4V, filler wire used

SECTION V

ANALYSIS AND CONCLUSIONS

In this section, several of the more important features of the program have been selected for further analysis. In the first part of the discussion, we shall cover the alloy chemistry, process and stability features of the alpha-two alloy. The second segment deals with the structural and processing features of the gamma alloys.

Previous studies have demonstrated that alloys from the Ti-Al-Nb-V system exhibit the best balance of tensile and stress-rupture properties. However, although the yield and ultimate tensile strength of Ti-25Al-10Nb-4V met goal values, the stress-rupture properties still fell somewhat below the aim of equivalence to the nickel alloy IN713 on a density corrected basis. In an attempt to compensate for this shortcoming, a further modification was made to alloy chemistry for the current year of the contract, by substituting one percent molybdenum for vanadium. As both the stress-rupture and tensile capability of this new alloy exceed goal levels, a major success could be claimed. Any enthusiasm must be tempered, however, by the grain size effects noted on the high temperature properties. It is unclear how much of the increase can be traced to composition and how much to structure, but it is clear that the molybdenum addition does change the basic alloy characteristics. This may be seen from the marked increase in elastic modulus, values at room temperature being 124×10^6 KPa (18×10^6 psi) compared with 89×10^6 KPa (12×10^6 psi) for the basic alloy. The observation indicates that further studies could identify alloys with a variety of property mixes that could possibly be tailored for specific requirements. For example, low modulus could be key for components that operate in environments with larger thermal variation, such as case struts, where stresses are governed by the product of elastic modulus and thermal expansion coefficient. On the other hand, in the outer shell of a case which operates in less extreme thermal cycles, high stiffness for clearance control could be important.

As noted above in the results section, the strong influence of grain size not only on stress-rupture but also on fracture toughness and low cycle fatigue was unexpected. It is clear that if isothermal forging in the beta phase field is to be used for this class of material, then the exact thermomechanical sequence must be controlled. In the past, acceptable grain sizes have been achieved by several sequences that culminate in a large reduction in the alpha:beta phase field, followed by beta heat treatment. Isothermal beta forging with excellent structural control has been demonstrated for conventional titanium alloys so that an effective sequence for the aluminides would seem possible.

The stability of the alpha-two alloy, as reflected in tensile tests after exposure, was rather poor with major reductions in ductility noted. These lower properties were due in part to the surface modification, but the major contribution is considered to be the structural changes that increased the strength of the alloy. The exact nature of these changes remain to be defined in more detail, but the preliminary results reported here indicate that an instability in the beta phase is responsible. Modification of the heat treatment to produce a more stable phase, for example by aging at a lower temperature, would be one approach to this. It is also clear that the large grain size of the material served to exacerbate the embrittlement. Preliminary results on the properties of Ti-25Al-10Nb-4V after the same exposure, that have been generated recently internally, confirm these postulates. This alloy, processed to fine grained condition, exhibited a slight reduction in elongation from ~3 to ~2 percent at room temperature with no change in the reduction in area values (~4 percent). The specific pre-exposure heat treatments utilized also resulted in only minor changes in strength properties after exposure indicating an increased degree of alloy stability.

The small scale alloy development effort for the gamma alloys did not add much to our previous knowledge. The decision to rely on forging to seal internal defects was a mistake, and this added to the analytical problem. However, it is probable that even if sound material had been produced, the ductility of the alloy series containing 47 percent aluminum would have been too low. Properties of the selected alloy Ti-48Al-1V-.1C were similar to material previously produced from small ingots and processed in the same manner. The slightly lower stress-rupture properties can probably be traced to a lower solution treatment temperature and a slightly different structure. Impact

values for the alloy were rather low but should be contrasted with the surprisingly good fracture toughness values. Reasons for the apparent disparity in levels may be related to a strain rate sensitivity which has not been recognized previously. It is not clear if the property balances measured in wrought alloys will be adequate for engine use especially as the low ductility values seem to be retained to quite high temperatures. Recent evidence on contract F33615-79-C-2091 has indicated that the properties of the cast product form may be increased and could be adequate for blade and other similar components. The one characteristic identified in this year's study which is encouraging is the excellent stability measured in post-exposure testing. This augurs well for high temperature utilization of the material.

The processing trials indicated that gamma alloys can be processed with conventional technology as long as care is exercised. Castability is attractive because of the low degree of surface contamination measured, although the ability to produce tight radii satisfactorily is not good. Gating and configurational changes to reflect the fill and fluidity characteristics of gamma aluminides should result in the ability to cast a variety of structures. The difficulty in healing porosity probably reflects the good creep resistance of the material. Hot isostatic pressing at 1260C (~2300F) will produce a high quality product without modifying the macrostructure appreciably. Finally, the quite extensive machining trials conducted showed that a variety of metal removing processes are applicable to gamma alloys but over rather restricted parametric ranges. Thus in producing aluminide shapes, care should be exercised in machining practice, and it could be useful to consider some of the more advanced electrical machining processes in order to minimize damage and produce a quality surface.

The main conclusions that can be drawn from this project are as follows:

A. For Alpha-Two Alloys

1. The alloy Ti-25Al-10Nb-3V-1Mo shows the best balance of tensile and stress-rupture properties found to date. Introducing molybdenum into the system increases the elastic modulus.
2. Beta grain size was shown to have major effects on creep, stress-rupture, low cycle fatigue and fracture toughness. Improved process schedules should result in finer grained forgings with better properties.

A. For Alpha-Two Alloys (Cont'd.)

3. The stability of the alloy after exposure at intermediate temperatures was poor and tentatively traced to an instability in the beta phase. Modified heat treatments are considered to be a method for alleviating this problem.
4. Processing studies continue to show that many of the methods of forging, joining, etc. developed for conventional titanium alloys can be applied to alpha two systems. Changes in process details, such as lubricants for closed die forgings, may be required.

B. For Gamma Alloys

5. The alloy screening program did not identify an alloy with superior properties to Ti-48Al-1V-0.1C. Properties of this alloy were consistent with earlier results, but the ductility and impact resistance tended to be low. This should be contrasted with the promising fracture toughness levels.
6. Evidence was obtained of structural effects on fatigue properties of larger grained regions leading to easier crack nucleation and consequently lower lives.
7. Alloy stability appeared excellent after exposure at intermediate temperatures with only minor changes in properties.
8. Additional processing studies showed that castings of the material of reasonable quality and good shape definition could be produced. Sharp radii lead to some porosity problems. Machining parameters were established for the alloy, but the conditions which give good stable surfaces tended to be more restricted than for alpha-two alloys.

REFERENCES

1. M. J. Blackburn, D. L. Ruckle and C. E. Bevan, "Research to Conduct an Exploratory and Analytical Investigation of Alloys," AFML-TR-78-18, March 1978.
2. M. J. Blackburn and M. P. Smith, "The Understanding and Exploitation of Alloys Based on the Compound TiAl (Gamma)," AFML TR-79-4056, May 1979.
3. M. J. Blackburn and M. P. Smith, "The Understanding and Exploitation of Alloys Based on the Compound TiAl (Gamma Phase)," AFML TR-78-78, June 1978.
4. M. J. Blackburn and M. P. Smith, "Research to Conduct an Exploratory Experimental and Analytical Investigation of Alloys," AFWAL TR-80-4175, November 1980.
5. T. E. O'Connell, "Study of Intermetallic Compounds," AFML TR-79-4177, December 1979.
6. J. B. McAndrew and H. D. Kessler, "Ti-36Al as a Base for High Temperature Alloys," Trans-AIME, Vol. 206, 1384 (1956).
7. J. B. McAndrew and C. R. Simcoe, WADD TR60-99, April 1960.
8. J. B. McAndrew and C. R. Simcoe, ASD TR61-446, Part I (March 1962) and Part II (June 1963).
9. M. J. Blackburn and M. P. Smith, "Research to Conduct an Exploratory and Analytical Investigation of Alloys," AFWAL TR-81-4046, June 1981.
10. T. E. O'Connell, "Production of Titanium Aluminide Products," Interim Report FR-15425, September 1981, F33615-78-C-5144.
11. M. J. Blackburn and M. P. Smith, "R&D on Composition and Processing of Titanium Aluminide Alloys for Turbine Engines," Third Interim Technical Report, 24 July 1981.
12. T. E. O'Connell, "Production of Titanium Aluminide Products," Interim Report FR-12559, 20 December 1979, F33615-78-C-5144.
13. Design, Manufacture and Evaluation of Titanium Aluminide Components, Contract F33615-79-C-2091.